5-2016

CLL METABOLISM IS REGULATED BY PROGNOSTIC FACTORS, MODULATED BY STROMA AND ABROGATED BY PI3K INHIBITION

Hima Vangapandu

CLL METABOLISM IS REGULATED BY PROGNOSTIC FACTORS, MODULATED BY STROMA AND ABROGATED BY PI3K INHIBITION

by

Hima V. Vangapandu, M.S.

APPROVED:

_____

Varsha Gandhi, Ph.D
Advisory Professor

_____

Peng Huang, M.D., Ph.D

_____

Gary Gallick, Ph.D

_____

David McConkey, Ph.D

_____

Zahid H. Siddik, Ph.D

_____

Timothy Thompson, Ph.D.

APPROVED:

_____

Dean, The University of Texas
Graduate School of Biomedical Sciences

CLL METABOLISM IS REGULATED BY PROGNOSTIC FACTORS, MODULATED BY STROMA AND ABROGATED BY PI3K INHIBITION

A

DISSERTATION

Presented to the Faculty of

The University of Texas

MD Anderson Cancer Center

Graduate School of Biomedical Sciences at Houston

In Partial Fulfillment

of the Requirements

for the Degree of

DOCTOR OF PHILOSOPHY

By

Hima V. Vangapandu, M.S.

Houston, TX

May, 2016

Copyright

Dedication

To my parents for the unconditional love and support I received throughout the course of my study

Acknowledgement

I would like to extend my deepest gratitude towards my Ph.D. advisor, Dr. Varsha Gandhi. Your constant guidance, support and exceptional mentorship on my academic career development has been the most invaluable experience of my graduate training; from commitment and dedication to science and teaching, made you my role model. Without your generous support and advice, I could not have reached my career milestone so efficiently.

I would like to thank my second mentor, Dr. Christine Stellrecht, for being so kind and patient with me, every time I asked for advice. Your help, motivation and mentoring helped me greatly. My stay in the lab during my Ph.D. work would not be the same without you.

I thank my committee members, for Drs. Gary Gallick, Peng Huang, David McConkey, Bradley McIntyre, Zahid Siddik and Timothy Thompson for their valuable input and recommendations on my projects and enhancing my critical thinking as a scientist.

Also, I thank Dr. Plunkett for his encouragement and helpful suggestions on my project at lab meetings.

Many thanks to,

My current and former lab mates, Kumudha Balakrishnan, Betty Lamothe, Mary Ayres, Aloke Sarkar, Carly Yang, Shadia Zaman, Viral Patel, Fabiola Gomez and Prexy Modi for providing for helpful tips on lab techniques and good company.

All members of Experimental Therapeutics Academic Program (ETAP) making my stay in school enjoyable!

CLL METABOLISM IS REGULATED BY PROGNOSTIC FACTORS, MODULATED BY STROMA AND ABROGATED BY PI3K INHIBITION

Hima V. Vangapandu, M.S.

Advisor: Varsha V. Gandhi, Ph.D.

Metabolism of chronic lymphocytic leukemia (CLL), a disease characterized by the relentless accumulation of mature B cells has been little explored. Bone marrow stromal cells provide a survival benefit to CLL cells, in part through PI3K/AKT pathway. Compared with proliferative B-cell lines, metabolic fluxes of oxygen and lactate were low in quiescent malignant B lymphocytes from CLL patients. Glycolysis (extracellular acidification rate, ECAR) was consistently low in CLL samples, but oxygen consumption (OCR) varied considerably. Higher OCR was associated with poor prognostic factors such as ZAP 70 positivity, unmutated IgVH, high β2M levels, and higher Rai stage. Co-culture with the NK-tert stromal line increased basal OCR and maximum respiratory capacity of CLL at 2 or 24 hours of interaction, without significant changes in glycolysis. Two other stromal lines displayed similar induction of OCR in CLL. The levels of ribonucleotide triphosphate pools in CLL cells were augmented with stromal interaction. PI3K inhibitors, duvelisib (IPI-145) and idelalisib (GS1101), and the AKT inhibitor MK-2206, dramatically reduced OCR, ECAR, and ribonucleotide pools in CLL cells. In concert, genetic ablation of PI3K in a malignant B cell line also diminished OCR and ECAR. Collectively, these data suggest that stroma affects metabolomics in quiescent CLL cells, driven in part by the PI3K/AKT pathway.

Table of contents

CHAPTER 2. MATERIALS AND METHODS

List of Figures

List of Tables

List of Abbreviations

4E-BP1	eukaryotic translation initiation factor 4E-binding protein 1
β-2M	beta 2 microglobulin
2-DG	2- deoxy-D-glucose
AA	antimycin A
ACC1	acetyl coA carboxylase
AKT	protein kinase B
ATP	adenosine 5’ triphosphate
BAFF	B cell activating factor
BCR	B cell receptor
BSA	bovine serum albumin
CAD	carbamoyl-phosphate synthetase 2, aspartate transcarbamoylase, and dihydrooratase
Cas9	CRISPR associated protein 9
CD	cluster of differentiation
Ci	Curie
CIP	calf-intestinal alkaline phosphatase
CLL	chronic lymphocytic leukemia
CRISPR	clustered regularly interspaced short palindromic repeats
CTP	cytosine 5’ triphosphate
DHODH.....	.dihydroorotate dehydrogenase
DMSO	dimethyl sulfoxide
DPM	disintegrations per minute
ECAR	extracellular acidification rate

ETC	electron transport chain
FACS	fluorescence activated cell sorting
FBS	fetal bovine serum
FCCP	carbonyl cyanide-4-(trifluoromethoxy) phenylhydrazone
GAPDH	glyceraldehyde-3-phosphate dehydrogenase
GFP	green fluorescent protein
GTP	guanine 5’ triphosphate
HPLC	high performance liquid chromatography
IC50	half-maximal inhibitory concentration
Ig	immunoglobulin
IgVH	immunoglobulin heavy chain variable region
LDH	lactate dehydrogenase
MAPK	mitogen activated protein kinase
MCL	mantle cell lymphoma
MRC	maximal respiratory capacity
mRNA	messenger ribonucleic acid
mTOR	mammalian target of rapamycin
NADH	nicotinamide adenine dinucleotide
NRF1	nuclear respiratory factor
NTP	nucleotide triphosphate
OCR	oxygen consumption rate
OxPhos	oxidative phosphorylation
PBMC	peripheral blood mononuclear cells
PBS	phosphate buffered saline
PI	propidium iodide

PI3K	phosphoinositide 3-kinase
PIK3CD	phosphatidylinositol-4,5-bisphosphate 3-kinase, catalytic subunit delta
rpm	rotations per minute
ROS	reactive oxygen species
RT-PCR	reverse transcriptase polymerase chain reaction
S6	ribosomal protein S6
SD	standard deviation
SDF-1	stroma derived factor -1
SRC	spare respiratory capacity
STAT	signal tranducer and activator of transcription
TFAM	mitochondrial transcription factor A
TMRE	tetramethylrhodamine, ethyl ester, perchlorate
UCP2	uncoupling protein 2
UTP	uracil 5’ triphosphate
ZAP70	zeta chain associated protein 70 kDa

CHAPTER 1. INTRODUCTION

Chronic lymphocytic leukemia

Chronic lymphocytic leukemia (CLL) is a frequently occurring indolent malignancy characterized by the relentless accumulation of quiescent, immunologically dysfunctional mature B cells that fail to undergo apoptosis. Although different compartments such as bone marrow, spleen, lymph nodes, and peripheral blood provide diverse microenvironments, which affect the characteristics of CLL cells in general, the population is either slowly proliferating or quiescent with the majority of cells being in G_0 phase of the cell cycle (Chiorazzi et al. 2005). However, these cells are transcriptionally and translationally active, suggesting that CLL cells are not inert and should have an active metabolomics profile (Balakrishnan et al. 2014).

Mature CLL cells are CD5 and CD19 positive (Marti et al. 1989, Matutes et al. 1994) and overexpress anti-apoptotic proteins of BCL-2 family including like BCL-2, MCL-1, BCL-XL (Kitada et al. 1998). Pro-apoptotic proteins like BAX and BCL-XS are under expressed (Caligaris-Cappio and Hamblin 1999).

Prognostic factors

CLL is the most common leukemia in the western world. According to NCI's SEER (Surveillance, Epidemiology and End Results Program), the incidence of CLL is 4.5 per 100,000 individuals, making it the most common leukemia in the Western world (Rozman and Montserrat 1995). It mostly affects adults above the age of 60. Risk of contracting CLL for first degree relatives of patients is higher, almost three times likely to those with no CLL history in the family (Cuttner 1992).

CLL has a heterogenous disease course as some patient have an indolent disease and a long clinical course, whereas others have a rapid progression of the disease. The clinical course of CLL can be predicted by the following prognostic factors: Rai and Binet are two staging systems which are widely used to categorize CLL patients based on clinical characteristics i.e., lymphocyte counts (lymphocytosis) and lymph node enlargement. Rai staging is widely used in North America and is based on lymphocyte counts (Rai et al. 1975). Patients with early Rai stage disease (0, 1) have a greater than 10 year life expectancy (Brown 2011).

In addition to the patients' clinical stage, there are several cellular markers that strongly correlate with prognosis. The expression levels of ZAP 70 (zeta chain (TCR) associated protein kinase 70 kDa) is one such marker. ZAP 70 is a receptor tyrosine kinase expressed on the surface of CLL B cells (Orchard et al. 2004, Rassenti et al. 2004). It is closely related to SRC kinase and is one of the membrane components associated with early activation of T lymphocytes and natural killer (NK) cells (Mustelin and Tasken 2003). Usually higher expression of this protein is found in CLL in the lymph node as compared to peripheral blood CLL B cells. A study reported that ZAP 70 positive CLL cells have stronger adherence capacity to stromal cells and enhanced signaling with the microenvironment as compared to their counterparts (Stamatopoulos 2009, Lafarge et al. 2014, Lafarge et al. 2015).

Somatic mutation in the immunoglobulin variable region heavy chain (IgVH) divides CLL disease into two subsets. The one in which IgVH is mutated is responsive to therapy as compared to the subset where the gene remains unmutated. Presence of somatic mutations in IgVH indicates that the cells have encountered an antigen and thus are indicative of a more

mature B-cell. A telomere analysis has revealed that UM CLL has a more active disease in terms of cell proliferation; and as a result acquire more genetic lesions, whereas, MU-CLL tend to undergo less number of cell divisions (Damle et al. 2004). IgVH unmutated (UM) cells also respond better to B cell stimulation than the ones with IgVH mutated (MU) gene (Lanham et al. 2003). Patients with UM-CLL tended to have high-risk genomic aberrations such as del17p and del11q, whereas favorable aberrations such as del13q were overrepresented in the MU-CLL group (Krober et al. 2002). There is also a correlation between expression of both ZAP 70 positivity and IgVH unmutated status (Crespo et al. 2003). ZAP 70 positive and IgVH unmutated patient cohort usually do not respond well to treatment.

CD38 is another marker, whose expression on the cell surface signifies a cell population that has recently left the lymph node, indicating cell activation that is associated with a proliferative nature (Damle et al. 2007). CD38 is necessary for cell to cell interactions during B cell development (Malavasi et al. 1994). If the expression is ≤20%, it is categorized negative for CD38 and >20% as positive.

Serum levels of both β2 microglobulin (β2M) and lactate dehydrogenase (LDH) are also prognostic marker for this disease. CLL cells are known to secrete β2 microglobulin (β2M). High serum levels of β2M have been associated with shorter survival. Similarly, high serum lactate dehydrogenase (LDH) levels are also indicative of poor clinical outcome to therapy. Additional risk factors include cytogenetics of the CLL cells (discussed in detail in the next section), age of the patients and gender; patients 60 years and above have a higher risk of contracting the disease and progression and in terms of gender, males are affected more than females.

Cytogenetics

Genomic aberrations like 17p, 11q, 13q deletions, Trisomy (12+) are common in the landscape of CLL. The most frequent among these is 13q deletion. miR-15a and mir-16-1 coding genes present on chromosome 13q have found to be frequently deleted (55% of CLL cases) and therefore are implicated in pathogenesis (Dohner et al. 2000). Anti-apoptotic proteins, BCL-2 and MCL-1 are downstream targets of miR-15a and miR-16-1. Subsequently, these oncogenes (BCL-2, MCL-1) are expressed at higher levels after deletion of these microRNAs. Patients with isolated 13q deletions have a favorable clinical course and overall survival.

11q deletion occurs in 10-20% of CLL patients leading to poor prognosis. 11q chromosome encompasses the ATM gene which is required for double stranded DNA repair. In a study by Dohner *et al*, incidence of 11q deletion second most in CLL after 13q deletion (Dohner et al. 2000)

Tumor suppressor, TP53 is located on chromosome 17p. Previous studies demonstrated 17p13 locus deletion corresponded to shorter median survival compared to their counterparts with normal karyotype (Dohner et al. 2000) and high incidence observed in fludarabine refractory CLL. The frequency of the chromosome 17p deletion in CLL is 10% (Dohner et al. 2000). A recent study reported that this deletion occurs 25-40% in refractory disease (Fink et al. 2006).

Trisomy 12 (extra copy of chromosome 12) is another common chromosomal anomaly in CLL with a frequency of 10-20%. Despite its frequency, little is known regarding genes associated with trisomy 12 or the mechanism of disease progression.

Treatment

Standard treatment of care for CLL is chemo-immunotherapy including fludarabine (a purine nucleotide analogue), cyclophosphamide (an alkylating agent) and rituximab (monoclonal antibody against CD20) (FCR). The only curative therapy for refractory CLL is allogenic bone marrow transplantation (Dreger et al. 2014). Median overall survival for patients with CLL is 8 to 12 years (Wierda et al. 2007). In recent years, several agents that target B- cell receptor pathway have been used in the clinic that include, Bruton's tyrosine kinase (BTK) inhibitor, ibrutinib and Phosphosphotidylinositide 3- kinase delta (PI3K δ) inhibitor, idelalisib. Also, several antibodies have shown promising response to CLL, that target CD 20 obinutuzumab and ofatumumab; targeting CD52, alemtuzumab and many other antibodies against CLL antigens are currently in testing in clinical trials, as they are better tolerated than chemotherapeutic agents.

Microenvironment

The literature is replete with data demonstrating that the supporting microenvironment (generally evaluated as bone marrow stromal cells) provides a survival advantage to CLL cells (Kurtova et al. 2009). CLL cells, in contact with stroma, showed increased expression of BCL-2 family of anti-apoptotic proteins (Patel et al. 2014). In this way they derive protection from both spontaneous as well as drug-induced apoptosis. Previous investigations from our group established that short-term (24 hours or less) interaction of CLL cells with stromal cells increased the transcription and translation rate of the CLL cells, including the transcription of early response genes such as MCL-1 (Balakrishnan et al. 2014). This expansion in macromolecule synthesis was without an increase in CLL cell replication, which remained inert.

CLL cells respond to the surrounding microenvironment *in vivo* by the activation of specific signaling pathways in the tumor cells mediated by direct cell to cell contact or secretion of soluble factors. The B-cell receptor (BCR) and CD19 pathways in parallel, are pivotal for survival and maintenance of CLL B cells, and are activated by microenvironmental factors (Herman et al. 2011, Cui et al. 2014). Cells in the microenvironment can be broadly classified into macrophages, fibroblasts, T cells, nurse-like cells (modified dendritic cells). Crosstalk between these cells promotes CLL cell trafficking, survival and proliferation (Herishanu et al. 2011).

SDF-1 (Stroma derived factor-1), BAFF (B cell activating factor), APRIL and CD40 are some cytokines secreted by the microenvironment that promote CLL cell survival and protect against spontaneous and drug induced apoptosis. The SDF-1 –CXCR-4 axis has been widely studied and is linked to prolonged survival of CLL B-cells (Burger et al. 1999, Barretina et al. 2003). SDF-1 is important for tissue relocalization and is necessary for the cross talk between stromal cells and CLL cells. BAFF and APRIL are necessary for B cell survival (Nishio et al. 2005).

Topographic interactions of CLL cells are dynamic as they shuttle amidst bone marrow, lymph node and blood. They come in contact with stroma cells in the first two compartments. CLL-stroma interactions can potentially rewire the metabolic pathways in these cells. CLL cells have strong binding affinity to stroma cells. In fact, some of the CLL cells migrate beneath the stromal cells, a process known as ‘pseudoemperipolesis’(Burger et al. 1999). In this way they derive protection from both spontaneous as well as drug-induced apoptosis. NK.Tert, HS-5 (human bone marrow derived stromal cells) and M2-10B4 cells

(derived from mouse) are well established cell lines that have been used to mimic the stromal microenvironment *in vivo*.

ATP generating pathways

There is overall increase in energy demand in malignant cells including CLL cells for survival and sustenance of homeostatic processes (Vander Heiden et al. 2009). The efficient pathway for generating cellular ATP is mitochondrial oxidative phosphorylation (OxPhos) in a normal functional cell, whereas, glycolysis is used to generate ATP under hypoxic conditions. However, in most solid cancers, cells exhibit increased glycolysis with production of lactate, even in normoxic condition a phenomenon termed 'aerobic glycolysis or 'Warburg effect'. This rewiring was initially thought to be a result of mitochondrial dysfunction in cancer cells. However, studies show that mitochondria are still functional in cancer cells and generate ATP (DeBerardinis et al. 2008, Ward and Thompson 2012). Recent studies demonstrate that cells rely on glycolysis even when the mitochondria in the cells are functional (Hsu and Sabatini 2008, Koppenol et al. 2011, Lim et al. 2011). Certain cancer cells get addicted to a particular substrate to fuel metabolic pathways (Glycolysis, OxPhos, TCA cycle and Pentose Phosphate Pathway). Flux from the metabolic pathways also provides biosynthetic precursors other than ATP. Therefore, understanding how these metabolic flux changes as CLL cells come in contact with the microenvironment is of primary importance.

Under normal conditions, glucose is converted to pyruvate via a multistep process and the latter is fed into tricarboxylic acid cycle (TCA). This process is termed as glycolysis (Figure 1). In the absence of oxygen, pyruvate gets converted to lactate and produces only 2

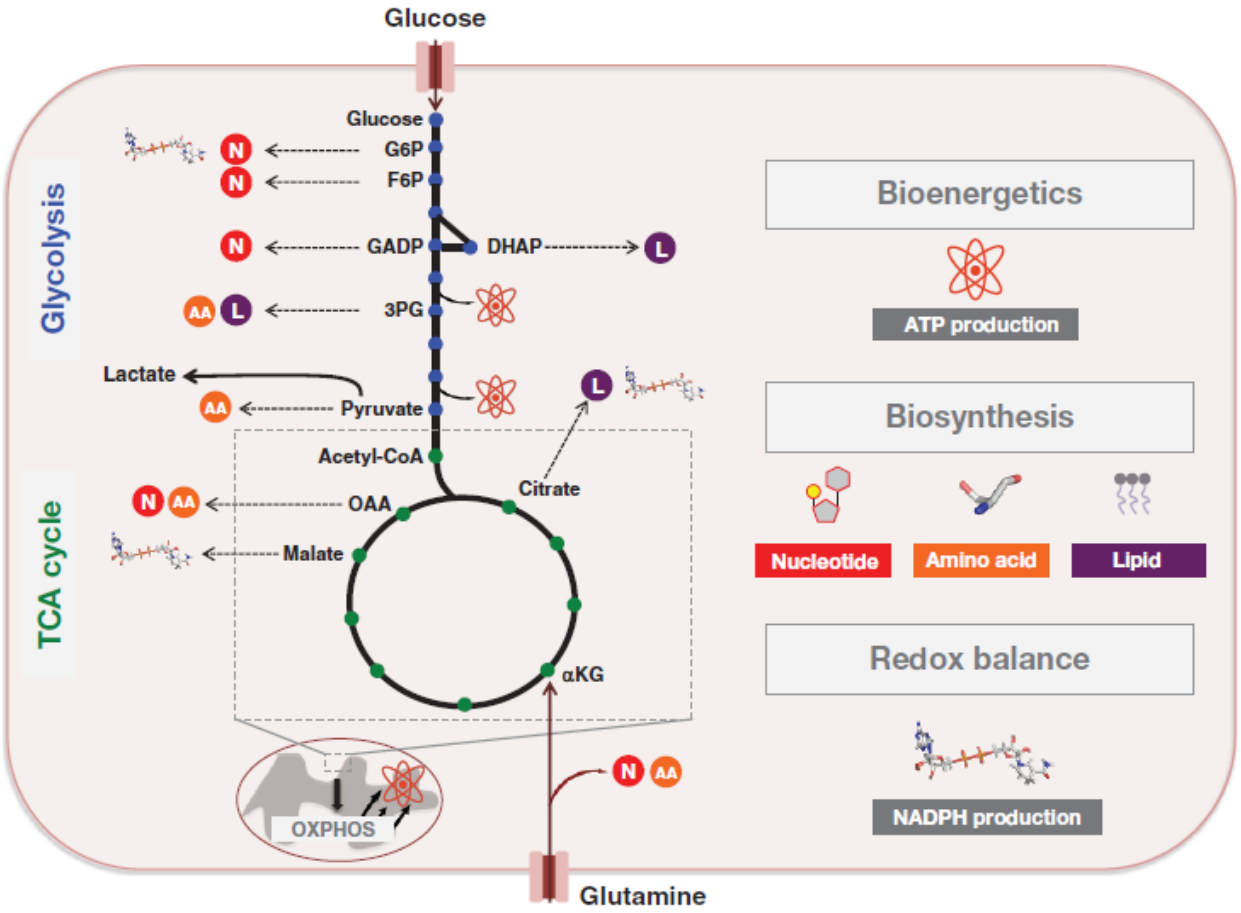

Cantor JR, Sabatini DM, Cancer cell metabolism: one hallmark, many faces. Cancer Discovery 2012. Used with permission. Copyright License Number 3762030060159

Figure 1. Schematic of the interconnection between metabolic pathways and byproducts in the cell.

Glucose taken up by the cell undergoes a series of reactions to produce pyruvate which enters the Tricarboxylic acid cycle (TCA) cycle as Acetyl CoA. Pyruvate can also be converted to lactic acid. This process is termed glycolysis. As an end product, glycolysis yields 2 molecules of ATP. The intermediate products from glycolysis are utilized in macromolecule biosynthesis. Glutamine taken up by the cell is converted to α-ketoglutarate in the TCA cycle. TCA cycle intermediates are also utilized in nucleotide, amino acid and lipid biosynthesis. The TCA cycle occurs in the mitochondrial matrix and provides the precursor NADH for the electron transport chain. Through a series of oxidation and reduction reactions in the electron transport chain, ADP is phosphorylated to form ATP. This process is termed 'Oxidative Phosphorylation'. G6P- glucose 6 phosphate, F6P- fructose 6 phosphate, GADP- glyceraldehyde 3-phosphate dehydrogenase, 3PG- 1,3 bisphosphoglycerate, OAA- oxaloacetate, α-KG- α-ketoglutarate.

ATP molecules per glucose utilized. In cancer, due to hypoxic conditions, cells produce increasing amounts of lactic acid via glycolysis. The rate of glycolysis within a cell can be measured using lactic acid production via pH measurement. The intermediates from glycolysis are utilized by pentose phosphate pathway, nucleotide synthesis and TCA cycle. The NADH generated by the TCA cycle feeds into Oxidative Phosphorylation (OxPhos) pathway.

The electron transport chain (ETC) consists of five complexes that reside in the mitochondrial membrane (Figure 2). ETC maintains the proton gradient and contributes to ATP synthesis (Mitchell 1961). NADH is an electron donor and oxygen is an acceptor. Complex I oxidizes NADH to NAD, and complex II oxidizes FADH to FAD and the electrons are accepted by oxygen at complex IV, which is then reduced to water. In this way, through a series of oxidation and reduction reactions, an electrochemical gradient is maintained as the electrons are pumped out of the intermembrane space to the cytoplasm. At complex V (F_1F_0 ATP synthase), the protons (H^+) are allowed to flow back from mitochondrial matrix to the cytosol energetically favoring ADP and phosphate reaction to form ATP. OxPhos can be measured by the amount of oxygen consumed by the ETC to generate 36 moles of ATP.

Glucose provides the source of carbons for bioenergetics and biosynthesis of macromolecules. Similarly, glutamine is the most abundant amino acid. Not only is it essential for protein translation, it acts as a nitrogen donor for nucleotide and amino acid synthesis, and for protein translation (Wise and Thompson 2010). Glutamine also supplies carbon for biosynthesis. Cancer cells often get addicted and become heavily dependent on one of these sources beyond the extent of meeting the energy demands.

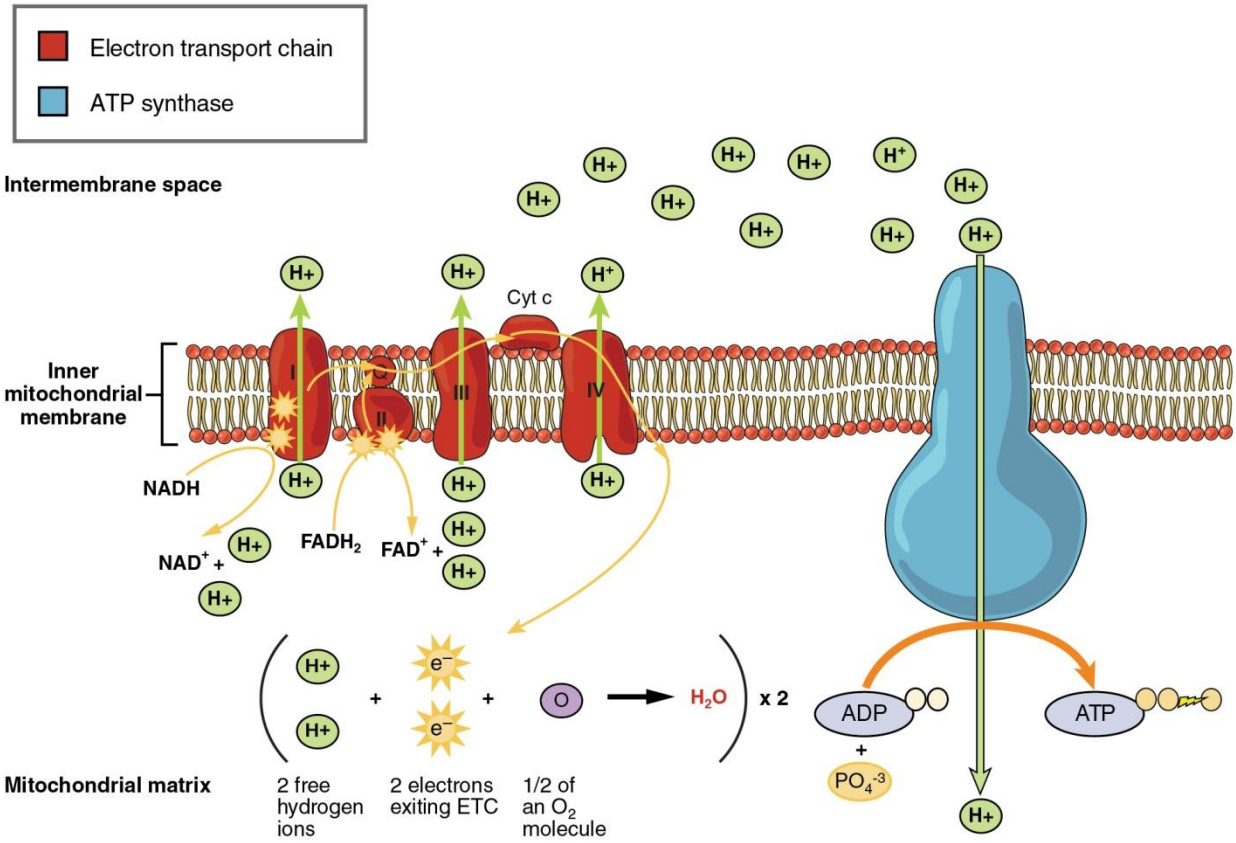

Taken from Wikimedia Commons

Figure 2. Schematic of mitochondrial electron transport chain.

There are five complexes embedded in the inner mitochondrial membrane of the electron transport chain. Electrons are transported from nicotinamide adenine dinucleotide (NADH) to complex I, while NADH is oxidized to NAD^+. Similarly, electrons are transferred from flavin adenine nicotinamide (FADH) to complex II. This electron transfer creates an electrochemical gradient by causing efflux of protons. These protons enter the mitochondrial matrix via complex V or ATP synthase, by causing changes in configuration of the proton pump, leading to phosphorylation of ADP to ATP.

The dynamic nature of CLL makes it more difficult to determine its metabolic phenotype as it changes with the context. My study explores the metabolic phenotype of CLL in suspension and in contact with stromal microenvironment.

B cell Receptor Pathway (BCR)

The BCR pathway activation is directly linked to CLL pathogenesis (Ghia et al. 2008). BCR has an immunoglobulin (IgM) bound to a heterodimer CD79 (α, β). When an extrinsic signal/antigen stimulates the dimerization of IgM and CD79 (α, β), the dimerized complex is phosphorylated by the SRC kinases, LYN and SYK, which in turn activates a signalosome including second messengers, non-receptor tyrosine kinase, BTK, adaptor protein, GRB2, and guanine nucleotide exchange factor, VAV. Along with co-stimulatory molecules such as CD19, the signal gets amplified and activates several downstream effectors including phosphoinositide 3-kinase (PI3K) (Woyach et al. 2012) (Figure 3). When PI3K is activated, the p85 subunit forms a complex with CD19 which further activates the p110 subunit, resulting in phosphorylation of phosphatidylinositol 4, 5-bisphosphate (PIP2) to PIP3. Upon formation of PIP3, AKT is activated (Vanhaesebroeck et al. 2001, Cantley 2002, Foster et al. 2003). BCR also activates mitogen activated protein kinase (MAPK) which controls cell survival and proliferation. By sequential phosphorylation of messengers, BCR activates transcription factors, MYC, NF-κB and NFAT.

The B cell receptor also mediates cell adhesion by 'inside out' signaling via integrins. Due to intrinsic signals BCR activates integrins leading to a conformational change in the structure of the latter, resulting in adhesion or migration. Activation of LYN, PI3K, BTK,

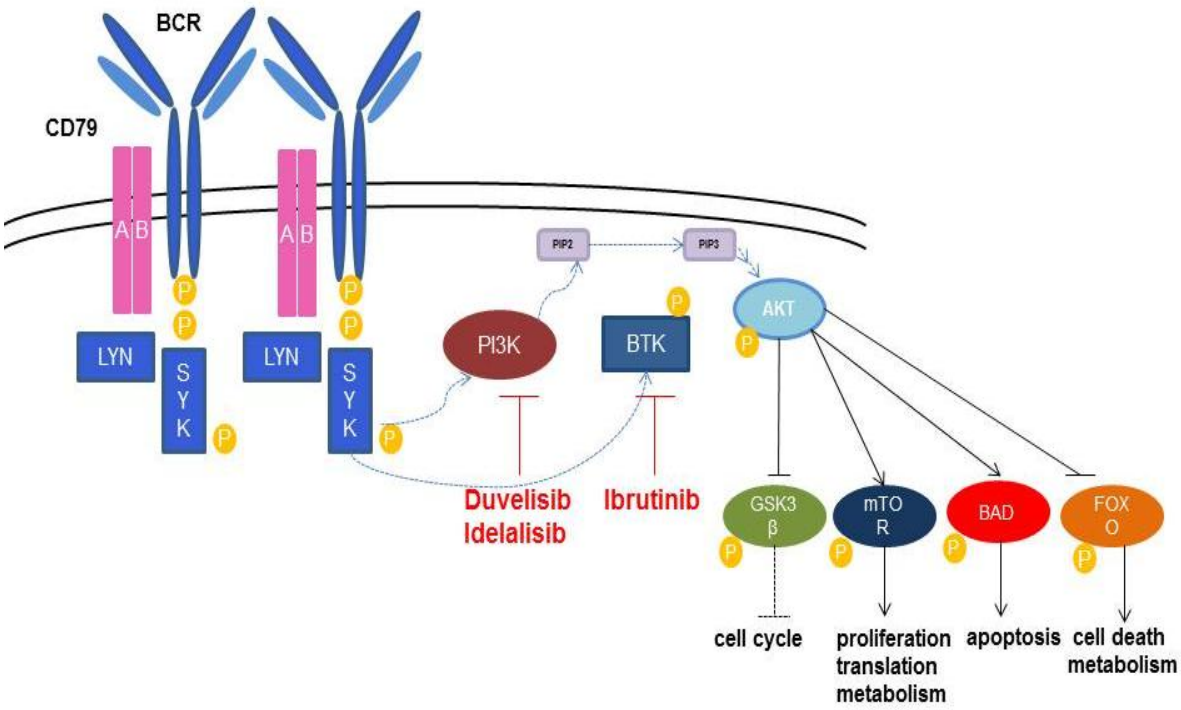

Figure 3: B cell receptor pathway in chronic lymphocytic leukemia.

B cell receptor upon encountering an antigen, gets activated. CD79 (α, β) gets phosphorylated by SRC kinases, LYN and SYK, which in turn activates a signalosome including BTK, GRB2, VAV etc., Along with CD19, BCR recruits PI3K to the membrane, where the latter phosphorylates PIP2 to PIP3, that activates AKT. AKT signals to its downstream effectors, GSK3β (cell cycle, glucose metabolism), mTOR (translation, metabolism and proliferation), BAD (apoptosis, cell survival) and FOXO (cell death, metabolism).

and PLC-γ are responsible for 'inside out' signaling through integrins (Spaargaren et al. 2003).

In spite of its prominence in regulating various signaling pathways, the surface expression of BCR relatively low in CLL for unknown reasons (Vuillier et al. 2005).

PI3K/AKT axis

A primary node in the BCR pathway is the PI3K/AKT pathway, which promotes downstream activation of survival factors in CLL cells (Figure 3). An additional survival axis is initiated from the CD19 receptor, which also cascades through PI3K. PI3K serves a myriad of functions including cell survival, proliferation, differentiation, chemotaxis, metabolism, apoptosis and cytoskeletal reorganization. As mentioned previously, PI3K converts PIP2 to PIP3 and this reaction can be reversed by a phosphatase, PTEN, dephosphorylates and converts PIP3 back to PIP2. SRC homology 2- containing inositol 5' phosphatase (SHIP) has a similar role and decreases PIP3 levels upon engagement with FcγRIIB1 (Ono et al. 1996).

There are 4 class I isoforms of PI3K, α, β, γ and δ. While the α and β isoforms of PI3K are ubiquitously expressed, the δ and γ isoforms are majorly found in leukocytes (Vanhaesebroeck et al. 1997, Sawyer et al. 2003). PI3K α has been shown to regulate cellular metabolism, insulin signaling and angiogenesis in solid tumors, whereas the β isoform has been found to be active in platelets (Hamada et al. 2005, Zhao et al. 2006, Yuan et al. 2008, Kim et al. 2009).

The PI3K α and β are essential in mice. Their deletion in mice leads to embryonic lethality (Bi et al. 1999, Bi et al. 2002).

PI3K γ knockout mice are viable; however, they display a decreased number of splenic T cells and impaired T cell function along with decrease in cytokine production (Hirsch et al. 2000, Li et al. 2000, Sasaki et al. 2000). Immune cells that lack δ isoform (in knockout mice), display impaired immune responses and chemotaxis and reduced immunoglobulin production (Clayton et al. 2002).

The PI3K γ and δ isoforms are overexpressed in CLL and have non-overlapping functions**.** The gamma isoform signaling confers immune tolerance and cell migration capacity to CLL cells and is also necessary for eliciting responses from T cells (Alcazar et al. 2007), whereas the delta isoform mediates cell proliferation and differentiation. The expression levels of the delta isoform increases upon contact with the microenvironment.

Based on the structure of the PI3K class I molecule, they are divided into two subtypes, class IA and class IB. The class IA consists of one of the catalytic subunits isoforms, p110α, β or δ which pairs with regulatory subunit of PI3K, p85. Class IB uniquely is made up of a catalytic subunit p110γ that associates with regulatory subunit p101 and p84 (Stephens et al. 1997) (Figure 4).

p110 α is commonly mutated in solid cancers and harbors hotspots, whereas, the mutation frequency in other isoforms it is still not clear. However, overexpression of δ and γ isoforms was reported in hematological malignancies, brain and colorectal cancers (Skorski et al. 1997, Benistant et al. 2000, Mizoguchi et al. 2004, Sujobert et al. 2005, Hickey and Cotter 2006). PI3K delta becomes activated by binding of ligands to tyrosine kinase receptors or BCR crosslinking.

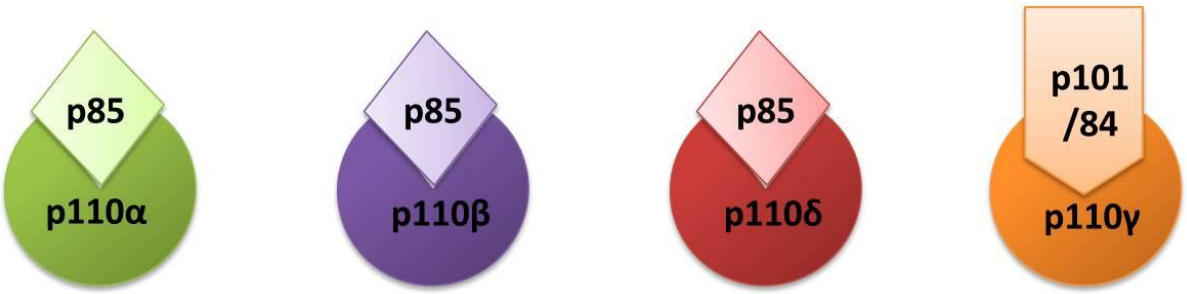

Class IA	Class IA	Class IA	Class IB
Coded by PIK3CA	Coded by PIK3CB	Coded by PIK3CD	Coded by PIK3CG
Ubiquitously expressed	Ubiquitously expressed	Leukocytes	Leukocytes
Proliferation, metabolism	Platelet activation	Survival, chemotaxis, proliferation	Immune response

Figure 4. PI3K class I isoforms and their characteristics

Classically, PI3K signaling is associated with AKT activation. AKT is activated upon translocation to the plasma membrane when it is recruited by PIP3 (via PH domain) and phosphorylated at Thr308 by PDK1 (phosphoinositide-dependent protein kinase-1). AKT promotes cell survival by phosphorylating and inactivating BAD, a member of pro-apoptotic machinery. BAD otherwise dimerizes with BCL-XL, an anti-apoptotic protein and renders it non-functional (Datta et al. 1997). Similarly, it phosphorylates and inactivates FOXO preventing its nuclear translocation (Brunet et al. 1999). Several FOXO target genes are members of pro-apoptotic machinery (BIM, FAS) and cell cycle inhibitors (p21, p27). Therefore AKT consequently inhibits their transcription. AKT also promotes cell proliferation by phosphorylating GSK3β, hampering its kinase activity, which in turn cannot phosphorylate cyclin D1 and renders it functional (Diehl et al. 1998).

AKT has three different isoforms, encoded by the genes *AKT1*, *AKT2* and *AKT3*. AKT 1 and 2 isoforms are ubiquitously expressed and AKT 3 is expressed predominantly in brain and testes (Yang et al. 2003). AKT 1 is vital for CLL cell survival (Hofbauer et al. 2015). AKT is also used as a surrogate marker for response to treatment in CLL . Phospho-AKT levels decline with various targeted therapies including with PI3K inhibitors.

PI3K/AKT downstream metabolic effectors

Several investigations have established that the PI3K alpha–mediated signaling cascade influences cellular metabolomics, including glycolysis and energy production (Engelman et al. 2006). Recent studies further demonstrated a role for AKT in this pathway. AKT-independent signaling is also involved in activation of cellular metabolomics (Hahn-

Windgassen et al. 2005, Arvisais et al. 2006). However, the role of PI3K delta/gamma in regulating metabolomics has not been elucidated.

Activation of AKT is linked to increased glycolysis in cancer cells. Phosphorylation of AKT at Ser473 promotes glucose uptake by mobilizing glucose transporters (GLUT4) to the cell membrane (via AS160 activation) (Jiang et al. 2003, Sano et al. 2003) as well as its utilization (Kohn et al. 1996). Insulin mediated glucose uptake is largely mediated by AKT2 (Whiteman et al. 2002). AKT also regulates hexokinase and phosphofructokinase activity, two of the ten enzymes critical in the glycolysis pathway (Deprez et al. 1997, Gottlob et al. 2001, Rathmell et al. 2003). Recently, PI3K was implicated in regulating Aldolase mobilization from the cytoskeleton and enhance glycolysis, in an AKT independent manner (Hu et al. 2016). Aldolase is a key enzyme in glycolysis that converts Fructose 1,6 bisphosphate into dihydroxyacetone phosphate and glyceraldehyde 3-phosphate.

Although the mechanism remains unknown, mitigation of PI3K activities lead to decrease in mitochondrial respiration in cancer cells leading to hypoxia (Kelly et al. 2014). Another study demonstrated that inhibition of PI3K/AKT pathway diminished oxygen consumption in head and neck cancers by phosphorylation and subsequent inhibition of pyruvate dehydrogenase activity (Cerniglia et al. 2015). Active AKT was also reported to translocate to mitochondria and phosphorylate ATP synthase along with other mitochondrial resident proteins, thereby resulting in upregulation of mitochondrial respiration in immortalized hepatocytes (Li et al. 2013).

The PI3K/AKT pathway cross talks with mTOR **(**mammalian target of rapamycin), a master regulator of cellular metabolism. mTOR activity is highly augmented in cancer cells

(Laplante and Sabatini 2012). mTOR has been shown to mediate mitochondrial oxidative phosphorylation by hexokinase inhibition in epithelial cancers (Lu et al. 2015).

Targeted therapy in CLL

The microenvironment in CLL simulates constitutive activation of BCR and PI3K pathways (Cuni et al. 2004, Burger and Chiorazzi 2013) Therefore, inhibiting these pathways might be an effective anti-cancer strategy for CLL patients. Recently, two targeted agents were approved for CLL. Ibrutinib, which targets BTK, was approved in 2014 by the FDA. The second drug that was approved for CLL treatment was idelalisib, a PI3K δ isoform specific inhibitor. Selective targeting of PI3K pathway is essential because pan-PI3K inhibition using Wortmannin and LY294002 results in adverse effects, as α and β isoforms are expressed in all cells.

Duvelisib (IPI-145)

Duvelisib is an orally available PI3K class I δ/γ inhibitor that is in Phase III clinical trials for CLL as a monotherapy. It is also being tested in combination with rituximab and bendamustine as for follicular and non-Hodgkin's lymphomas (NCT02576275, www.clinicaltrials.gov). It prevents the activation of PI3K δ/γ isoforms by binding competitively and reversibly to the p110 ATP binding site of the isoforms. It inhibits the δ/γ isoforms with an IC_{50} of 1/50 nM and Ki value is 23/243 pM. It inhibits adaptive and innate immune responses (Winkler et al. 2013). Therefore, it is used for the treatment of autoimmune and inflammatory diseases. Studies have demonstrated that duvelisib diminishes PI3K signal transduction via blocking the AKT pathway. However, its effect on cellular metabolism has not been investigated. Inhibition of both δ/γ isoforms is much more effective

than inhibition of delta alone (Subramaniam et al. 2012)**.** Both duvelisib and idelalisib are very similar in structure (Figure 5).

Duvelisib treatment *in vitro* has been shown to inhibit CCL3, CCL4 secretion from CLL cells and prevent migration of CLL cells beneath the stroma cells. It was also shown to inhibit CLL proliferation induced by CD40-IL2-IL-10. Importantly, this drug also overcomes acquired resistance to ibrutinib that occurs after monotherapy due to acquired BTK missense mutation at cysteine to serine 481 residue located in the catalytic domain. Duvelisib also inhibits IL2, TNF-α and IFN-γ secretion by T cells (Dong et al. 2014).

Idelalisib (GS 1101)

Idelalisib is a selective inhibitor of PI3K p110 δ used to treat refractory/relapsed CLL and follicular lymphoma treatment. Idelalisib was first approved for clinical use as first line treatment for CLL by the FDA in 2014. It was highly successful in clinical trials for CLL and indolent lymphomas (Fruman and Cantley 2014, Gopal et al. 2014). The IC_{50} of idelalisib for the δ isoform is 19 nM and the Ki value is 1pM; for the α, β, γ isoforms, the IC50 is 8600, 4000, 2100 and the Ki value is 453, 211 and 110pM. Idelalisib treatment results in inhibition of PI3K downstream signaling cascade. It also forces the CLL cells out of the lymph node into blood circulation leading to lymphocytosis (Herman et al. 2010). Similar to duvelisib, idelalisib also alters cytokine production from T cells and NK cells. It also induced apoptosis in the presence of protective microenvironmental factors like BAFF, TNF-α, and fibronectin (Herman et al. 2010). Idelalisib was used along with bendamustine and rituximab in a phase III clinical trial on 416 patients with relapsed CLL and lead to prolonged progression free survival of 23 months compared with 11 months on bendamustine and rituximab

combination only. Therefore, the combination of these drugs emerged as a new treatment option for patient with relapsed or refractory CLL.

MK2206

MK2206 is an allosteric pan AKT inhibitor (Hirai et al. 2010)**.** It binds to AKT in a non-ATP competitive manner.MK2206 is used in combination therapy for treating advanced solid tumors. Its IC_{50} values for isoforms AKT1, AKT2 and AKT3 are 8, 12 and 65 nM respectively.MK2206 is currently in Phase I and II clinical trials as a combination therapy agent for CLL along with bendamustine and rituximab for CLL and small B cell lymphocytic leukemia and for non-small cell lung and pancreatic cancers (www.clinicaltrials.gov). MK2206 achieved promising results when tested in combination with erlotinib, lapatinib as well as docitaxel and carboplatin against human cancer cell lines (Hirai et al. 2010).

MK2206, when used in combination with bendamustine, in clinical trials evoked a positive response from patients. Single dosage of MK2206 decreased cytokine production, mobilized lymphocytes out of the lymph nodes, and lead to an inhibition of AKT activity by decreasing phosphorylation at Ser473 residue (Ding et al. 2014). It induces caspase mediated apoptosis. It also decreases MCL-1 protein levels and increased PARP cleavage indicating apoptosis.

Duvelisib

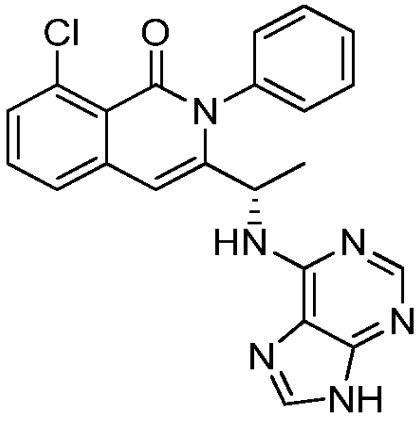

Chemical name: 8-chloro-2-phenyl-3-[(1S)-1-(7H-purin-6-ylamino)ethyl]isoquinolin-1-one

Idelalisib

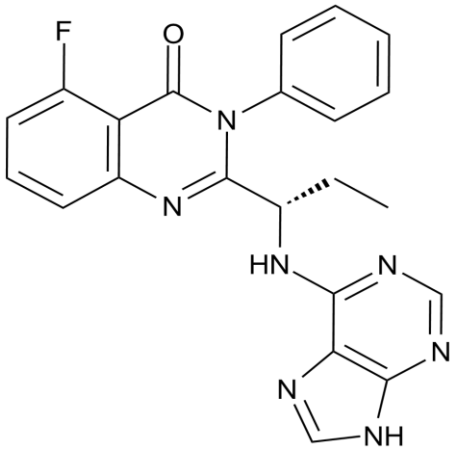

Chemical name: 5-fluoro-3-phenyl-2-[(S)-1-(9H-purin-6-ylamino)-propyl]-3H-quinazolin-4-one

MK2206

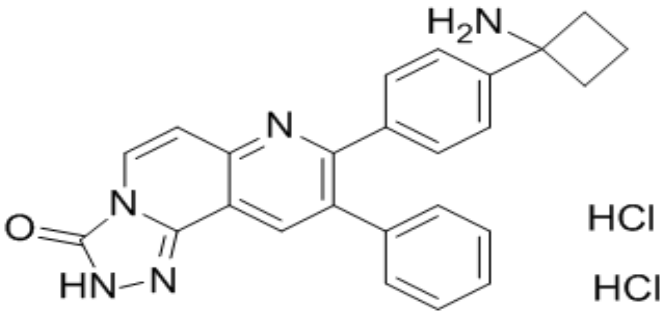

Chemical name: 8-[4-(1-aminocyclobutyl)phenyl]-9-phenyl-2H-[1,2,4]triazolo[3,4-f][1,6]naphthyridin-3-one

Figure 5. Chemical structure of PI3K and AKT inhibitors.

Hypothesis & Aims

Although CLL cells are quiescent, transcription and translation processes are active in these cells. Microenvironment provides survival advantage to CLL cells. Stroma cell lines derived from human bone marrow mimic the microenvironment. Interaction with stroma activates B cell receptor pathway, where PI3K is an active node. PI3K is an important regulator of cellular metabolism. Global RNA synthesis and protein synthesis increase in CLL upon interaction with stroma.

Based on this background, and existing knowledge of CLL-stroma interactions, I hypothesize that stroma interaction upregulates metabolism in CLL lymphocytes through a mechanism involving PI3K pathway. CLL lymphocytes are metabolically active and may show different metabolic profiles that are in line with the aggressiveness of the disease based on prognostic markers. Changes in metabolomics should enhance the nucleotide biosynthesis needed for increased gene transcription. In accordance with these expectations, pharmacological intervention in this pathway is expected to inhibit metabolic changes and reduce the survival of CLL cells.

Aim 1: Elucidate the bioenergetics profile of primary CLL cells peripheral blood lymphocytes, encompassing two major energy (ATP) generating pathways, glycolysis and mitochondrial oxidative phosphorylation (OxPhos) and determine the relationship to CLL prognostic factors.

Aim 2. Determine the impact of stroma on energy generating pathways, oxidative phosphorylation and glycolysis in primary CLL cells.

Aim 3. Delineate the role of PI3K pathway in induction of glycolysis and OxPhos in CLL cells.

CHAPTER 2. Materials and Methods

Patient sample collection

Peripheral blood samples were collected from 107 CLL patients. All patients had given written informed consent in accordance with the Declaration of Helsinki and under a protocol approved by the Institutional Review Board of The University of Texas MD Anderson Cancer Center. All experiments were performed using freshly-isolated CLL cells from peripheral blood samples. Purity of B cell population is 95% or higher determined by CD19 and CD5 double positive staining. Patient characteristics are summarized in Table 1.

Isolation of CLL cells

Peripheral blood mononuclear cells (PBMCs) were isolated using Ficoll Hypaque density gradient centrifugation method (Atlanta Biologicals, Norcross, GA). Blood collected in 20 mL heparinized tubes was centrifuged for 10 min at 20ºC. The top layer of plasma was removed and the blood was diluted at a ratio of 1:3 with 1X phosphate-buffered saline (PBS) and carefully layered over 10 mL of Ficoll in a 50mL conical tube. The tube was centrifuged at 1500rpm for 20 min at 20ºC. The mononuclear cells at the interphase were gently removed and washed twice with 1X PBS. Cell counts were taken using Beckham Coulter counter and cells were resuspended in RPMI 1640 supplemented with L-glutamine and 10% Human Serum. Cells were cultured at a density of $1x10^7$ cells/mL. All experiments were performed using freshly isolated CLL cells from peripheral blood samples; purity of this cell population was ≥95%.

PBMCs from healthy donors were isolated using the Ficoll technique as described above.

Pt #	Age	Sex	# Prior Rx	WBC	% LYM	β2M	LDH	RAI	ZAP	IgVH	CD38	Cytogenetics
3	58	F	0	114.8	94	3.6	876	4	Pos	UN	86	2011: 46,XX[20]
4	61	M	0	183.1	97	3.1	516	1	Neg	MU	1.3	53,XY,+6,+7,+11,+15,+18,+19,+20[1]/46,XY[19]
5	72	M	0	50.5	89	2.8	515	1	np	MU	NA	not performed
6	46	M	3	172.6	89	np	956	4	Pos	UN	43	not performed
7	89	F	0	14.8	91	3.1	387	3	np	MU	NA	not performed
8	55	F	0	71.8	92	1.7	562	1	Pos	NR	NA	not performed
9	51	M	0	132	83	2.6	563	1	Pos	UN	26	45,X,add(Y)(q12),t(1;3)(p36.3;q21),-19[1]/48,XY,+X,-2,+3,+5,+6,+11,+12,-15,-16,-22[1]/46,XY[18]
10	53	F	0	124.9	85	1.4	512	1	Pos	UN	NA	46,XX[20]
11	62	M	0	92.7	90	2.7	591	1	Pos	UN	58	46,XY,add(18)(q23)[8]/46,XY[12]
12	62	F	0	160.3	93	2.2	511	0	Neg	MU	Neg	not performed
13	50	F	0	21.8	70	1	426	1	Pos	MU	NA	not performed
14	77	M	1	70	95	4.4	429	1	Neg	NR	NA	2005: 46,XY[20]
15	51	F	1	76.7	97	4.2	1238	4	Pos	UN	19.3	46,XX,del(20)(q11.2q13.1)[8]/47,XX,del(11)(q13q22),+12[2]/47,XX,del(11)(q13q22),+12,-17,+mar[1]/47,XX,del(9)(q22q34),del(11)(q13q22),+12,add(13)(q34),-17,+mar[2]/46,X,add(X)(p22.1),t(1;5)(p13;q13),-4,-11,+12,-17,-22,+3mar[2]/46,XX[5]
16	53	F	0	34.4	93	2.5	383	0	Pos	MU	NA	46,XX,del(13)(q12q14)[3]/46,XX[17]
17	72	M	1	74.6	96	3.9	521	4	Pos	MU	NA	46,XY[20]
18	71	M	0	12.2	41	2.7	498	1	Pos	np	NA	45,X,-Y[8]/46,XY,del(11)(q22)[1]/46,XY[11]
19	54	M	0	27.7	56	1.9	289	3	Pos	UN	18.8	46,XY[20]
20	54	F	0	102.6	94	1.9	605	0	Pos	UN	5.4	No mitotic cells recovered
21	60	M	0	76.2	88	1.5	771	4	Neg	NR	15	46,XY[20]
22	64	F	0	281.	92	2.6	746	1	Neg	MU	NA	2002: 46,XX[20]

				5								
23	69	F	2	24	95	3.1	553	0	NR	Neg	NA	not performed
24	61	M	0	70.9	83	7	975	4	Pos	UN	21	42~46,X,-Y,del(2)(q32),del(11)(q23),del(17)(p13.1),+0~2mar[cp10]/46,XY[8]
25	65	M	0	33.7	84	2.5	512	1	np	np	NA	not performed
27	53	M	0	57.4	84	1.7	525	1	Pos	MU	NA	not performed
28	76	F	3	200.5	87	4.9	691	3	Pos	UN	NA	not performed
29	44	F	0	92	76	2	1417	0	Neg	UN	NA	not performed
30	51	F	1	26.3	83	4.4	886	2	Pos	UN	19.5	46,XX,del(20)(q11.2q13.1)[9]/47~48,XX,del(11)(q13q22),+12,-17,+1~2mar[cp3]/
31	79	F	0	104.5	90	2.9	609	2	Pos	UN	0.2	45,XX,del(13)(q12q14),-19[1]/45,X,-X,t(10;20;12)(q21;q13.3;q13)[1]/46,XX[18]
32	70	M	3	89.3	93	2.5	495	1	Neg	UN	23.4	46,XY,der(1;10)(p10;p10)[1]/46,XY,del(11)(q13q23)[1]/46,XY[18]
33	59	M	1	131.4	98	3.1	636	1	np	UN	NA	not performed
34	77	M	3	49.5	86	2.4	578	0	Neg	MU	NA	not performed
35	68	M	2	112.8	87	3.3	571	2	np	UN	NA	not performed
36	61	F	0	25	74	2.2	483	1	Pos	MU	NA	46,XX[20]
37	56	M	1	39.1	89	4.3	440	2	Pos	UN	62.3	45,XY,t(1;8)(q31;q21),-2[1]/46,XY[19]
38	91	M	1	224.9	84	20.8	823	3	Pos	UN	83.9	not performed
39	68	M	1	241.5	94	4.1	953	1	Pos	NR	17.8	45,X,-Y[5]/46,XY,del(11)(q21q23)[2]/45~47,XY,del(11)(q21q23),del(13)(q12q32),der(19)t(4;19)(q21;q13.3)[cp7]/46,XY[8]
40	70	M	3	96.1	95	3	550	1	Neg	UN	NA	46,XY,der(1;10)(p10;p10)[1]/46,XY,del(11)(q13q23)[1]/46,XY[18]
41	62	F	0	15.6	84	7.4	845	4	Pos	UN	84.2	44,XX,add(7)(q36),-9,del(13)(q12q32),der(17;18)(q10;q10)[3]/44,idem,add(15)(p11.2)[2]/44,idem,add(22)(p11.2)[3]/46,XX[12]
42	66	M	0	45	87	2.8	554	1	Neg	NR	NA	46,XY[20]
43	83	M	0	20.7	70	2	434	0	Neg	MU	NA	not performed

44	70	F	0	95.9	78	2.8	467	0	Neg	MU	NA	No analyzable metaphases recovered
45	64	F	6	64.9	90	1.6	770	4	Pos	NR	NA	not performed
46	62	F	0	31.2	89	2.1	538	0	np	MU	NA	No mitotic cells recovered
47	61	M	0	30	52	2.1	501	0	Neg	MU	NA	46,XY[20]
48	66	F	1	75.5	85	5.7	554	4	Pos	UN	0.7	39,X,-X,-7,add(8)(p23),-9,-20,-21,-21,-22,-22,+mar[1]/44,XX,add(1)(p36.1),del(2)(p13),-16,add(17)(p13),-18[1]/45,XX,t(5;17)(q31;p13),del(6)(q21),-20[1]/46,XX,add(6)(p21),add(14)(q32)[1]/46,XX[16]
49	83	F	4	52.9	85	3.7	2067	0	Pos	UN	47	47,XX,+12[19]/46,XX[1]
51	68	F	1	34.6	90	1.8	np	0	Neg	MU	1.5	not performed
52	59	F	0	72.3	88	2	741	1	Pos	UN	1.7	47,XX,i(7)(q10),+12[16]/46,XX,i(7)(q10)[cp2]/46,XX[2]
54	49	M	1	43.4	89	2.2	np	4	Neg	UN	3.5	not performed
55	54	M	0	43.9	73	2.1	448	1	Pos	UN	NA	not performed
56	71	M	0	32.4	72	2.2	518	1	Neg	MU	NA	not performed
57	53	M	0	32.9	75	2	387	1	Neg	MU	NA	No mitotic cells recovered
59	61	F	0	62.3	91	2.4	660	1	Neg	MU	NA	46,XX[20]
60	67	F	0	36.8	89	1.6	479	1	Pos	NR	69	46,XX[20]
61	76	F	2	107.2	83	3.9	ND	1	ND	UM	3	not performed
63	53	M	1	42.5	85	1.4	578	4	Neg	UN	3.5	46,XY[20]
64	74	F	1	125	92	3	462	2	Neg	UN	0.2	not performed
65	56	F	0	113.3	86	3.4	430	2	Neg	MU	NA	not performed
67	65	M	1	123.8	91	3.7	687	4	Pos	NR	NA	not performed
69	84	M	1	36.6	92	np	367	1	np	NR	NA	not performed
70	65	F	1	140.2	95	3.3	514	1	Neg	MU	NA	46,XX[20]
73	57	M	0	82	89	4.1	712	4	Pos	UN	85.6	45,XY,-9,der(15)t(13;15)(q22;p11.2),add(17)(p11.2),+mar[1]/45,idem,t(8;9)(q24;q22),

												t(12;16)(q13;q24)[6]/46,XY,del(3)(q21)[1]/46,Y,-X,add(9)(q22),+mar[1]/46,XY[11]
74	78	M	0	27.6	89	np	436	4	Pos	MU	NA	46,XY[20]
75	75	F	0	120.5	91	3.5	379	3	Pos	MU	0.9	46,XX[11]
76	83	F	4	77.1	87	3.9	2087	0	Pos	UN	NA	not performed
81	51	F	0	19.7	76	1.7	504	0	Pos	MU	NA	not performed
83	67	F	0	25.2	84	3.1	572	3	Neg	UN	NA	46,XX[23]
84	69	F	0	127.2	97	3.7	547	1	Pos	UN	1.5	46,XX,t(8;14)(q24.2;q32)[5]/46,XX,t(4;11)(q25;q23)[1]/46,XX[14]
86	68	M	0	111.9	90	3.8	963	0	Pos	UN	NA	47,XY,+12[6]/46,XY[14]
88	48	M	0	46.1	89	1.4	440	0	np	MU	NA	not performed
89	70	F	0	30.1	82	4.1	720	0	Neg	MU	NA	not performed
91	37	F	0	45.4	92	1.6	474	0	Neg	MU	NA	not performed
103	64	F	0	19.4	58	2.3	383	0	Neg	MU	NA	46,XX[20]
104	57	M	0	66.5	92	1.9	498	1	Neg	MU	NA	46,XY[20]
105	42	F	2	132.8	79	6.1	795	2	np	UN	NA	not performed
105b	58	M	1	56.6	88	4.3	615	1	Pos	UN	91	45,X,-Y[4]/45~46,XY,+2,i(17)(q10),del(20)(q11.2q13.3)[cp7]/46,XY,t(13;14)(q21;q32)[1]/46,XY[8]
106	65	M	0	32.6	88	2.2	623	0	Neg	MU	NA	47,XY,+12[5]/46,XY[15]
107	47	F	0	23.6	82	2.2	529	0	Neg	MU	NA	not performed
108	56	M	0	32.4	80	1.3	533	0	Neg	MU	NA	46,XY[20]
115	47	M	0	18.3	87	1.6	367	1	Neg	MU	NA	No mitotic cells recovered
112	72	M	0	55	89	4.3	715	0	Pos	NR	NA	not performed
110	78	M	2	41.9	79	3.8	414	1	Neg	MU	NA	not performed
116	83	F	0	42.8	80	3.2	550	3	np	MU	NA	not performed
118	67	M	1	27.6	81	3.8	481	0	Neg	MU	NA	46,XY[20]

119	43	F	0	23.3	69	2.1	392	0	Neg	UN	NA	46,XX,del(9)(q13),del(11)(q21),+2mar[cp4]/46,XX[16]
117	67	F	0	97.4	97	1.5	556	0	Neg	MU	NA	not performed
120	69	M	2	38.3	91	3.4	558	0	Pos	MU	0.2	48,XY,+12,+19[5]/48,idem,-13,-16,+2mar[1]/46,XY[14]
121	54	M	0	51.3	83	2.7	511	0	Pos	UN	NA	not performed
122	62	M	0	48.5	92	1.8	483	0	Neg	MU	NA	46,XY[20]
123	71	M	0	165.3	89	3.9	475	3	Pos	MU	57	46,XY,del(11)(q13)[cp2]/46,XY[18]
124	76	F	0	141	94	3.3	490	0	Neg	NR	NA	not performed
125	49	M	0	40.4	84	1.7	429	1	Pos	UN	8.9	45,XY,t(2;14)(p12;q32),-11[1]/46,XY[19]
126	66	M	0	16.2	83	4	506	1	Neg	MU	0.6	Insufficient yield of analyzable metaphases/46,XY,t(4;10)(p16;q24)[1]/45,XY,-3,-14,+mar[1]/46,XY[8]
127	71	F	0	49.1	94	2.4	527	2	Neg	MU	NA	not performed
128	56	F	0	106.2	95	3.1	519	4	Pos	UN	54.5	45,XX,-17,der(20)t(17;20)(q21;p13))[5]/46,XX[15]
130	62	M	0	16.9	52	1.7	417	1	Neg	MU	1	46,XY[20]
132	75	F	0	107.4	95	3.7	623	4	Neg	UN	NA	not performed
133	76	F	0	77.3	93	2	567	2	Neg	NR	NA	not performed
134	63	M	0	136.3	93	3.6	785	1	Pos	UN	NA	not performed
135	50	M	1	40.9	91	1.8	486	0	Neg	MU	NA	46,XY[20]
136	63	M	0	55.3	81	2.5	530	0	Pos	UN	NA	46,XY,add(17)(p13)[4]/46,XY[16]

MU=Mutated; np= not performed; NR= Not Reported; UN= Unmutated; NA= not available

Table 1. List of CLL patients and their characteristics.

B cell isolation

Normal B cells were isolated by negative selection using Easy Sep^{TM} human B Cell Enrichment Kit (Stem Cell Technologies, Vancouver, CA).

Cell lines

Stromal cell lines and their culture conditions as well as conditions for Mino and JeKo-1 mantle cell lymphoma cell lines are in Table 2. CLL cells were co-cultured with stromal cell lines in a ratio of 100:1. All cell lines were periodically checked for Mycoplasma contamination using MycoTect kit (Invitrogen, Waltham, MA).

Drugs

Duvelisib (IPI-145) was obtained from Infinity Pharmaceuticals and used at 1 μM concentration to treat cells in all experiments. Idelalisib (GS1101) was obtained from Gilead Sciences and MK-2206 from Selleck Chemicals; 1 μM idelalisib and 2.5 μM MK-2206 were used in the experiments. All compounds were dissolved in 100% DMSO. DMSO-treated cells were used at the same time point as controls.

Cytotoxicity assays

Cells were stained with annexin V/propidium iodide and counted using flow cytometry. $5x10^5$ cells were collected in 5 mL tubes and resuspended in 100 μL of 1X Annexin binding buffer with 5 μL of Annexin –FITC. Samples were incubated in the dark for 15 min at room temperature and 300μL 1X Propidiumiodide buffer (with 1X PBS and 50 μg/mL of PI) was added to the reaction and analyzed by Flow Cytometry (BD Accuri, Franklin Lanes, NJ). 10,000 events per sample were recorded.

Stroma cell line	**Origin**	**Source**	**Culture conditions**
NK-Tert	Human	Dr. Jan Burger, MD Anderson Cancer Center	MEM +10% human serum, 10%FBS, 0.4µg/mL hydrocortisone, 0.1µg/mL 2-Mercaptoethanol(Manshouri et al. 2011)
M2-10B4	Mouse	Dr. Jan Burger, MD Anderson Cancer Center	DMEM +10% FBS
HS-5	Human	ATCC®	DMEM +10% FBS
MCL cell line	**Origin**	**Source**	**Culture conditions**
JeKo-1	Human	Dr. Hesham Amin, MD Anderson Cancer Center	RPMI 1640, 10%FBS
Sp53	Human	Dr. Hesham Amin, MD Anderson Cancer Center	RPMI 1640, 10%FBS
Mino	Human	Dr. Hesham Amin, MD Anderson Cancer Center	ATCC® RPMI 1640, 20%FBS

Table 2. Source of cell lines and culture conditions

Extracellular flux assays

Extracellular flux assays (Seahorse Bioscience, Chicopee, MA) were used to measure the oxygen consumption rate (OCR) and extracellular acidification rate (ECAR) of CLL cells. XF96 wells were coated with Cell Tak solution diluted in sodium bicarbonate buffer and water to enhance adsorption (20.5 µL Cell Tak + 1610 µL 1M sodium bicarbonate + 62 µL distilled molecular biology grade water). Cell Tak solution (17 µL) was used to coat the plate and incubated for 20 min for adsorption to take place at room temperature. Excess Cell Tak was drained and the plate was washed twice with 1X PBS and allowed to dry for 1hr in a laminar flow cabinet. Stromal cells (5×10^3) were first plated on Cell-Tak–coated XF microplates and were allowed to adhere for 4-6 hours. CLL cells (5×10^5) were plated onto the stromal cells in RPMI-1640 + 10% human serum. CLL cells were cultured on 6-well plates, with or without duvelisib for 24 hours. The day before extracellular flux analysis, the assay cartridge was hydrated with 200 µL of XF calibrant overnight at 37ºC in a non-CO_2 incubator. Cells were counted and plated onto XF microplates. RPMI-1640 medium was replaced with XF base (OCR) or glycolysis base (ECAR) media as recommended by Seahorse Bioscience. All the compounds used in the flux assays are listed (Table 3). Five technical replicates for each condition were plated. The plate was centrifuged at 100 g for 5 min at 20ºC and checked under microscope to make sure the CLL cell adhered to the Cell-Tak /stroma cells. The plate was pre-incubated at 37ºC non-CO_2 incubator for 30 minutes. The drugs were loaded into drug injection ports in the assay cartridge for cell mitochondrial stress test A: Oligomycin (1.25 µM), B: Carbonyl cyanide-*p*-trifluoromethoxyphenylhydrazone or FCCP (1 µM), C: Antimycin A (0.75 µM) + Rotenone

(1 µM) (Figure 6). Glycolysis stress test A: Glucose (10 mM), B: Oligomycin (1.5 µM), C: 2-Deoxy-D-Glucose (100 mM). Glycolysis and cell mitochondrial stress tests using standard mixing and measuring times recommended by Seahorse.

Oligomycin is mitochondrial uncoupler. It disrupts the ATP synthase activity by binding to the F_0 component of the complex. Once oligomycin is added, oxygen consumption required for ATP synthesis declines, whereas the oxygen required for maintaining the electron transport chain remains (Figure 7). If the mitochondria is defective or is targeted by a drug then the proton leak increases as well. The consumption of oxygen is coupled to the electron transport towards the production of ATP. The proton current generated by basal respiration supplies the ATP synthase and the proton leak. An approximate measure of the mitochondrial ATP synthesis in the basal state can be obtained from the decrease in respiration by inhibiting the ATP synthase with oligomycin. Therefore, to calculate the coupling efficiency, we can deduct the oxygen consumed after addition of oligomycin, from the basal state. FCCP is an ionophore that disrupts the mitochondrial membrane gradient, causing the cell to consume oxygen to rescue the membrane potential for the ETC activity. The oxygen consumption capacity of the cell in response to the stress induced by FCCP is termed 'Maximal Respiration'. The quantitative difference between the basal respiration and maximal respiration is termed 'Spare respiratory capacity' of the cell. To ensure the oxygen consumed is mitochondrial, Antimycin A and Rotenone, (inhibitors of mitochondrial complexes III and I activities respectively) are injected together. After their addition, the oxygen consumption must decline steeply and rapidly indicating that the oxygen consumed was indeed used by the ETC. However, non-mitochondrial respiration does get recorded and those values get deducted from the basal and maximal reparation values.

Assay	**Cell type**	**Compound/Injection**	**Optimal Concentration**
OCR	CLL/MCL/Stroma	Glucose	17 mM
OCR	CLL/MCL/Stroma	Sodium Pyruvate	2 mM
OCR	CLL	Human Serum	1 %
OCR	CLL/MCL/Stroma	Oligomycin	1.25 mM
OCR	CLL/MCL/Stroma	FCCP	0.5-1 μM
OCR	CLL/MCL/Stroma	Antimycin A	0.75 μM
OCR	CLL/MCL/Stroma	Rotenone	1 μM
ECAR	CLL/MCL/Stroma	L-Glutamine	2 mM
ECAR	CLL/MCL/Stroma	D-Glucose	10 mM
ECAR	CLL/MCL/Stroma	Oligomycin	1.5 μM
ECAR	CLL/MCL/Stroma	2-Deoxy-D-Glucose	100 mM

Table 3. List of compounds and drugs used in the extracellular flux assays.

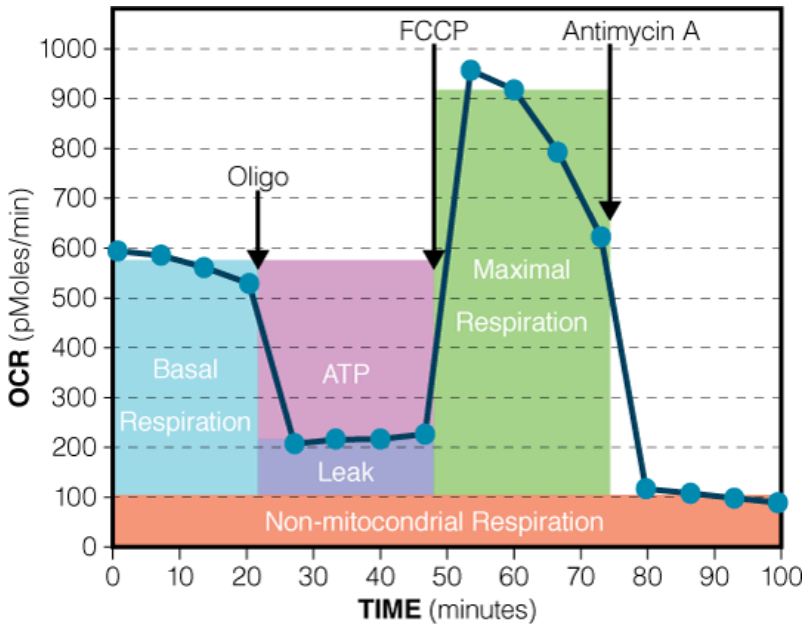

Figure 6: Graphical representation of cell mitochondrial stress profile.

The two hour test measures different parameters of mitochondrial respiration, when subject to stress by addition of drugs – Oligomycin (ATP coupler), followed by FCCP (uncoupler) and Antimycin A and Rotenone (inhibitors of complex III and I activity).

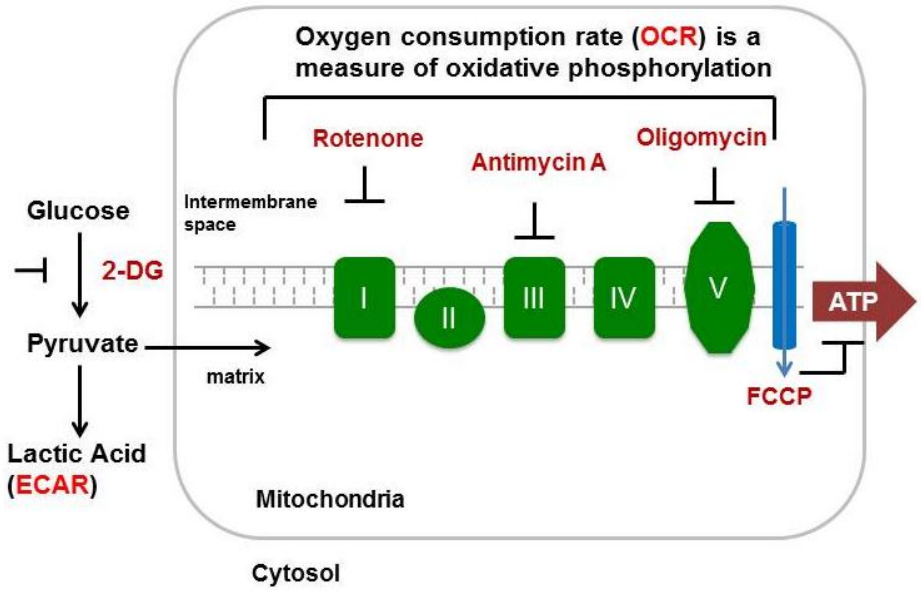

Figure 7. Biological targets of the drugs used in the extracellular flux assays.

2-Deoxy-D-glucose is a competitive inhibitor for hexokinase in the glycolysis pathway. Rotenone and Antimycin A target Complex I and III respectively. Oligomycin inhibits complex V activity and FCCP affects the inner mitochondrial membrane.

Similarly, for ECAR, glucose (10 mM) is injected, followed by oligomycin that disrupts ATP production as discussed before; therefore, the cell has to rely on glycolysis to meet its energy demands (Figure 8). The capacity of the cell to utilize glycolysis as a source of ATP determines its glycolytic capacity. A final injection of 2-Deoxy-D-Glucose ensures the readout (mPH) is due to lactic acid production (end step of glycolysis).

Optimization of cell numbers and drug concentrations for the XF assay:

For optimal read outs from the mitochondrial and glycolysis stress tests, it is critical to plate sufficient number of cells in a monolayer to minimize variations. Optimization assays were run before starting the experiments for each cell type to determine the concentrations for each drug and the number cells to be used. NK.Tert cells were plated in 5000, 7500, 10,000 (Figure 9A). 5000 stroma cell gave an optimal readout for ECAR/OCR. M2-10B4 and HS-5 cells were tested similarly (plated in 5000, 7500, 10000, 15000 cells counts) (Figure 9B).

All drugs and substrates used in extracellular flux assays were titrated for optimal concentrations. Optimal concentration can be defined as the minimum amount of drug required to induce a response in OCR or ECAR. The protocol followed for the XF assays are as recommended by Seahorse Bioscience. Three minutes of mixing followed by four minutes of measurement of oxygen concentration or acidity of the medium. This cycle repeats after addition of each drug.

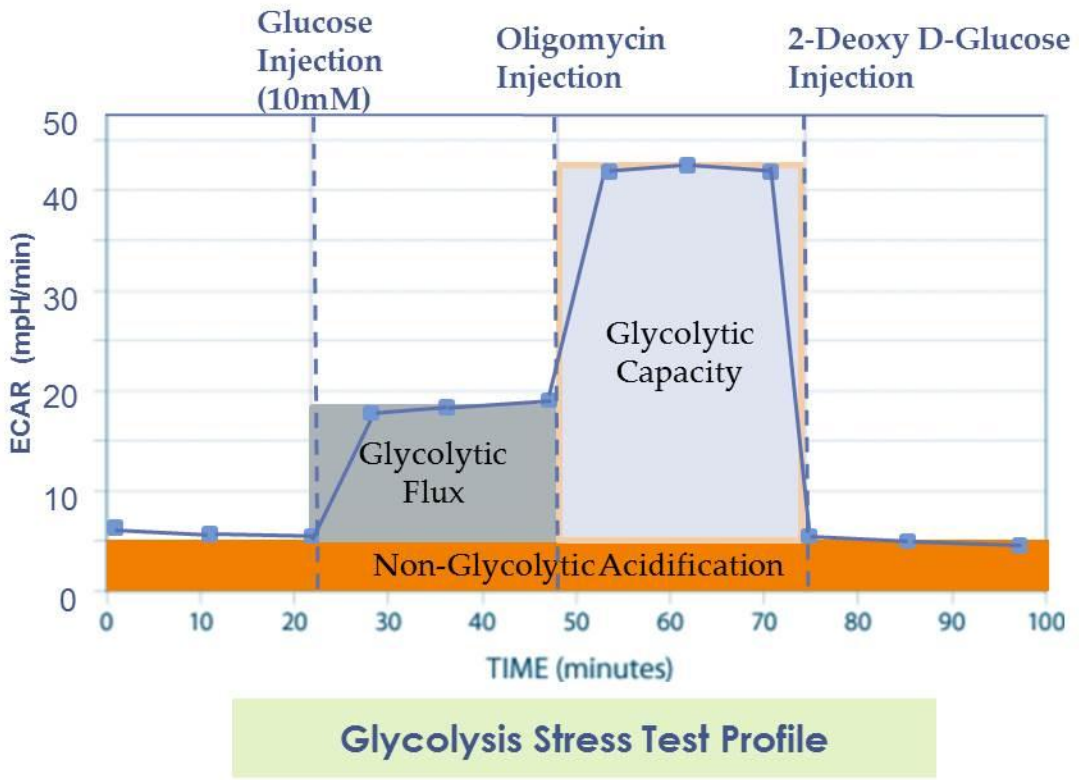

Figure 8: Graphical representation of glycolytic stress profile.

This test measures glycolysis by the decrease in pH levels in the media. Glucose utilization by the cells is measured after addition of glucose, followed by addition of oligomycin (ATP synthase inhibitor) and injecting 2-Deoxy-D-glucose to cut off the non- glycolytic acidification.

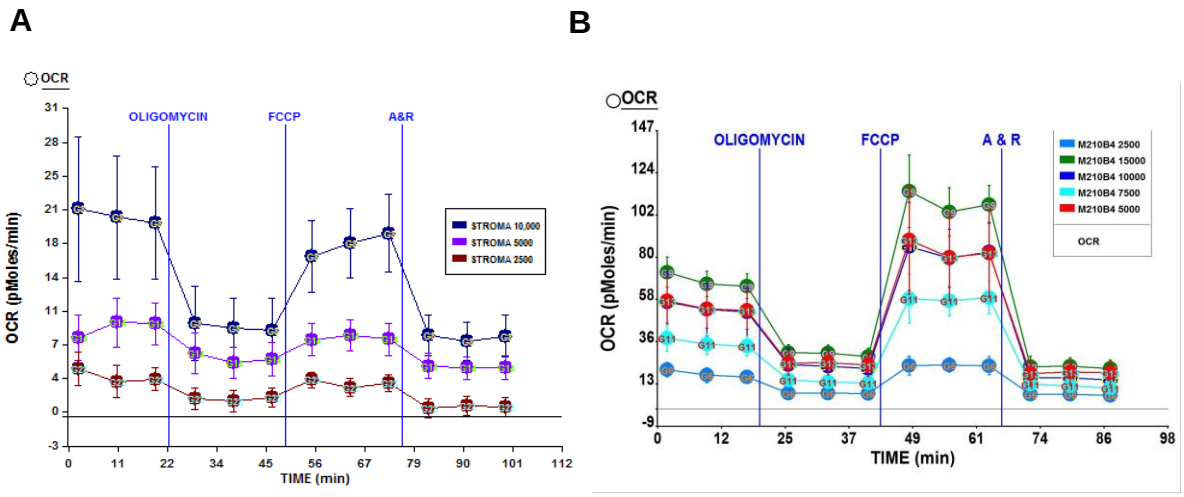

Figure 9: Optimization of stroma and CLL cell numbers for extracellular flux analysis.

A. NK.Tert cells cultured in MEM media were plated on XF96 plates at different cell numbers (2500, 5000, 10,000) and allowed to adhere for minimum of 6 hours.Five technical replicates were plated for each concentration. The media was replaced with XF test media supplemented with fresh 17.5 mM Glucose and 2 mM sodium pyruvate. The pH was adjusted to 7.4-7.6. Oligomycin (1.25 µM), FCCP (1 µM) and Antimycin A + Rotenone (0.75 µM+1 µM) were added in the order shown above. B. M2-10B4 cell numbers (2500, 5000, 7500, 10,000, 15000) were optimized as described in (A)

Fibronectin coating

CLL samples were assayed for OCR and ECAR using fibronectin (Sigma Aldrich, St. Louis, MO) as the adhesive at different concentrations (10, 15, 20μg/mL). XF96 plates were coated according to the manufacturer's protocol.

Cytokine stimulation assays

CLL cells were incubated with stroma derived growth factor-1 (SDF-1, 250, 500 ng/mL), B cell activating factor (BAFF 100 ng/mL), SDF-1 and BAFF in combination, IgM (10 μg) for 24hr and analyzed for ECAR and OCR.

Conditioning media experiments

CLL cells were cultured in conditioning media obtained from stroma cell culture. NK.Tert and M2-10B4 cells are grown in the media described in Table 2. Media is freshly added on day 1 to stroma cells. After 24hr culture, conditioning media from these cultures were obtained without disturbing the stroma layer (day 2) and added to CLL cells. CLL cells are then cultured in this media for 24hr before assaying for extracellular flux.

Ribonucleotide pools extraction

After 24 co-culture, CLL cells were carefully removed in 15 mL conical tubes, centrifuged at 1500 rpm at 4C for 5 min. The pellets were then washed with 10 mL of ice cold PBS and pelleted by centrifugation. After PBS was aspirated, 0.5 mL of ice-cold 0.4 N perchloric acid was added to the pellet, mixed well and incubated on ice for 5 min. The cells were repelleted by centrifugation and the supernatant was transferred to a clean Eppendorf tube. The 0.25 mL percloric acid was added to the pellet and extraction was repeated. The

supernatant was added to the first supernatant and its pH was adjusted with KOH to 6-7. The supernatant was spun down and the resultant supernatant was carefully removed with a glass syringe without disturbing the precipitate at the bottom. Intracellular nucleotide pools were separated using High Pressure Liquid Chromatography (HPLC). The extracts were applied to an anion-exchange Partisil-10 SAX column and eluted at a flow rate of 1.5 ml/min with a 50-min concave gradient (curve 9; Waters Alliance 2695 separations module; Waters 2487 Dual λ absorbance detector) from 60% 0.005 M $NH_4H_2PO_4$(pH 2.8) and 40% 0.75 M $NH_4H_2PO_4$ (pH 3.7) to 100% 0.75 M $NH_4H_2PO_4$ (pH 3.7). The column eluate was monitored by UV absorption at 257 nm, and the nucleoside triphosphates were quantitated by electronic integration with reference to external standards. The intracellular concentration of nucleotides contained in the extract was quantitated using the number of cells and cell size (median).

Immunoblotting

Proteins from cell pellets were extracted using Cell lysis buffer (Cell Signaling Technology, Danvers, MA) supplemented with Protease inhibitor (EDTA free miniSTOP, Roche, Basel, Switzerland) and Phosphatase inhibitor (PhosSTOP, Roche), 25 mM boiled sodium orthovanadate and 10 µg/mL phenylmethanesulfonylfluoride (PMSF) in 1.5 mL Eppendorf tubes. Cells were incubated on ice for 30 min with occasional vortexing. The cells were centrifuged at 14000 rpm at 4ºC for 15 min.

All steps were performed on ice. Supernatant was removed into a clean Eppendorf tube and protein was quantified using Bradford assay. 40-50 µg of protein was diluted with lysis buffer and ¼ th of sample buffer (Loading dye + 5% β-mercaptoethanol) was boiled at

95ºC for 5 min. The denatured protein was loaded onto 4-12% Bis-Tris gradient gel (BioRad, Hercules, CA) and the 1X XT MOPS (BioRad) was used as the electrolyte. The gel was transferred to a membrane using 1X Transfer Buffer (100 mL 1X Tris Glycine buffer + 200 mL Methanol+ 700 mL milliQ water) at 400 mA for 1 hour at 4ºC. The membrane was probed with 1X blocking buffer for 1 hr at room temperature. The membrane was incubated overnight with 1:1000 dilution of the primary antibody (All antibodies used are listed in Table 4). The next day, after removing the primary antibody, the membrane was washed with 1X wash buffer (1X PBS + 0.01 % Tween-20) twice for 5 min followed by 1 wash with 1X PBS. The membrane was incubated with 1:4000 dilution of the secondary antibody (Odyssey) for 1 hr at room temperature protected from light. The wash procedure mentioned above was repeated and the blot was scanned using an Odyssey Infrared Imaging System (LI-COR Biosciences, Lincoln, NE). The protein expression was quantitated by utilizing Image Studio ™ Lite Ver 4 (LI-COR). For serum starvation experiments the cells in growth media were counted and washed twice with 1X PBS, before resuspending in RPMI 1640 media supplemented with 0.5% FBS for 2 hours. For IgM stimulation experiments, cells were serum starved as mention before and 10 µg of IgM was added to 1 mL of media containing cells (1×10^7 CLL cells/ 3×10^6 JeKo-1 cells).

Glucose/glutamine uptake assays

CLL cells were suspended in glucose free or glutamine-free media and either [^{3}H]2-deoxy-D-glucose (0.5 µl, specific activity 28 Ci/mmol) for 60 min or [^{3}H]L-glutamine (1 µl

Primary Antibody	Company	Species	Dilution
OXPHOS cocktail	Abcam	Rabbit	1:500
p-STAT3 Tyr 705	Santa Cruz Bio	Rabbit	1:250
P-STAT3 Ser727	Cell Signaling	Rabbit	1:1000
STAT3 total	Cell Signaling	Mouse	1:1000
p-AKT Thr308	Cell Signaling	Rabbit	1:1000
p-AKT Ser473	Cell Signaling	Rabbit	1:1000
AKT total	Cell Signaling	Mouse	1:1000
UCP2	Novus Biologicals	Rabbit	1:1000
DNA pol γ	Cell Signaling	Rabbit	1:1000
NRF1	Santa Cruz	Rabbit	1:250
p-S6 Ser235	Cell Signaling	Rabbit	1:1000
S6 Ribosomal protein	Cell Signaling	Mouse	1:1000
p-ERK44/42 Ser	Cell Signaling	Rabbit	1:1000
p-ERK 44/42 total	Cell Signaling	Mouse	1:1000
GAPDH	Genetex	Rabbit; Mouse	1:20000
p-ACC1 Ser79	Cell signaling	Rabbit	1:1000
GLUT4	Abcam	Mouse	1:1000
PI3K p110δ	Santa Cruz	Rabbit	1:1000

Table 4. List of primary antibodies used in western blotting procedure.

specific activity 50.3 Ci/mmol) was added and incubated for 20 min (both reagents from Perkin Elmer, Waltham, Massachusetts) in a 12 well plate. At the end of the incubation period the plate was placed on ice and 1 mL ice cold 1X PBS was added to each well to stop the uptake and collected into 15 mL conical tube and washed with 1X PBS to get rid of excess radioactive compound and the cells were quenched with 1 mL 1N sodium hydroxide and placed in a 37ºC water bath overnight. The next day 1 mL of quenched cells was added to 19 mL of counting liquid and radioactivity was quantified using the scintillation counter. The disintegrations per minute were quantified by the cell number. For control experiments, CLL cells were stimulated by addition of insulin 10 μg/mL (Sigma, St. Louis, MO) after 4 hr of incubation with the drug and 15 minutes before addition of either [^{3}H] 2-deoxy-D-glucose for untreated/treated cells. CLL wells were also stimulated with anti-IgM (10μg/mL/10^7cells) to activate the B cell receptor pathway after 24hr of drug treatment and 15 minutes before addition of either [^{3}H] 2-deoxy-D-glucose for untreated/treated cells.

Flow cytometry analysis for measurement of mitochondrial reactive oxygen species, membrane potential, and mass

CLL cells ($5x10^6$) were washed and stained with 1:1000 Mito SOX Mitochondrial Superoxide Indicator in RPMI 1640 + 1% FBS for 10 min at 37ºC in a CO_2 incubator and washed with 1X PBS and resuspended in 1X PBS to measure mitochondrial reactive oxygen species using Flow cytometry. This dye selectively targets mitochondria and is oxidized by generation of superoxide. Similarly, cells were simultaneously stained with 500 nM (working concentration) Mitotracker Deep Red FM to stain for live cell mitochondria and Tetramethylrhodamine, Ethyl Ester, Perchlorate to measure the mitochondrial outer membrane potential (MOMP) and incubated for at least 30 min and analyzed by Flow and

30,000 events were recorded per sample. All the three reagents are light sensitive and samples were protected from light throughout the assay. All reagents were obtained from Life Technologies Grand Island, NY. Geometric means of histograms were quantified using FlowJo, LLC software (Ashland, OR).

Metabolite Mass Spectrometry

CLL cells were co-cultured with NK.Tert cells for 24hr, washed and cellular metabolites were extracted using 80% methanol by following the protocol provided by Mass spectroscopy facility at Beth Israel Deaconness Medical Center. The samples were sent for polar metabolite analysis.

The changes in metabolites after co-culture were calculated by the ratio of values obtained for each metabolic after co-culture vs suspension culture. The metabolites were then grouped into pathways using Kyoto Encyclopedia of Genes and Genomes (KEGG) IDs.

CRISPR-Cas9 gene editing

BCR knockout

(These experiments were conducted in collaboration with Dr. Richard E. Davis laboratory, Department of Lymphoma/Myeloma, UT MDACC)

CRISPR Cas9 px330 plasmids with BCR target DNA sequence constructs were donated by Dr. Davis. JeKo-1 cells (6×10^6) were transfected (10 µg of plasmid DNA/million cells) by electroporation (Neon® transfection system, Invitrogen) according to the manufacturer's protocol. No DNA and non-specific plasmid were used as negative control. GFP only transfection was used as a positive control to measure transfection

efficiency. JeKo-1 cells in culture were harvested, washed with 1X PBS, cells were counted by tryphan blue exclusion. Cells were pelleted by centrifugation and supernatant was carefully removed. The pellet was resuspended in R buffer (100 μL/10^6 cells). Appropriate plasmid DNA was added to sterile Eppendorf tubes and 100 μL of cells were added to each tube. 100 μL electroporation tip was used to mix the cells with the DNA and placed in the electroporation Tip chamber contacting 3 mL of E2 electroporation buffer. JeKo-1 cells were then pulsed once at 1500 V, for 20 mS. The cells were then plated in 3 mL DMEM media supplemented with 10% FBS in a 6 well plate. The cells were stained and analyzed for BCR heavy chain (IgM) and light chain (κ) expression, by flow cytometry, 72 hr post transfection. The cells were resuspended in 100 μL of FACS buffer with IgM and the corresponding light chain Ab (JeKo-1 κ, Mino –λ). The cells were incubated on ice for 20 min in the dark. The cells were then washed with FACS buffer and resuspended in 200 μL FACS buffer containing Pacific blue (Thermo Fisher Scientific, Waltham, MA) / Propidium Iodide (BD Biosciences, San Jose, CA) to stain for dead cells.

The knockout (KO) cells were stained and sorted by FACS on day 6 (Figure 10). After sorting, the cells were placed in DMEM media supplemented with 20% FBS +1 U Penicillin Streptomycin solution. Three KO clones were generated, where the Cas9 construct harbored DNA sequences complimentary to different regions of CH2 domain of BCR.

Targeting CH2 IGHM constant region http://crispr.mit.edu/job/8849455957183642

TS4: **CCCCCGCAAGTCCAAGCTCATCT**

TS5: **CAGGTGTCCTGGCTGCGCGAGGG**

TS6: **ACCTGCCGCGTGGATCACAGGGG**

IGHMC_gRNA_04_F CACCGATGAGCTTGGACTTGCGG

IGHMC_gRNA_04_R GATGAGCTTGGACTTGCGGGTTT

IGHMC_gRNA_05_F CACCGGTGTCCTGGCTGCGCGA

IGHMC_gRNA_05_R GGTGTCCTGGCTGCGCGAGTTT

IGHMC_gRNA_06_F CACCGACCTGCCGCGTGGATCACAG

IGHMC_gRNA_06_R GACCTGCCGCGTGGATCACAGGTTT

PIK3CD Knock in –Knock out

The knock in – knock out approach enabled us to viably mark the PI3K δ KO cells by expressing the GFP instead of PI3K δ from its DNA locus and consequently use the cells for further studies. The general approach was to knock in (KI) the GFP-STOP-polyA cassette right after translation initiation site of the PI3Kδ leading to PI3Kδ promoter driven expression of GFP instead of PI3Kδ. We have used the CRISPR/Cas9 system to introduce DNA double strand breaks at the desired location and at the same time provided template plasmid for homologous recombination mediated KI. The px330 plasmid (Addgene plasmid #42230, PubMed 23287718) coding for Cas9 and gRNA targeting PI3K δ (target site sequence: 5'- CATCTGGGAAGTAACAACGCAGG-3') was cloned according to the published protocol (PMID: 24157548). The target site was designed using CRISPR design tool at http://crispr.genome-engineering.org/ (PMID: 23873081). Electroporation was used (Neon Transfection System, Thermo Fisher Scientific) to deliver the px330 plasmid at the same time as the KI template plasmid (9 μg per 1e10 cells of each plasmid). The pSC-B-amp/kan plasmid (Agilent Technologies, Santa Clara, CA) was used to carry the KI template sequence that consisted of (from 5' to 3'): left homology arm (400 bp of PI3K δ DNA

sequence upstream of translation initiation site), kozak sequence (GCCACC), GFP with STOP codon, bGH PolyA signal sequence, and right homology arm (300bp of PI3Kδ sequence downstream of translation initiation site). The homology arms contained silent mutations preventing targeting of the template plasmid or PI3K δ locus after the KI. The PI3K δ KO GFP positive cells were identified and sorted to purity using FACS. As a control for KI specificity, px330 plasmids with non-specific target site were electroporated together with template plasmid. No GFP positive cells were detected in the specificity control.

px330 and px 335 plasmids were cloned with two different target (beginning of exon 3 for PI3KD gene) inserts. PI3KD homology arm sequence is used as the repair template with Green Fluorescent Protein insert.

1. Annealing the oligo: The oligos (custom ordered from IDT) were reconstituted and diluted to 100 pmol/µl. 10 µl PCR buffer, 5 µl forward oligo, 5 µl reverse oligo, 80µl ddH_2O were mixed and placed in a thermal cycler with slowly decreasing temperature as follows: 95°C 2 min, 90°C 2 min, 85°C 5 min, 70°C 5 min, 65°C 5 min to stop at 20°C. The resulting product would be double stranded oligos at 5 pmol/µl.

P110delta_gRNA_01_F	CACCGCATCTGGGAAGTAACAACGC
P110delta_gRNA_01_R	AAACGCGTTGTTACTTCCCAGATGC
P110delta_gRNA_02_F	CACCGCAGGATGCCCCCTGGGG
P110delta_gRNA_02_R	AAACCCCCAGGGGGCATCCTGC
P110delta_gRNA_03_F	CACCGAGTTACCTCAGCTGAGC
P110delta_gRNA_03_R	AAACGCTCAGCTGAGGTAACTC

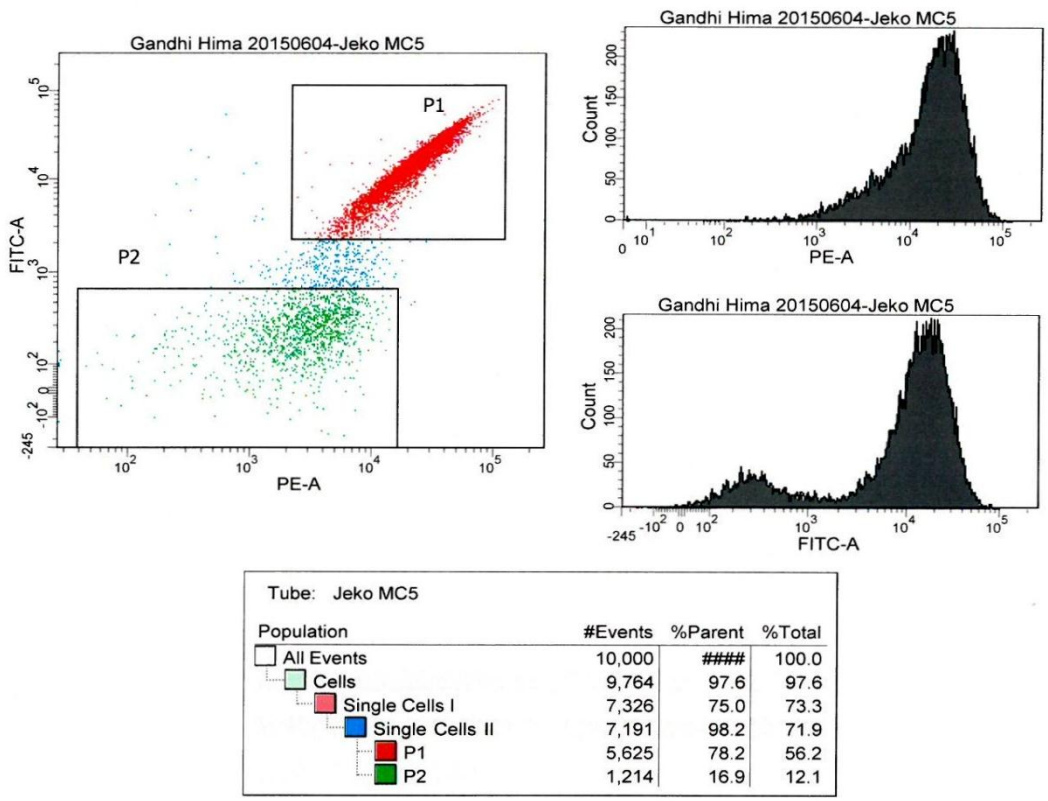

Figure 10. Sorting B cell receptor knockout cells from Cas9 transfected JeKo-1 cells.

On day 4 after transfection of JeKo-1 (1×10^7) cells with Cas9 plasmid containing BCR target sequence, the cells were stained with IgM-FITC and κ-PE (1:100 ratio) for 20 minutes on ice and sorted for IgM negative population as shown.

2. Phosphorylation of the oligos: 20 µl of previous reaction (200pmol of 5' ends), 5 µl of 10 X T4 DNA Ligase Buffer,1 µl of T4 Polynucleotide Kinase (10 units), 24 µl ddH2O were taken together in an Eppendorf tube and incubated at 37°C(water bath) for 30 minutes. Resulting concentration of ds phosphorylated oligos: 2 pmol/µl. The oligos were then diluted to 0.1 pmol/µl by adding 19 µL of ddH_2O to 1 µL of ds oligo.
3. Ligation of the oligo with px330 or px335 plasmids: These plasmids were first cut with restriction enzyme BbsI and treated with CIP (Calf-intestinal alkaline phosphatase).

   10 µL of the ligation reaction is set upon ice in an Eppendorf as follows

   1 µL of opened plasmid (40 ng/ µL), 0.5 µL of ds phosphorylated diluted oligo (0.1 pmol), Buffer 1 µL, Ligase 0.5 µL, ddH_2O 7 µL. The reaction was gently mixed by pipetting up and down and incubated at 16°C overnight.

   The combination of the oligos with the px plasmids are as follows:

   px330- oligo 1, px330- oligo 2, px335- oligo 1, px335- oligo 3
4. Transformation of bacteria: The reaction was then chilled on ice and 2 µl of the reaction was added to 100 µl of competent cells (StrataClone Blunt PCR Cloning Kit from Agilent Technologies). 20 µl of bacteria was spread on an agar plate with ampicillin. β-galactosidase was used for blue white colony screening and placed in 37°C incubator overnight. The next day, 3 white colonies were picked and streaked on agar plate with ampicillin. After 6hrs of incubation at 37°C, the bacteria from the streaks were inoculated

In 2 mL of LB broth supplemented with 100 µg/mL ampicillin and incubated at 37ºC for another 6 hrs. This culture was used to prepare a mini prep using Qiagen mini prep kit.

5. Sequencing: The DNA obtained from minipreps was sent for Sanger sequencing at the DNA sequencing core facility at MD Anderson Cancer Center. Sequences of interest were verified with Finch TV (Geospiza Inc) and Lasergene SeqBuilder (DNASTAR™)
6. After sequence verification, more DNA was obtaining by using Qiagen Maxiprep Kit (Valencia, CA).

Repair Template: PI3KCD homology arm gene block was ordered from Integrated DNA Technologies.

1. The gBLOCK containing PIK3CD homology arms was captured into the Strataclone pSC plasmid.
2. The plasmid with p110delta_HA_1 was then opened with BbsI restriction enzyme to insert GFP-PolyA fragment to make final template for KI.
3. Co-transfection of JeKo-1 cells were as follows:
   i. Px330-1 (9 µg) + PI3KCD_HA (9 µg)
   ii. px330-2 (9 µg)+ PI3KCD_HA (9 µg)
   iii. Px335-1 (6 µg)+ Px-335-3 (6 µg) + PI3KCD_HA (6 µg)

The combination that gave the highest GFP + ve cells was used for further experiments. GFP expression was checked by Flow cytometry (Figure 11). Experimental set up consisted of no DNA control, non-specific control, GFP control and px330-1 plasmid transection.

Knock-in template sequence (with PI3K homology arms and GFP):

GGTCTCAGGGCACCTGACCAGCTGTCCTGCCATCTCCCTTCTGTGCCAGCTGGTG
GCCATGACTGGCTTTCGTGGATGTGTATGTTCCTGAGGAAAGATGATTTGCTGTG
CGTGCTCCTGTGGGGAGGACATGCAGTGTCTG**CCTGGGAGAAGAGGCAGCTGA**
GGCCGTGGCCCGGAGTAGTAGGAGCCACAAGCCACCCTGGGCAGGACGAG
GCCCTGAGGGAGGTGAGCTTTTTGTACCCGCAGGTCGGGAACTCACTCCTGAGC
TTCCTGCTGTCCAAGGACCCCACTGTTTTCCAGGGAGTCCCTTCCAAAGGTCTCA
CTCAACTCAGCTGAGGTAACTCATTTTGCCATTTCTTCATTTTTAG**GACAACTGT**
CATCTGGGAAGTAACAAGCCACCATGGAACCCGTGAGCAAGGGCGAGGAGCTG
TTCACCGGGGTGGTGCCCATCCTGGTCGAGCTGGACGGCGACGTAAACGGCCAC
AAGTTCAGCGTGTCCGGCGAGGGCGAGGGCGATGCCACCTACGGCAAGCTGACC
CTGAAGTTCATCTGCACCACCGGCAAGCTGCCCGTGCCCTGGCCCACCCTCGTGA
CCACCTTCACCTACGGCGTGCAGTGCTTCGCCCGCTACCCCGACCACATGAAGCA
GCACGACTTCTTCAAGTCCGCCATGCCCGAAGGCTACGTCCAGGAGCGCACCAT
CTTCTTCAAGGACGACGGCAACTACAAGACCCGCGCCGAGGTGAAGTTCGAGGG
CGACACCCTGGTGAACCGCATCGAGCTGAAGGGCATCGACTTCAAGGAGGACGG
CAACATCCTGGGGCACAAGCTGGAGTACAACTACAACAGCCACAAGGTCTATAT
CACCGCCGACAAGCAGAAGAACGGCATCAAGGTGAACTTCAAGACCCGCCACA
ACATCGAGGACGGCAGCGTGCAGCTCGCCGACCACTACCAGCAGAACACCCCCA
TCGGCGACGGCCCCGTGCTGCTGCCCGACAACCACTACCTGAGCACCCAGTCCG
CCCTGAGCAAAGACCCCAACGAGAAGCGCGATCACATGGTCCTGCTGGAGTTCG
TGACCGCCGCCGGGATCACTCTCGGCATGGACGAGCTGTACAAGTAAGATCAGC
CTCGACTGTGCCTTCTAGTTGCCAGCCATCTGTTGTTTGCCCCTCCCCCGTGCCTT
CCTTGACCCTGGAAGGTGCCACTCCCACTGTCCTTTCCTAATAAAATGAGGAAAT
TGCATCGCATTGTCTGAGTAGGTGTCATTCTATTCTGGGGGGTGGGGTGGGGCAG
GACAGCAAGGGGGAGGATTGGGAAGACAATAGCAGGCATGCTGGGGACATG**CC**
CCCTGGTGTGT**ACTGCCCCATGGAATTCTGGACCAAGGAGGAGAATCAGAG**
CGTTGTGGTTGACTTCCTGCTGCCCACAGGGGTCTACCTGAACTTCCCTGTG
TCCCGCAATGCCAACCTCAGCACCATCAAGCAGGTATGGCCTCCATCCGGTCC
TCAGACCTTGGTGCTCAGAGAGAGAGAGAGAGAGAGAGACACAGATAGACAGA
CAGACAGACAGACAGATGGACAGGTGGACAGACGGACAGACAGATGGACAGAT
GCACTGCTTTTCAGACTTGGGATCCTCAGATGAGAATTTTAAAAGATAAATAATG
GTTTGTTTGTTTGTTTGTTTGTTTTGAGACGGAGTTTCGCTCTTATTGCCCAGGCT
GGTGTGCAATGGCGCAATCTCGGCTCC

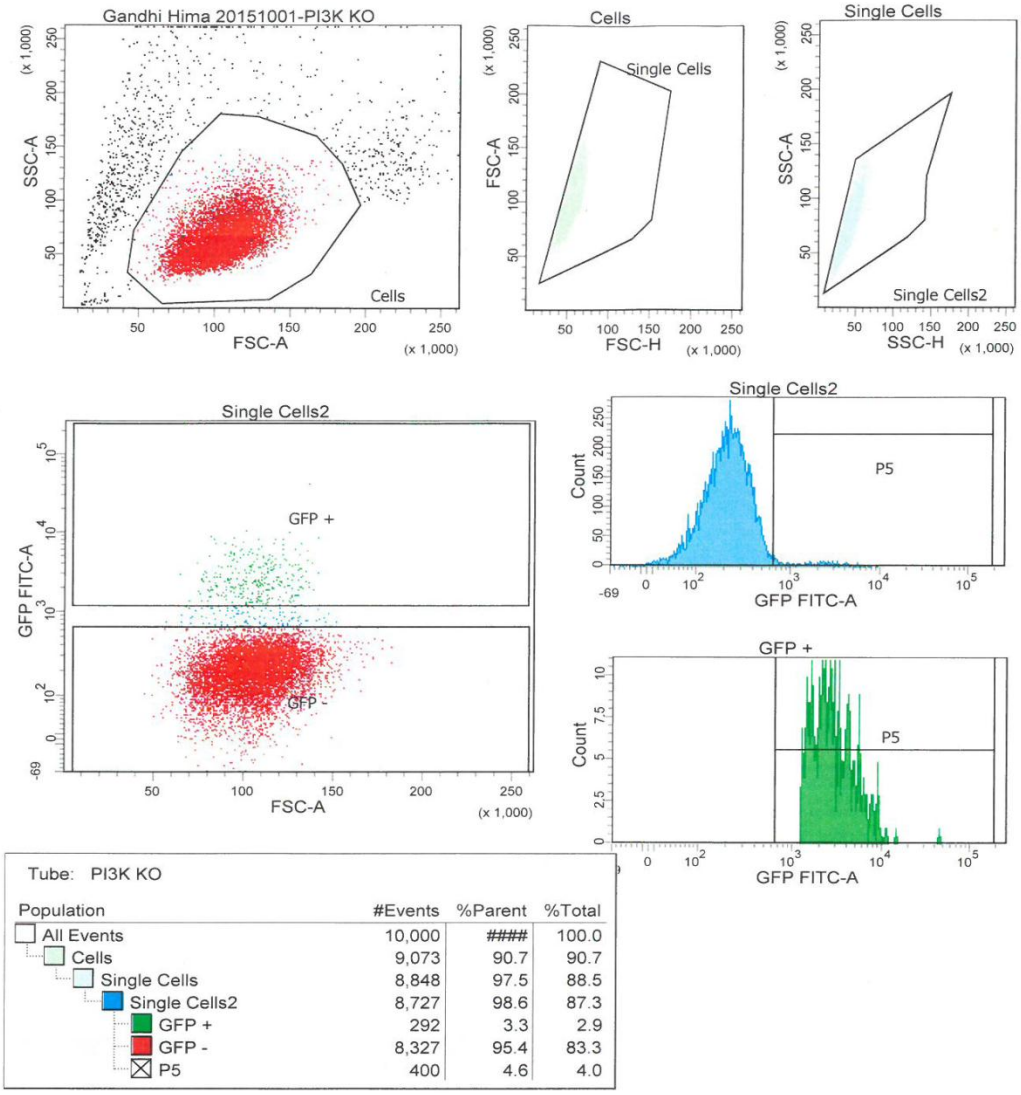

Figure 11. Sorting PIK3CD knockout cells from Cas9 transfected JeKo-1 cells.

On day 3, after co-transfection of JeKo-1 (1×10^7) cells with Cas9 and GFP containing PIK3CD repair template, the cells were sorted for GFP positive cells that were knockout for PIK3CD as shown.

Fluorescence Activated Cell Sorting

For BCR KO experiments, IgM-FITC conjugate and light chain antibodies (κ, λ) –PE conjugate obtained was from Life Technologies (Carlsbad, CA). The cells were counted by Trypan Blue staining and 2×10^7 cells were stained at 1 μL of sterile Abs /million cells in 1 mL of media and taken to the FACS facility. The KO cells were collected in RPMI 1640 containing 20 % FBS and 1 % Penicillin and Streptomycin solution. These cells were then centrifuged at 1500 rpm for 5 minutes and resuspended in RPMI 1640 + 10 % FBS + 1 % penicillin-streptromycin solution.

PCR for mtDNA copy number

QiaAMP DNA mini kit (Qiagen, Venlo, Limberg, Netherlands) was used and DNA was extracted from CLL samples according to manufacturer's protocol. qPCR SYBR green master mix was used to amplify the mitochondrial DNA from 4 CLL patient samples. All samples were run in triplicate. These experiments were conducted in collaboration with Dr. Benny Kaiparettu's laboratory, Baylor College of Medicine.

Electron Chain Transport activity analysis

Frozen cell lysates were lysed and then used for electron transport chain (ETC) enzyme assays. The enzymes were assayed at 30 °C using a temperature-controlled spectrophotometer; Ultraspec 6300 pro, Biochrom Ltd., (Cambridge, England). Each assay was performed in triplicate. The activities of the five enzymes were measured using appropriate electron acceptors/donors according to published procedures (Vu et al. 1998, Enns et al. 2005). These experiments were conducted in collaboration with Dr. Benny Kaiparettu's laboratory, Baylor College of Medicine.

Citrate synthase (CS) was used as a marker for mitochondrial content. Enzyme activities are expressed relative to total protein as nmol/min/mg protein.

Statistical analysis

Student's t-tests (two-tailed) and ANOVA were performed using Prism 6 software (GraphPad Software, San Diego, CA).

CHAPTER 3. RESULTS

As discussed in the Introduction Section, although CLL cells are quiescent, they are active in transcription, translation, and metabolomics. However, the metabolic activity of CLL cells has not been explored in detail in previous studies. To gain a deeper understanding of the bioenergetics of CLL cells in context of the microenvironment, and to test my hypotheses that stroma would modulate CLL metabolism and PI3K would play a crucial role regulating metabolism of these cells, I conducted the following three aims.

Aim 1: Elucidate the bioenergetics profile of primary CLL peripheral blood lymphocytes, encompassing two major energy (ATP) generating pathways, glycolysis and mitochondrial oxidative phosphorylation (OxPhos) and their relationship to CLL prognostic factors.

Aim 2. Determine the impact of stroma on energy generating pathways, Oxidative Phosphorylation and glycolysis in primary CLL cells.

Aim 3. Identify the role of PI3K pathway in induction of glycolysis and OxPhos in CLL cells.

Aim 1. Elucidate the bioenergetics profile of primary CLL peripheral blood lymphocytes

Aim 1.1. Elucidate the bioenergetic profile of primary CLL cells in relation to glycolysis and mitochondrial OxPhos.

Oxidative phosphorylation and glycolysis are the two major pathways leading to the production of ATP. Glycolysis is often upregulated in cancer cells to meet its energy demands (Warburg 1956). Cancer cells are highly proliferative and require energy for DNA

replication- and cell division- associated processes. However, the more prominent pathway that quiescent mature cells such as CLL rely on has not been well elucidated so far.

CLL metabolic profile

Glycolysis (measured as ECAR) and OxPhos (measured as OCR) profiles were analyzed in CLL patient samples using Seahorse extracellular flux analysis. The cells obtained from all of the CLL patients samples were cultured in RPMI 1640 +10% human serum before the analysis. Glycolysis and OxPhos were measured in 41 patient samples using cell mitochondrial stress test and glycolysis stress tests as described in Materials and Methods. Along with the CLL cells, peripheral blood mononuclear cells (mostly T cells) ($5x10^5$) and quiescent mature B cells obtained from 4 healthy donors were also analyzed for ECAR and OCR as were mantle cell lymphoma cell lines, (another B cell malignancy), JeKo-1, Mino, Granta and Sp53 (40,000 cells). These cell lines were actively proliferating, therefore, we expect their metabolism to be much higher than quiescent B cells.

A phenogram depicting the metabolic phenotype of cells was plotted using the data from all the cell types assayed above. The phenogram can be divided into four quadrants. Abscissa is taken as ECAR and ordinate as OCR. Lower left quadrant depicts metabolically less active cells as both ECAR and OCR have low values; lower right quadrant depicts cells that are more glycolytic owing to high ECAR, but low OCR values; upper left quadrant depicts aerobically active cells as OCR is high compared to ECAR; upper right quadrant denotes cells that are metabolically highly active as both oxygen consumption as well as glycolysis rates are high.

OCR and ECAR were lower in CLL lymphocytes (n=41) than in healthy mature B cells, PBMCs, or MCL cell lines, the latter were highly metabolic both aerobically and anaerobically (Figure 12). Among the malignant lymphocyte samples, there was very little glycolytic disparity, whereas mitochondrial respiration varied. The coefficient of variation for OCR was 57% versus ECAR at 42%.

Aim 1.2. Evaluate the metabolic profile of CLL patient samples in relation with the most-prevalent prognostic factors and cytogenetic profiles.

Impact of prognostic factors on CLL mitochondrial OxPhos and glycolysis

To understand the basis for these differences in OCR, we compared basal OCR with prognostic markers of the disease. These are factors that have been associated with aggressiveness of disease, the outcome of treatment in the clinic, and relapse and disease progression. These prognostic factors were ZAP 70 status, IgVH mutational status, Rai staging, β2 microglobulin, LDH levels, lymphocyte counts, CD38 status, gender, age and cytogenetics.

ZAP 70 is a tyrosine kinase receptor that is expressed on T cells and its expression in normal B lymphocytes is not known. However, in CLL cells, ZAP 70 is expressed (Rosenwald et al. 2001). ZAP 70 expression on the surface of malignant B cells is correlated with aggressive CLL disease. ZAP 70 expression is measured by immunohistochemistry or by flow cytometry. The patient is considered negative for ZAP 70, if it is expressed on less than <20% of the monoclonal B cells and if the expression is found on ≥20% of B cells, he/she is ZAP70 positive. For OCR, CLL cells from 20 ZAP 70 negative patients and 29

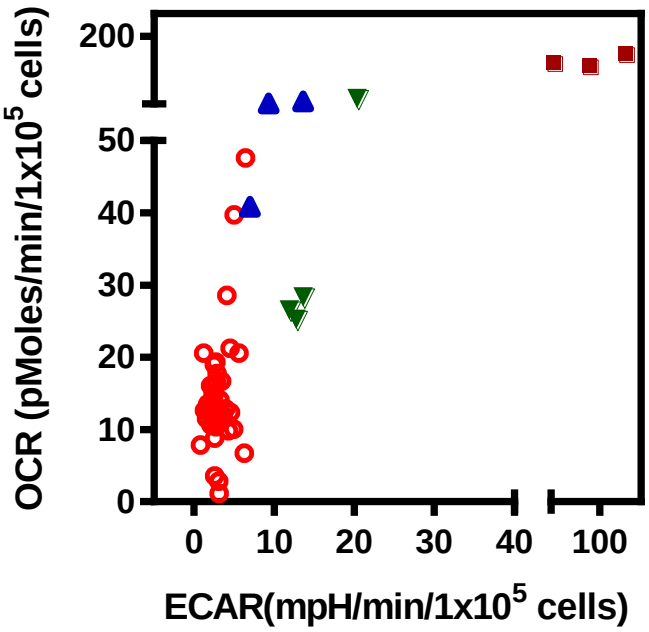

Figure 12. Phenogram of CLL cells compared with healthy and other malignant lymphocytes.

Bioenergetic profile of CLL cells($5x10^5$) from 41 patients (red circles) compared with peripheral blood mononuclear cells (PBMCs) from healthy donors (n = 3, blue triangles), B cells from healthy donors (n = 4, inverted green triangles), and proliferating B cell lymphoma cell lines (JeKo-1, Mino and Sp53, maroon squares). All cells were in suspension cultures. Extracellular Acidification Rate (ECAR) and Oxygen Consumption Rate (OCR) (n = 5 technical replicates for all extracellular flux experiments conducted) were measured and normalized to $1x10^5$ cells

ZAP 70 positive were analyzed. There is an overlap in the OCR values for the negative and positive samples which can be attributed to the variable levels of ZAP 70 in these cells as opposed to complete presence or absence. Statistical analysis (unpaired t-test) suggested that ZAP 70-positive samples had higher OCR compared to their counterparts (Figure 13A). ZAP 70 negative patients and 19 ZAP 70 positive were assayed for ECAR; however, these ECAR values were fairly similar and varied based on ZAP 70 expression (Figure 13B).

ZAP 70 status generally correlated with IgVH mutational status (Crespo et al. 2003). Absence of somatic mutations in IgVH marks aggressive disease. Somatic mutation occurs in the gene segments VH, D, JH that code for immunoglobulin heavy chain variable region. CLL is classified into two subsets based on the germline mutations of IgVH. Mutational status is confirmed by reverse transcriptase-polymerase chain reaction (RT-PCR). 19 CLL samples with IgVH mutation and 27 samples with unmutated IgVH were analyzed for OCR. Basal OCR was significantly higher in IgVH unmutated cohort than in mutated cohort (Figure 13C). Similarly, glycolytic flux was assayed for 11 IgVH mutated and 18 unmutated CLL samples. However, they did not display any correlation with IgVH status (Figure 13D).

Binet and Rai staging defines various stages of CLL disease. Among these two, Rai staging is commonly used in the USA and is mainly based on lymphocytosis (>15,000 lymphocytes/mm^3) in blood and prevalence of disease in bone marrow, lymph nodes and other sites. Staging is mainly used for treatment purposes and risk stratification. There are five stages- 0, 1, 2, 3 and 4; 0 and 1 being low risk for overall survival and 2-4 being high

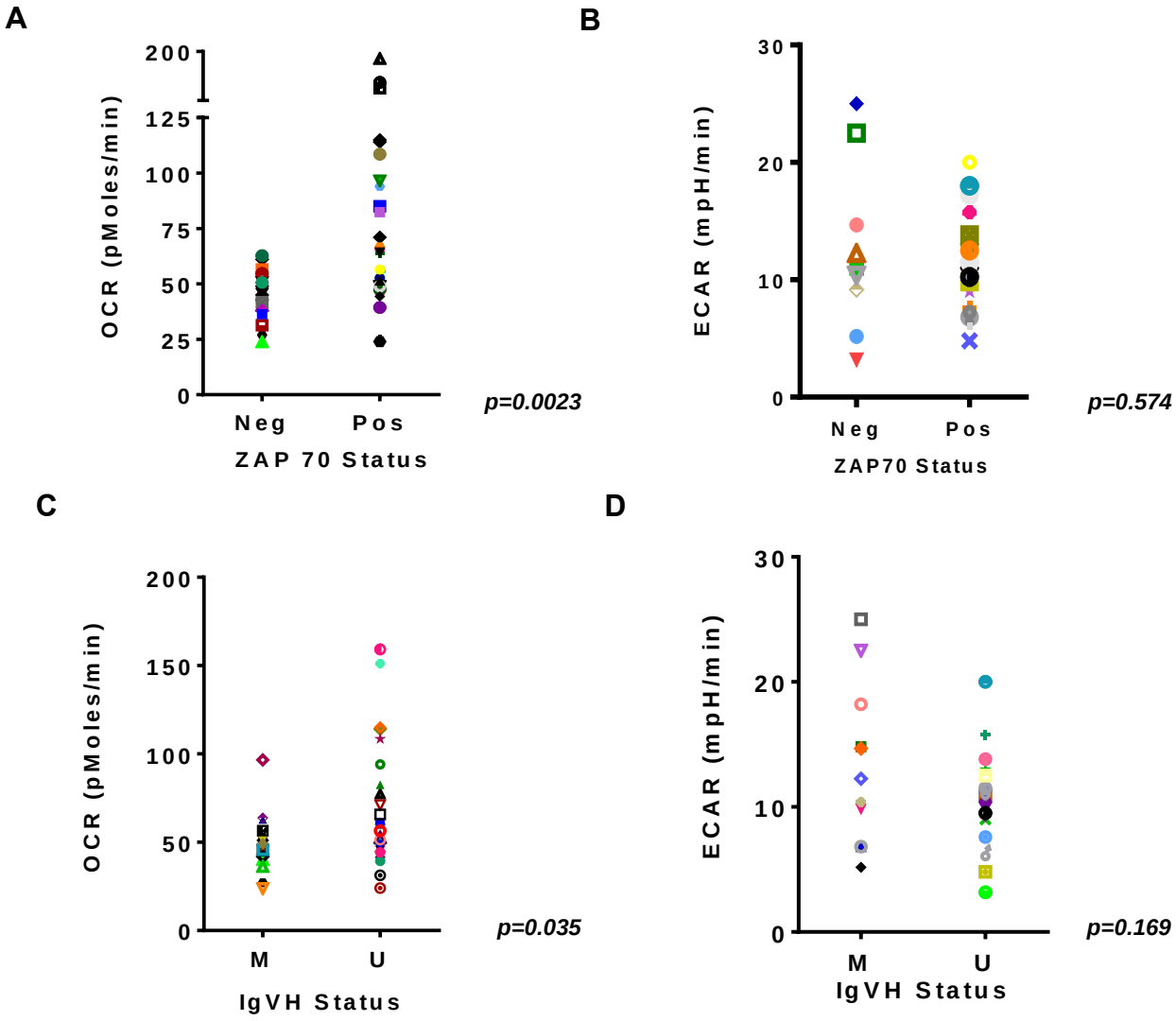

Figure 13. Correlation of CLL OCR and ECAR with ZAP 70 expression and IgVH mutational status.

CLL cells were assayed for OCR and ECAR, after isolation from peripheral blood. A. Basal OCR of CLL cells obtained from ZAP 70-negative (neg) (n=20) and ZAP 70-positive (pos) (n=29) patients were compared. B. Glycolytic flux from CLL cells of ZAP70-negative (neg)(n=9) and ZAP 70-positive (pos) (n=19) patients were compared. C. Similar to A, CLL cell basal OCR was compared based on the mutational status of IgVH in patients: mutated (M)(n=19) or unmutated (U)(n=27). D. Glycolytic flux from IgVH mutated (M)(n=11) and unmutated (U)(n=18) CLL cells were compared. Unpaired student's t-test was used to calculate statistical significance.

risk. 34 patients with low grade CLL and low grade (stages 0-1), and 20 with high grade were analyzed for OCR. Higher basal OCR correlated with advanced disease stage (Figure 14A). In contrast, when glycolytic flux from 25 low grade patients (stages 0-1), and 11 high grade CLL were compared, no significant difference was observed between the two groups (Figure 14B).

β2 microglobulin (β2M) is a cell membrane protein associated with HLA-antigens and its levels are elevated in serum of CLL patients with advanced disease. The cut-off levels for β2M according to CLL International Prognostic Index in healthy individuals is ≤3.5μg/mL. A value of >3.5 μg/mL is associated with high risk CLL disease. CLL patients with low serum (≤3.5μg/mL, n=39) β2M levels and with high levels (>3.5 μg/mL, n=15) were analyzed for OCR. High basal OCR marginally correlated with high β2M levels (Figure 15A). Whereas, ECAR analyzed for 18 CLL patients with low β2M levels and 7 with high levels did not correlate (Figure 15B).

Lactate dehydrogenase (LDH) is an enzyme that converts lactate into pyruvate. Elevated LDH levels are an indicator of tissue damage. In my study, patients are grouped according to their serum LDH levels- 8 patients had low levels (300-500 μg/mL) (L), 26 patients have intermediate levels 501-700 μg/mL (M), and 17 patients with high level >700 μg/mL (H, high). These samples were analyzed using a cell mitochondrial stress test (Figure 15C). Similarly, glycolysis stress tests were performed on CLL cells from patients with low (n = 5), medium (n = 11), high (n = 9) LDH levels (Figure 15D). In general, LDH levels did not associate with either OCR or ECAR.

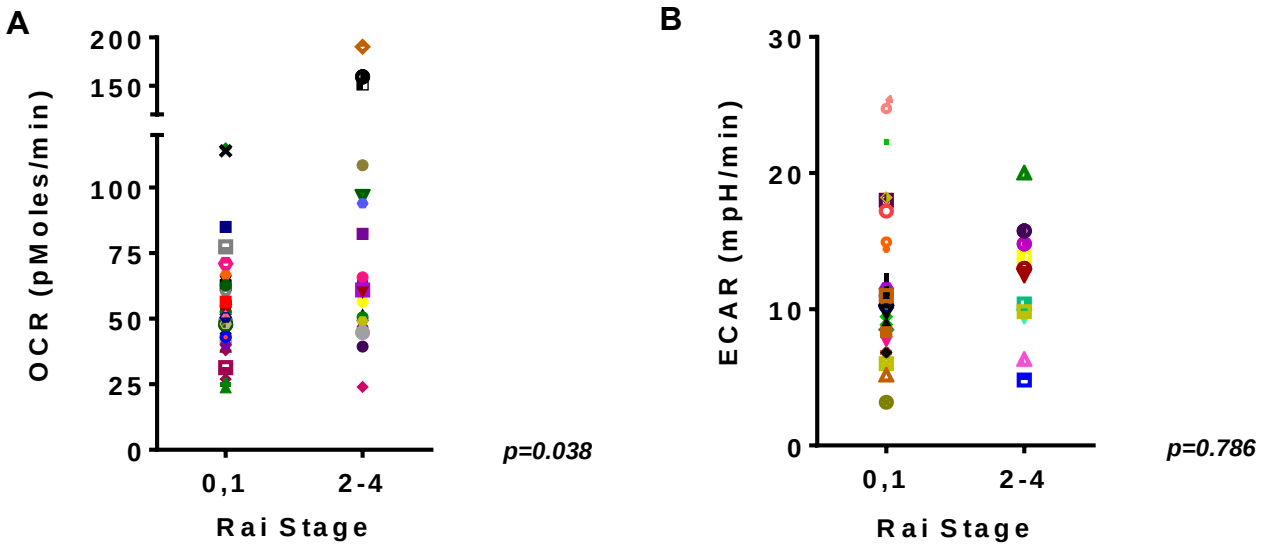

Figure 14. Correlation of CLL OCR and ECAR with Rai stage.

CLL cells were assayed for OCR and ECAR, after isolation from peripheral blood. A. Basal OCR of CLL cells were compared for patients classified by Rai stage: low grade (stages 0-1, n = 34), high grade (stages 2-4, n = 20). B. Glycolytic flux from low grade (stages 0-1, n = 25), high grade (stages 2-4, n = 11) CLL cells were compared. Statistical significance was calculated using unpaired student's t-test.

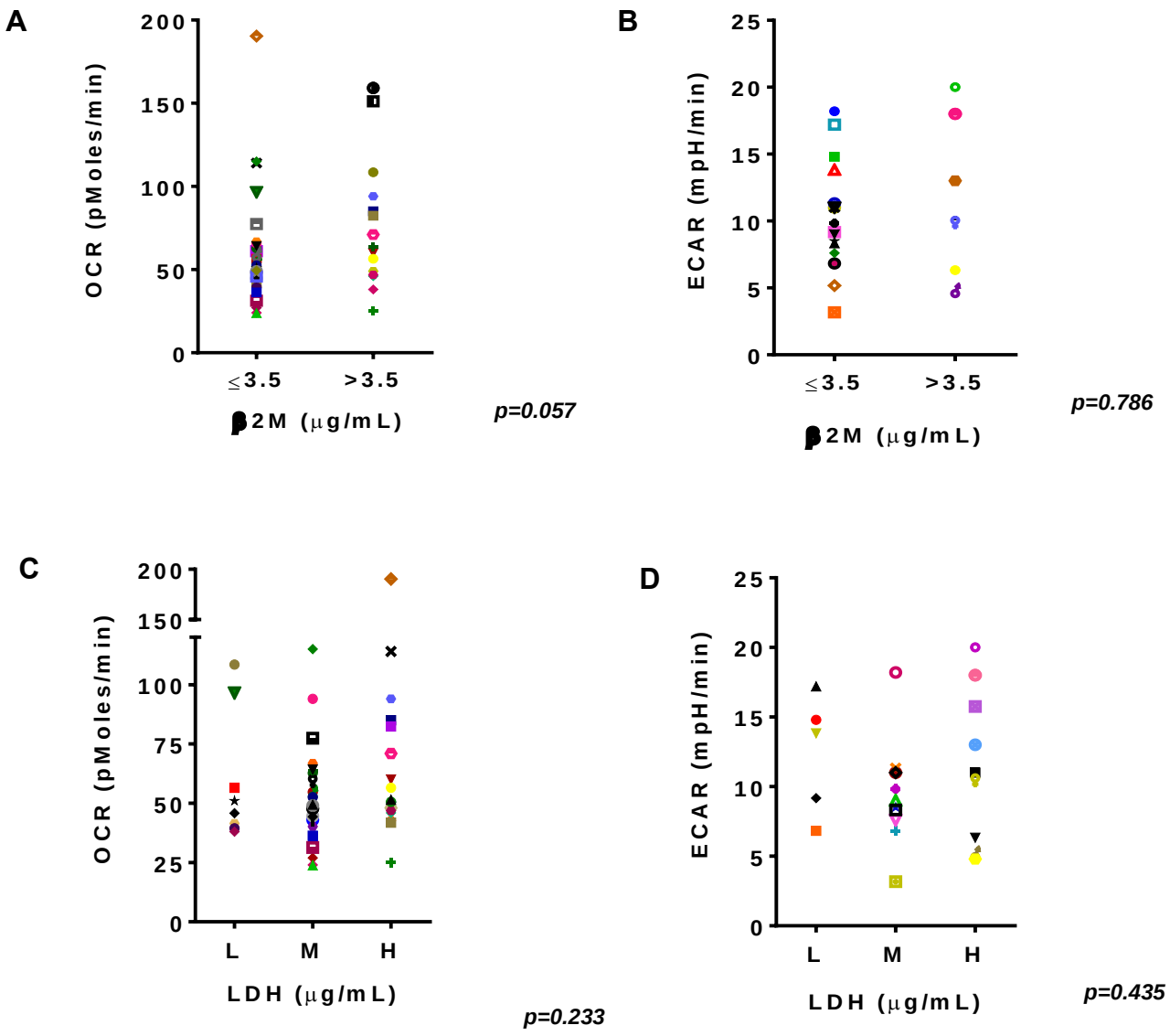

Figure 15. Correlation of CLL OCR and ECAR with LDH and β2 microglobulin levels.

A. Basal OCR from CLL cells were compared for patients classified according to β2M cut-off levels determined by CLL International Prognostic Index ≤3.5 μg/mL (n=39), >3.5 μg/mL (n=15), respectively. B. glycolytic flux of CLL cells were compared for patients with ≤3.5μg/mL (n=18), >3.5μg/mL (n=7) levels. Statistical significance was calculated using unpaired student's t-test for A and B. C. CLL OCR correlation with patient lactate dehydrogenase (LDH) levels. Basal OCR from CLL cells were compared for patients with different LDH levels: low (L) (300-500 μg/mL, n = 8), medium (M) (501-700 μg/mL, n = 26), high (H) (>700 μg/mL, n = 17). D. glycolytic flux of CLL cells were compared for patients low (L) (300-500 μg/mL, n = 5), medium (M) (501-700 μg/mL, n = 11), high (H) (>700 μg/mL, n = 9) LDH levels. Statistical significance was calculated using one way ANOVA.

The incidence of CLL is higher in males than in females (Ries L.A.G. 2003). To determine if CLL lymphocytes from men had higher metabolic profile, cell mitochondrial stress tests were performed for OCR on cells obtained from 27 male and 27 female patients. There was no statistical variation between the two cohorts (Figure 16A). However, when these cells were compared for glycolytic flux ECAR varied significantly between the two groups, with males (n=14) displaying higher glycolysis rates than females (n=13) (Figure 16B).

CLL onsets at a later stage in life and is most common in the elderly with adults above 60 years of age at a greater risk. Basal OCR of CLL cells were compared in patients of different age groups, 27 patients from ages 40-59, 14 patients from ages 60-69 and 13 patients from ages 70 and greater (Berger et al. 1978)(Figure 16C). ECAR was assessed for 12 patients from ages 40-59, 5 patients from ages and 8 patients from ages 70 and greater (Figure 16D). Both OCR and ECAR values did not correlate with age.

CD38 is a type II transmembrane glycoprotein that is expressed on the surface of hematopoietic cells. Its functions involve signal transduction and mediating cell to cell adhesion (Deaglio et al. 2011). The cut-off value for CD38 positivity is ≥20%, whereas cells with less than 20% surface expression of the receptor are considered negative. CD38 positive patients respond poorly to therapy (Durig et al. 2002) and have short survival. CD38 surface expression was measured by flow cytometry. 13 patients negative for CD38 and 7 patients positive for CD38 were assessed for OCR. Considering the sample size is relatively small, the difference between OCR of these two groups was not significant and thereby CD38 status did not impact OCR (Figure 17A).

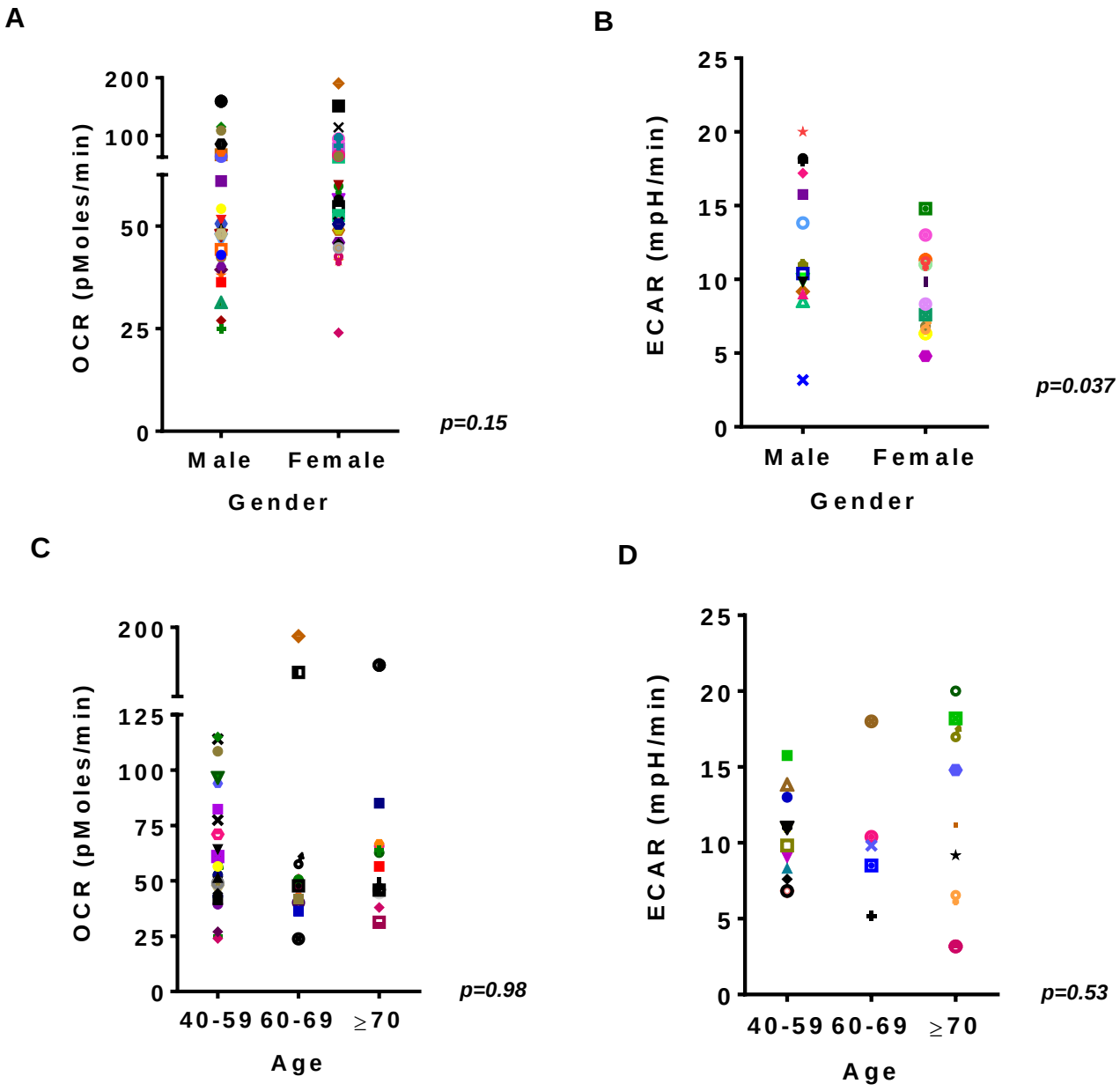

Figure 16. Correlation of CLL OCR and ECAR with patient's gender and age.

A. Basal OCR of CLL cells were compared based on the gender of the patient, male (n=27) or female (n=27). B. Glycolytic flux of CLL cells were compared based on the gender of the patient, male (n=14) or female (n=13). Statistical significance was calculated using student's unpaired t-test for A and B. C. Basal OCR of CLL cells were compared for patients of different age groups: 40-59, 60-69, ≥70 years (n = 54).D. Glycolytic flux of CLL cells were compared for patients of different age groups. Statistical significance was calculated using one way ANOVA.

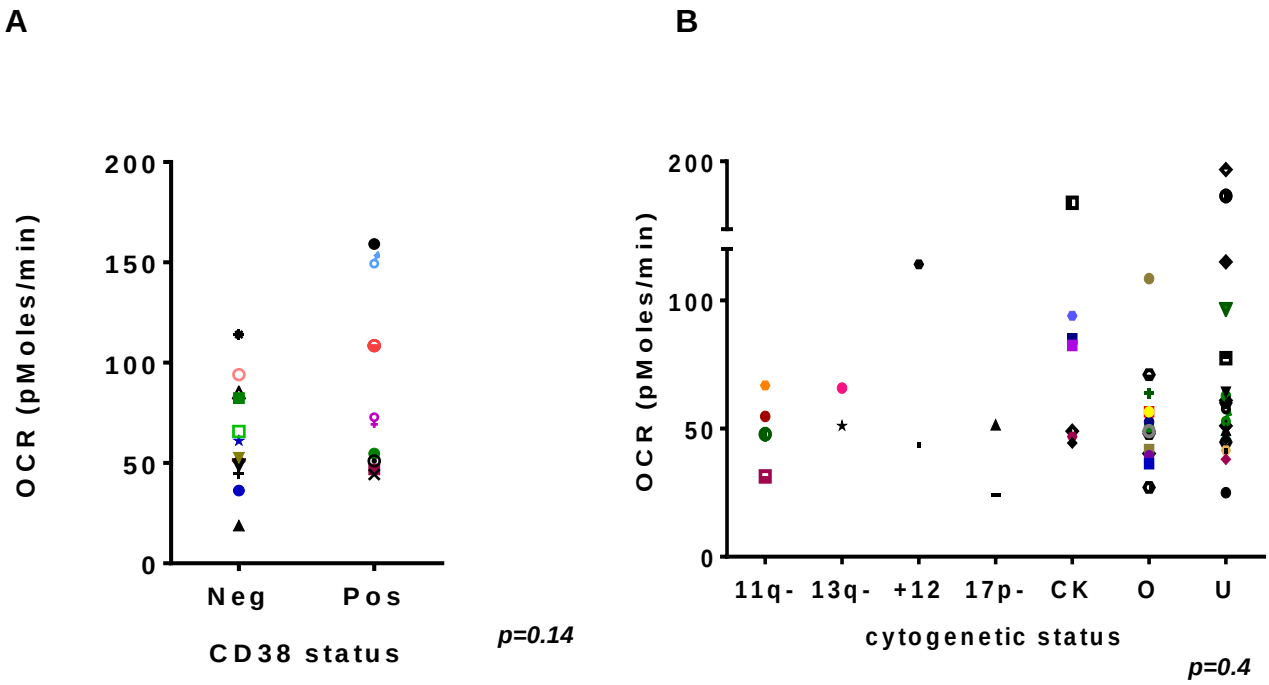

Figure 17. Correlation of CLL OCR and ECAR with patient's cytogenetic profile and CD38 status.

A. Basal OCR of CLL cells from patients expressing CD38 ≥20% (positive), <20% (negative) were compared. Statistical significance was calculated using unpaired student's t-test p=0.14 B. Basal OCR of CLL cells were compared for patients with various chromosomal abnormalities by extracellular flux analysis: 11q deletion (n = 4), 13q deletion (n = 2), 17p deletion (n = 2), trisomy 12 (+12) (n = 2). C.K. (n = 7) indicates complex karyotype with 2 or more of these deletions, O (n = 16) indicates other chromosomal abnormalities and U (n = 21) indicates unknown karyotype. Statistical significance was calculated using ANOVA p=0.4.

Impact of CLL cytogenetics on metabolism

The most common chromosomal aberrations that are identified in CLL are: 11q deletion, 13q deletion, 17p deletion and trisomy. These lesions are detected by fluorescence *in situ* hybridization (FISH) karyotyping. CLL patients were grouped based on the karyotyping results. 4 patients that are unique for 11q deletion without other major chromosomal anomalies mentioned before were grouped into 11q category. Similarly, 2 patients for 13q, 2 for 17p and trisomy 12 (+12) (n = 2). If two or more of these aberrations occur together, then the patients are categorized into complex karyotype pool (C.K.) 16 patients are classified into another cohort that exhibit other aberrations, but not these major ones listed. Karyotype for 21 patients were not done, therefore are unknown. It is difficult to correlate OCR data with cytogenetics as the sample size for these chromosomal anomalies was very small with a large portion of samples falling into the unknown category (Figure 17B).

Aim 2. Elucidate the impact of stroma on CLL-bioenergetics

Aim 2.1. Elucidate the impact of stroma on CLL OxPhos and glycolysis pathways.

CLL cells that are positive for ZAP 70 and have an IgVH unmutated status have an increased advantage for interaction with the microenvironment. Interaction with stromal cell *in vivo* and *in vitro* greatly enhances cell survival. Though a few studies touched upon the aspect of the metabolic advantaged conferred to CLL cells by interaction with stroma cells, there is still not much clarity of how stromal cells contribute to bioenergy or biosynthesis in CLL cells.

Metabolite analysis in CLL cells after stroma co-culture

My study aims at delineating the metabolic pathways that get activated in CLL cells and the change in metabolic fluxes upon interaction with stroma.

To study changes in metabolic pathways in CLL upon stromal interaction, CLL cells were obtained from 40 CLL samples and co-cultured with NK.Tert stromal cells and measured for cell death by Annexin-PI staining at the end of 24 hr. The stroma protected CLL cells from endogenous cell death (Figure 18). CLL cells were co-cultured with NK.Tert at a ratio of 100:1. CLL cells were carefully removed and harvested at the end of 24 hrs. Metabolites were extracted using 80% methanol and examined by the mass spectroscopy core for metabolite analysis. Metabolites in CLL varied in their concentrations post co-culture, and were categorized into different pathways according to their KEGG IDs (Figure 19). For this analysis, the top five hits that were identified included TCA cycle, gluconeogenesis, purine and pyrimidine synthesis, indicating that cellular metabolism is affected by co-culturing CLL cells with stroma. Some of the metabolites in the listed pathways were augmented upon co-culture. Both, bioenergy (TCA cycle) and biosynthesis (purine and pyrimidine synthesis) of CLL increased, contributing to the prolonged survival of these cells in the co-cultures. In addition, the top hit is degradation pathway of methionine, whose end products, succinyl coA and pyruvate feed into the TCA cycle

Furthermore, the metabolite analysis revealed that lactic acid levels in CLL cells were significantly elevated upon co-culture with stroma; this is in contrast with the results obtained from extracellular flux assays. Metabolite analysis also saw an increase in pyruvate levels (although not statistically significant), which might mean that lactic acid is getting

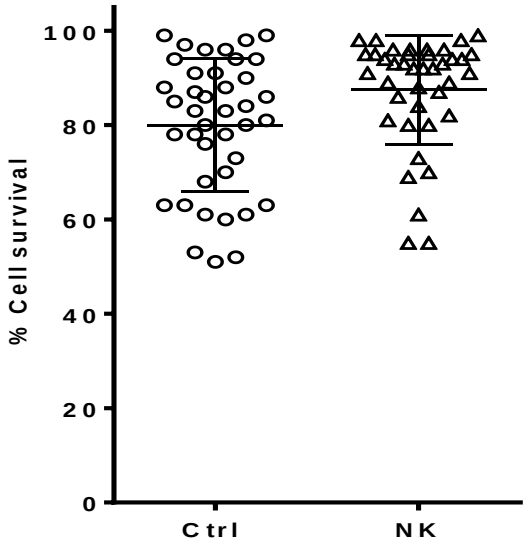

.

Figure 18. Effect of NK-Tert stromal cell co-culture on CLL cell survival.

CLL cells after isolation were either cultured in suspension (Ctrl) or co-cultured with NK.tert cells (NK) for 24hr. The cells were stained for Annexin-PI and the results were analyzed by flow cytometry. The results were analyzed by a paired student's t –test (n=40, $p<0.0001$).

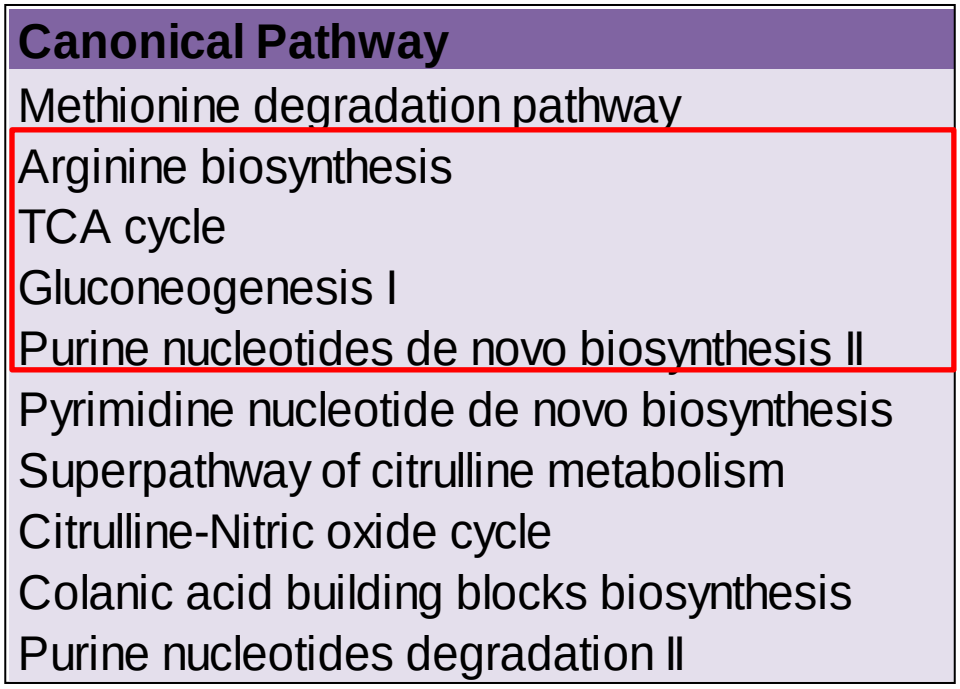

Figure 19. Effect of stroma on CLL metabolic pathways.

CLL cells from 5 patient samples were co-cultured with or without NK.Tert cells for 24hr. Metabolites were extracted with 80% methanol were assessed bymass spectrometry. Metabolites were grouped into major biochemical pathways and were analyzed using Ingenuity Pathway Analysis (IPA). Change in metabolite concentrations are expressed as stroma/suspension culture ratios.

converted to pyruvate. The metabolites that are synthesized by mitochondrial enzymes were analyzed. Orotate levels saw an increase in CLL cells post co-culture with stroma marking the increase in dihydroorotaate dehydrogenase activity

I further tested for changes in energy generating pathways, glycolysis and oxidative phosphorylation in the presence of stroma. Three stromal cell lines were employed in this study. Before CLL-stroma co-culture could be assayed for extracellular flux assays, the number of stroma cells necessary for a proper read out for OCR/ECAR needed to be optimized. NK.Tert cell line is derived from human bone marrow. These cells were marked by no spare respiratory capacity (SRC) for oxygen consumption, irrespective of cell numbers plated. HS-5, another cell line derived from bone marrow, was optimized for extracellular flux assays (See Materials and Methods). M2-10B4 cells obtained from mouse were tested similarly. These two cells lines displayed higher OCR as well as SRC when compared to NK.Tert.

Influence of stroma on CLL glycolysis

I first assessed the effect of stroma on glycolysis. CLL cells were co-cultured with NK.Tert cells for 24 hrs. Cell viability was measured in both suspension and co-culture in parallel cultures. These cells were assayed for glycolysis stress test (Figure 20A). Glycolytic flux represents the amount of glucose the cells can metabolize after injection with 10 mM glucose. The third value of OCR after glucose has been injected was recorded and non-glycolytic acidification value (obtained after addition of 2-Deoxy D-glucose) was deducted to obtain the value of glycolytic flux. The glycolytic flux was calculated for 29 patient samples.

Glycolytic capacity represents the extent to which cells can rely on glycolysis when aerobic ATP synthesis is disrupted by oligomycin (1.25 µM). This value was obtained in a similar way to that of flux-in that the third value after addition of oligomycin (or 20 minutes of mixing and measuring) was noted and the non-glycolytic acidification value was deducted from it. For all 29 patients, glycolytic flux and capacity values were obtained for CLL suspension, CLL-NK.Tert co-cultures and NK.Tert culture (Figure 20B-C). ECAR values from NK.Tert cells were deducted from the co-cultures. It is to be noted that co-cultures did not impact glycolysis of NK.Tert cells as no change was found in ECAR of NK.Tert cells assayed alone or after co-culture with CLL cells (CLL cells were removed from stroma cells after 24 hr).

CLL cells from 5 patient samples were assayed in presence of stroma, without any prior co-culture, to determine, if cell-to-cell contact causes an immediate change in metabolic flux (however, the experimental set up takes 2 hr). In CLL cells, the glycolytic flux and capacity were overall variable but did not induce statistically significant changes after co-culture with the NK.Tert cell line (in dotted lines, Figure 20 B-C).

Effect of stroma co-culture on CLL oxidative phosphorylation

In contrast, co-culture had a positive effect on mitochondrial respiration in CLL lymphocytes (Figure 21A); the 28 samples tested, either had increased basal OCR (18/28) or maximum respiratory capacity (MRC) (26/28) (Figure 21B-C).Basal OCR reading was taken before the cells were subjected to stress by addition of drugs. Basal OCR is calculated by taking the 3rd reading, which is 21 minutes after the start of the assay and after deducting the non-mitochondrial respiration value (12th reading, 3rd after the addition of Antimycin A and

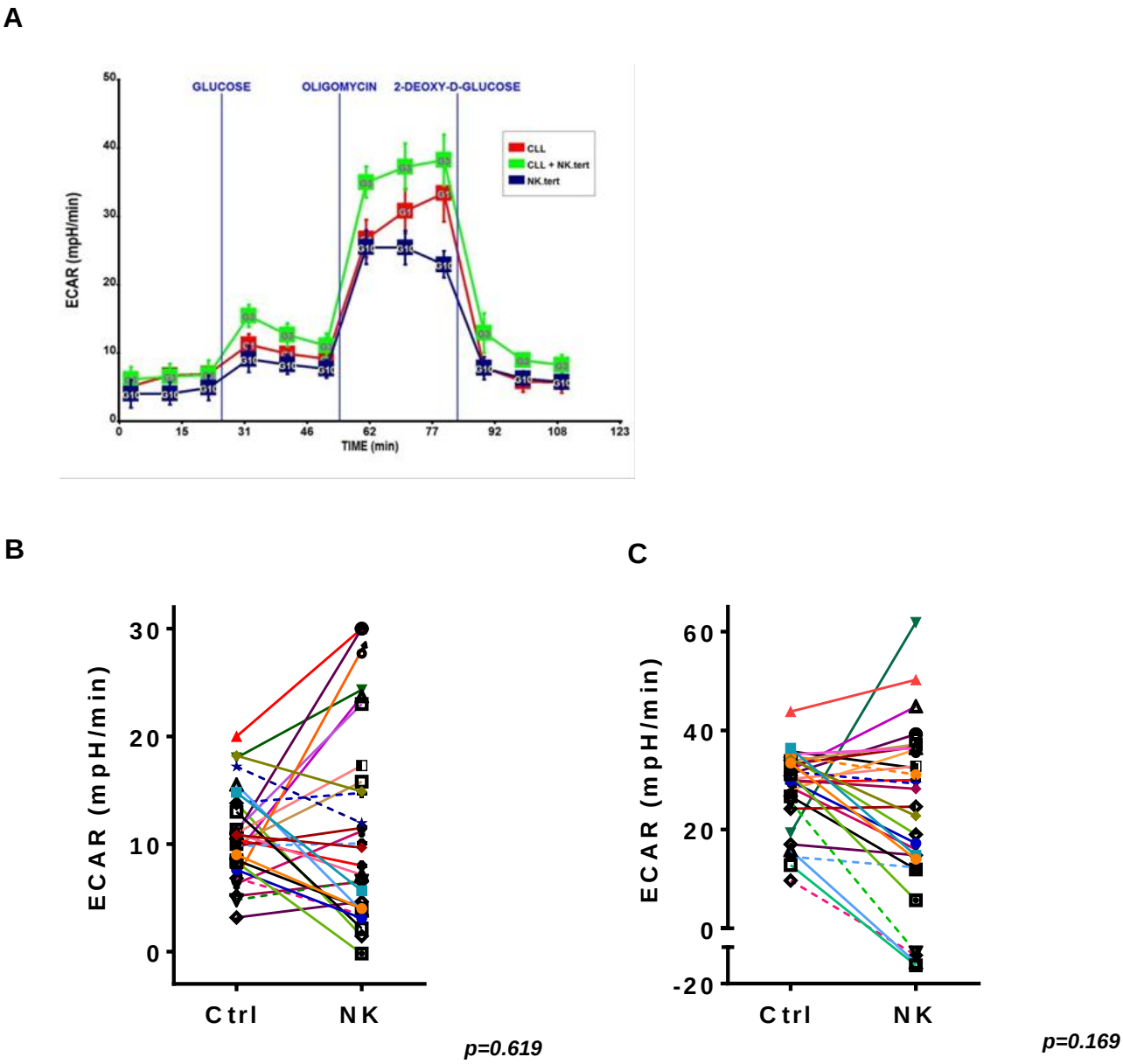

Figure 20. Effect of stromal cells on CLL glycolysis.

A. CLL cells were cultured in suspension (Ctrl) or co cultured with NK.Tert (NK) in XF96 well plates and then assayed for glycolysis. A. A representative glycolysis stress test profile from from a CLL patient (#9) cells in suspension culture (red curve), CLL-NK.tert co-culture (green curve), and only NK.tert cells (blue curve) assayed after 24 hr in culture. B. Similarly cultures as in figure A were assayed for either 2 hours (n = 9, dashed lines) or 24 hours (n = 20, solid lines) and glycolytic flux was measured. C. Glycolytic capacity of 29 CLL samples, 20 minutes after addition of oligomycin was measured. Statistical significance was calculated using paired student's t-test.

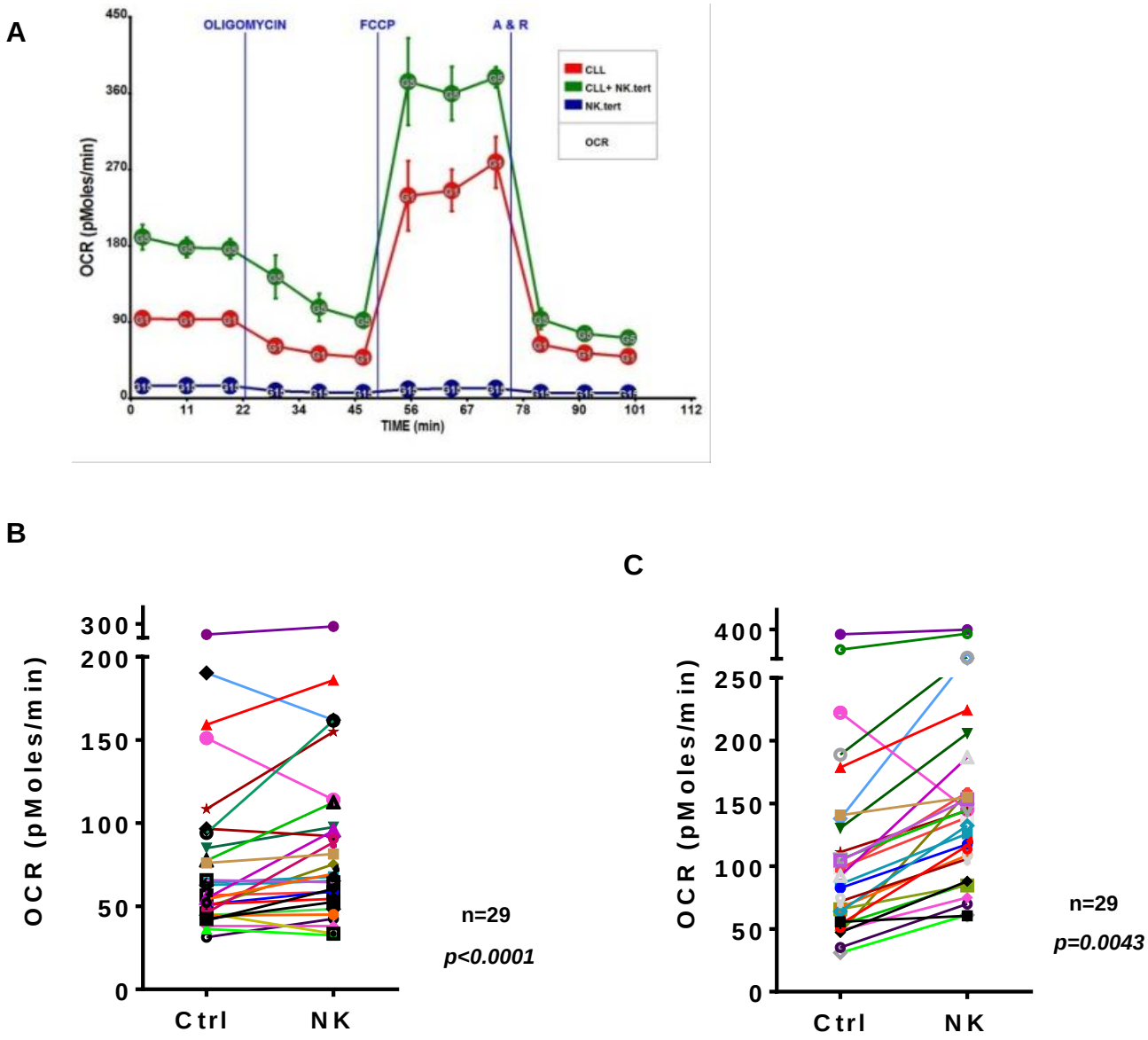

Figure 21. Effect of stromal cells on CLL oxidative phosphorylation.

A.CLL cells were cultured in suspension or co cultured with NK.Tert in XF96 well plates for 24hr and then assayed for oxygen consumption. Mitochondrial stress test profile of CLL patient sample (#30). CLL cells in suspension culture (red curve), co-culture on stroma (green curve), and only NK.tert cells (blue line) were assayed. B.CLL basal OCR was compared after 24 hours or 2 hours (n=12) in suspension (Ctrl) versus stromal co-cultures (NK). C. Similarly, CLL maximum respiration capacity was also analyzed pre– and post–co-culture for 24 hours (n = 28). Statistical significance was calculated using paired student's t-test.

Rotenone). MRC is the cellular respiratory capacity of complex I/II when uncoupled from the rate-limiting complex V. NK.Tert cells alone showed very low OCR, and this value was subtracted from the reading obtained in stromal co-culture CLL cells. Furthermore, CLL cell addition to stromal cell culture did not affect stromal OCR (Figure 22).

The basal OCR and MRC augmentation was also observed with 2 other stromal lines, HS-5 and M2-10B4. CLL cells from 8 patient samples were co-cultured with M2-10B4 and assayed for OCR (Figure 23). Similarly, cells from 3 patient samples were co-cultured with HS-5 (Figure 24). Co-culture with HS-5 stromal cells increased CLL OCR as well. Stroma-mediated increase in OCR was not due to an increase in the proliferation index, as CLL cells on stroma stained negative for Ki67 (not shown).

Correlation between CLL prognostic factors and stroma induced OCR

It would be interesting to investigate if stroma co-culture differently impacts CLL OCR in relation with prognostic markers. To start with, markers that affected OCR based on their expression levels were assessed. CLL samples in suspension and co-culture that are ZAP 70 negative (n=11), and those that are positive for ZAP 70 were analyzed (n=21). Both of the groups demonstrated a statistically significant increase in OCR (Figure 25A).

CLL samples in suspension versus co-culture that are IgVH mutated (n=11) and that unmutated (n=19) were compared for OCR and analyzed for statistical significance using paired student's t-test (Figure 25B). Both the groups showed an increase in OCR upon co-culture.

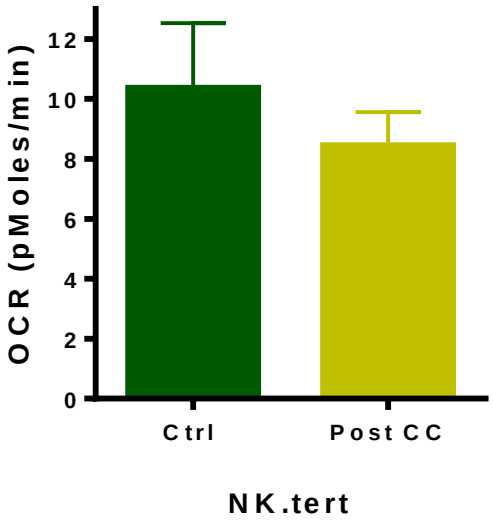

Figure 22. Effect of CLL co-culture on stroma OCR.

NK.tert cells were cultured alone (Ctrl) or with CLL cells (Post CC) for 24hrs (n=3) and were assayed for OCR. Statistical significance was calculated using paired student's t-test

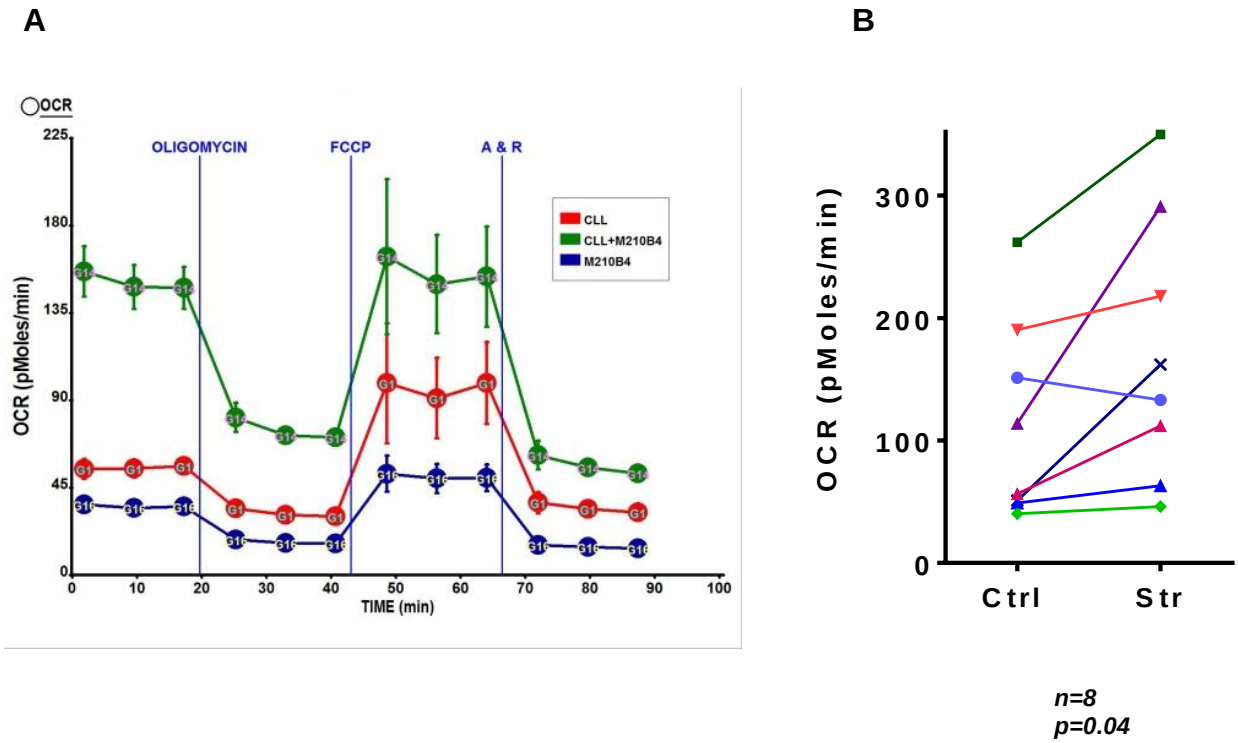

Figure 23. Effect of M2-10B4 stromal cell co-culture on CLL oxidative phosphorylation.

CLL cells were cultured in suspension or co-cultured with M2-10B4 in XF96 well plates for 24hr and then assayed for oxygen consumption. A. Cell mitochondrial stress test profile of one patient sample (#45). CLL cells in suspension (red curve), CLL-M2-10B4 co-culture (green line), and M2-10B4 cells (blue line) were analyzed. B. Basal OCR of 8 patient samples in suspension (Ctrl) or with M2-10B4 co-cultures (Str) described in A was compared. Statistical significance was calculated using paired student's t-test.

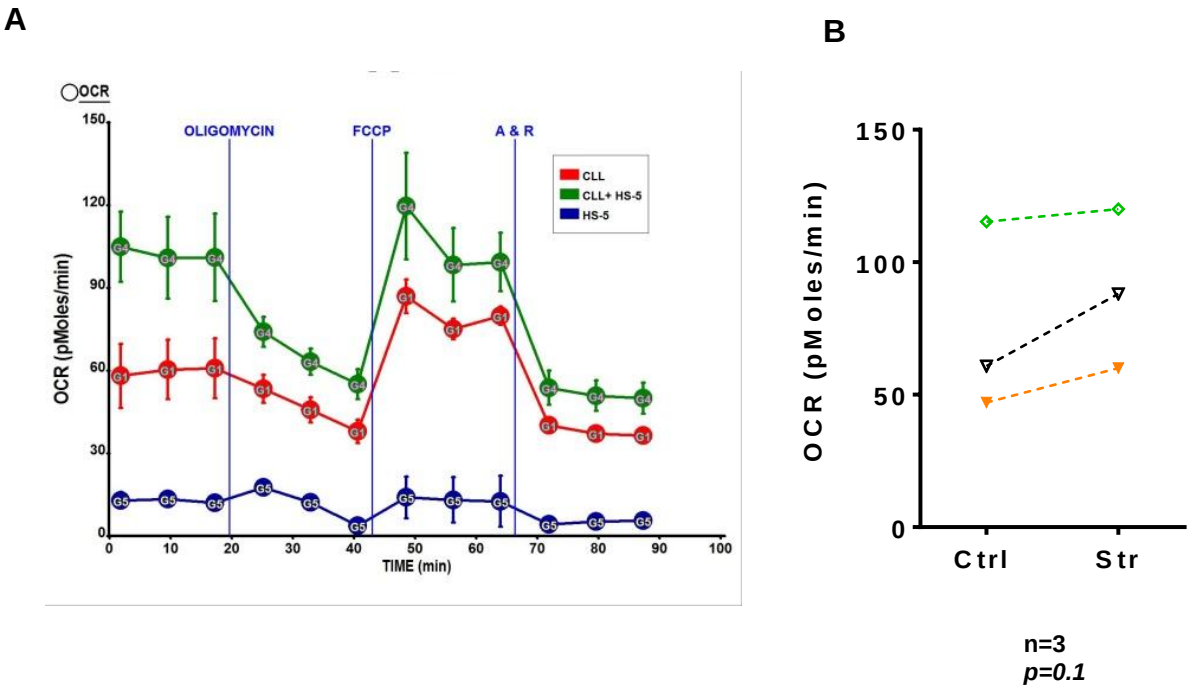

Figure 24. Effect of HS-5 stromal cell co-culture on CLL oxidative phosphorylation.

A. CLL cells cultured in suspension or co cultured with HS-5 in XF96 well plates for 24hr and then assayed for oxygen consumption. CLL cells in suspension (red curve), CLL-HS-5 co-culture (green line), and HS-5 cells (blue line) were analyzed. B. Basal OCR of 3 patient samples from suspension (Ctrl) versus HS-5 co-cultures (Str) described in A was compared. Statistical significance was calculated using paired student's t-test.

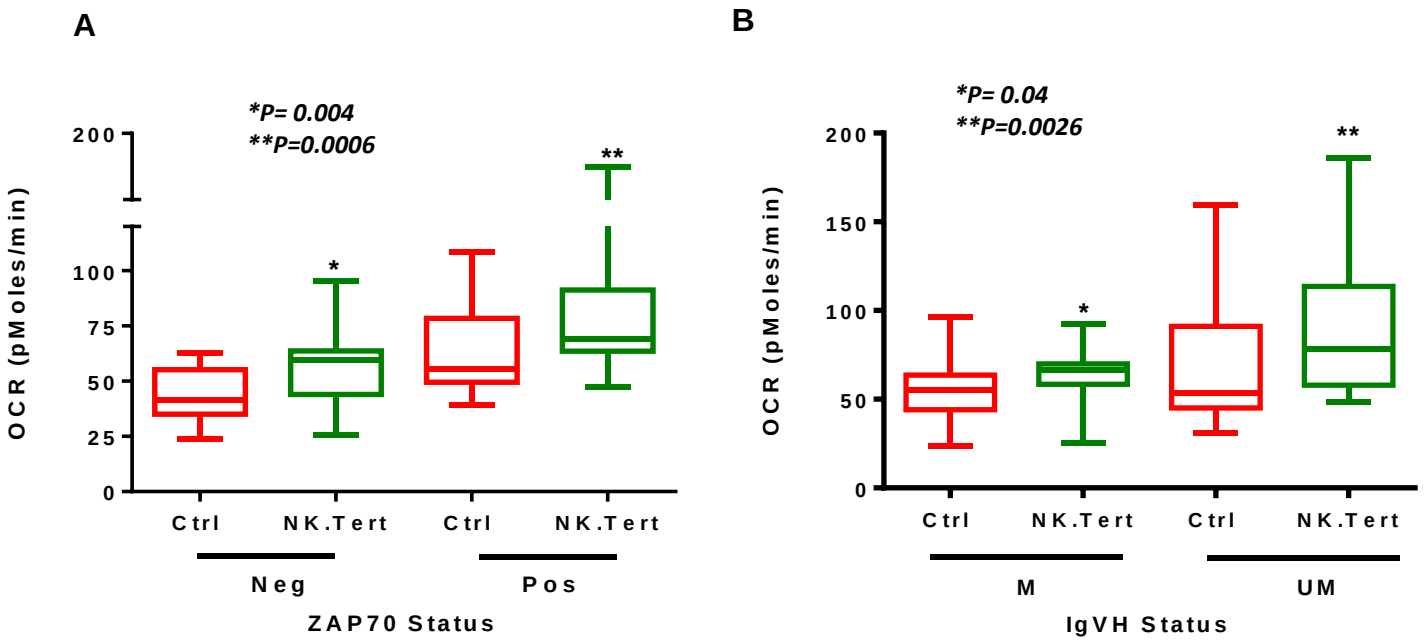

Figure 25. Differential impact of stroma on CLL OCR based on ZAP 70 status and IgVH mutation.

Basal OCR of CLL cells in suspension (Ctrl) or NK.Tert co-culture were compared for patients based on A. ZAP 70 expression; negative (n=11), positive (n=21) B. IgVH status, mutated (n=11), unmutated (n=19). Statistical significance was calculated using paired student's t-test.

Similarly, for CLL cells from patients with benign disease (Rai stage 0,1 (n=26)), displayed a statistical increase in OCR upon co-culture (Figure 26A). Whereas, patients with advanced disease did not show significant OCR induction. Similarly, in patients with low serum β2M levels (<3.5μg/mL (n=12)) and high β2M levels ≥3.5μg/mL (n=24)) -B), OCR was upregulated upon co-culture. Patients with intermediate LDH levels showed a significant increase in OCR on stroma (n=18), although stroma did not induce OCR in CLL patients with low or high LDH levels (Figure 26C).

Stroma upregulated OCR in CLL cells obtained from patients irrespective of gender and those that belong to ages 40-59 and greater than 70 (Figure 27). Basal OCR from patients that are CD38 negative showed a significant increase in basal OCR upon co-culture with stroma, whereas the positive cohort did not (Figure 28A). Stroma modulated CLL OCR did not correlate with patient chromosomal abnormalities (Figure 28B).

Aim 2.2. Determine if stroma regulates mitochondrial metabolism via cell-to-cell contact or secretion of growth factors.

The mechanism by which stroma upregulates CLL OxPhos is unknown. Growth factors secreted by stroma that promote cell survival, proliferation or chemotaxis may be responsible for changes in oxygen consumption. To test this possibility, the minimal essential medium in which NK.Tert cells were grown for 24hrs was added to freshly isolated CLL cells and assayed for OCR after 24hr. This did not increase CLL OxPhos in the two patient samples tested (Figure 29). Similarly, conditioned media in which M2-10B4 cells are cultured did not increase OCR in CLL cells.

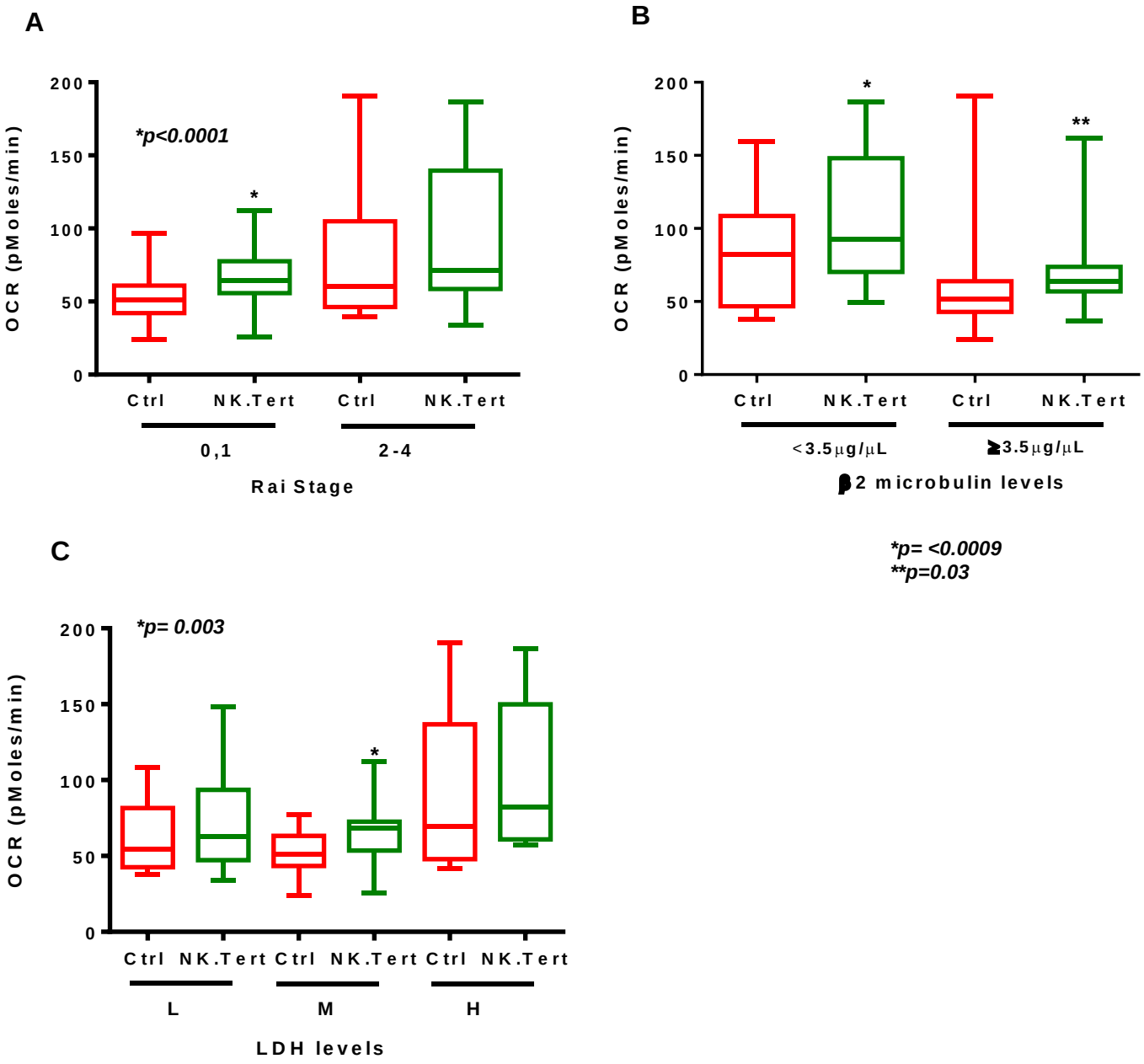

Figure 26. Differential impact of stroma on CLL OCR based on Rai stage, β2M and LDH levels.

Basal OCR of CLL cells assayed in suspension (Ctrl) vs NK.Tert co-culture were compared based on Rai stage, β2M and LDH levels of patients. A. benign Rai stage, 0,1 (n=26), advanced stage 2-4(n=16) B. β2 microglobulin levels <3.5µg/mL (n=12) and ≥3.5µg/mL (n=24) C.LDH levels Low, (301-500) (n=9); medium (501-700)(n=18) and high (≥700) (n=12). Statistical significance was calculated using paired student's t-test.

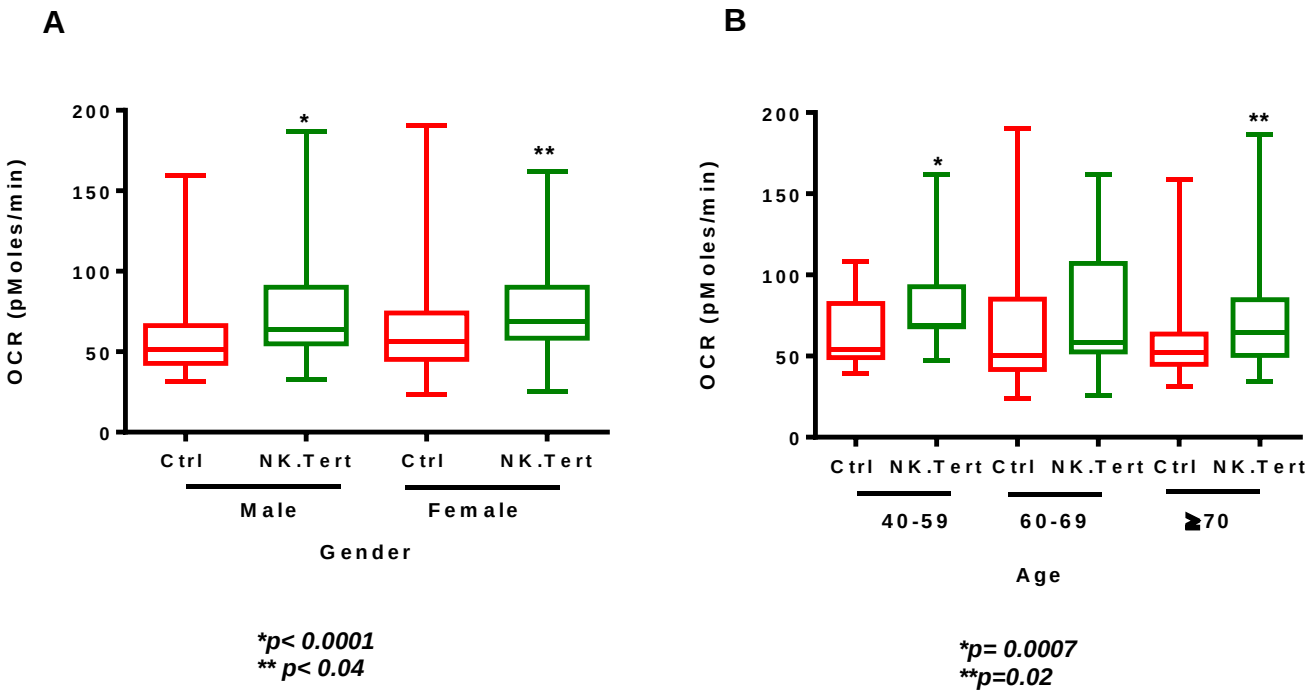

Figure 27. Differential impact of stroma on CLL OCR based on gender and age.

Basal OCR of CLL cells in suspension (Ctrl) versus NK.Tert co-culture were compared for patients based on gender and age A. Gender, male (n=21), female (n=18); B. Age (40-59) n=15, (60-69) n=12, (≥70) n=12; Statistical significance was calculated using paired student's t-test.

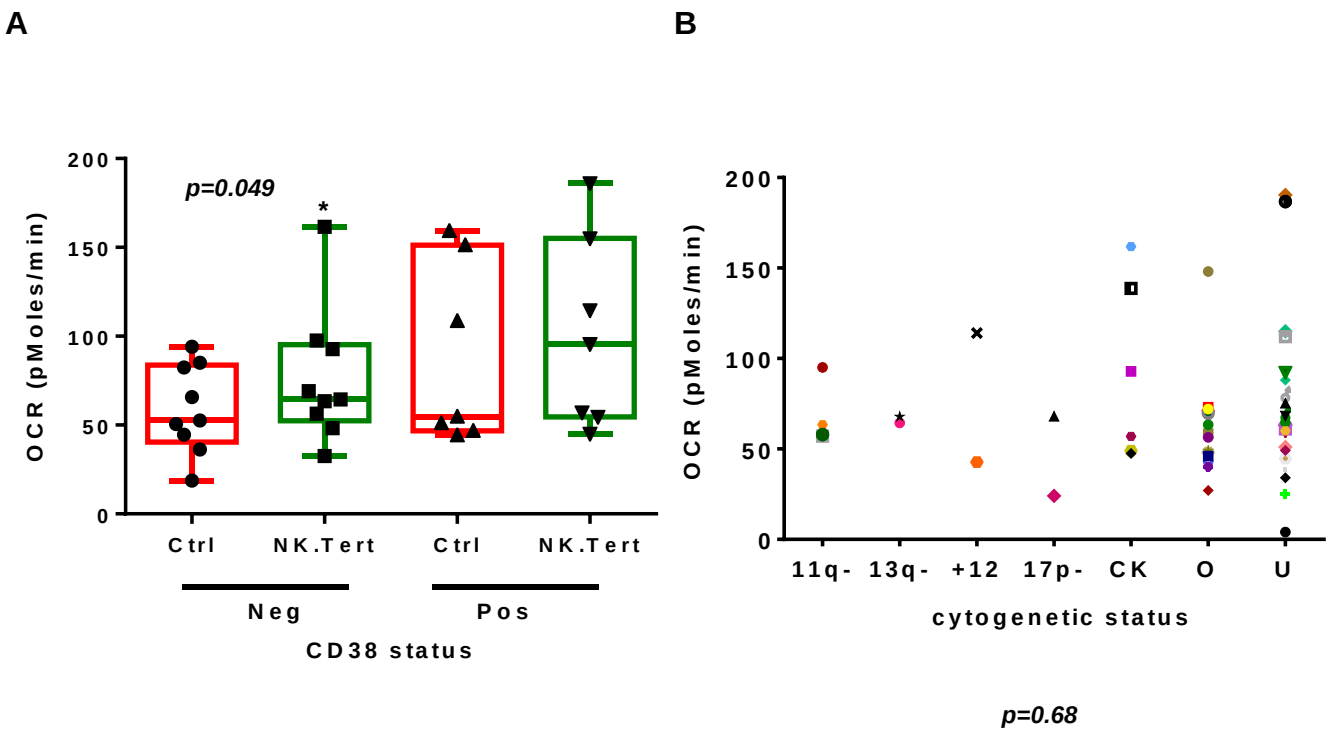

Figure 28. Stroma modulated CLL OCR correlation with patient chromosomal abnormalities.

A. Basal OCR of CLL cells in suspension (Ctrl) versus NK.Tert co-cultures from patients expressing CD38 ≥20% (positive), <20% (negative). Statistical significance was calculated using paired student's t-test. B. Basal OCR of CLL cells after co-culture were compared for patients with various chromosomal abnormalities: 11q (n = 4), 13q (n = 2), 17p deletions (n = 2), trisomy 12 (n = 2). C.K. (n = 6) indicates complex karyotype with 2 or more these deletions, O indicates other chromosomal abnormalities (n = 13), U indicates unknown karyotypes (n = 21) were compared. Statistical significance was calculated using one way ANOVA p=0.68

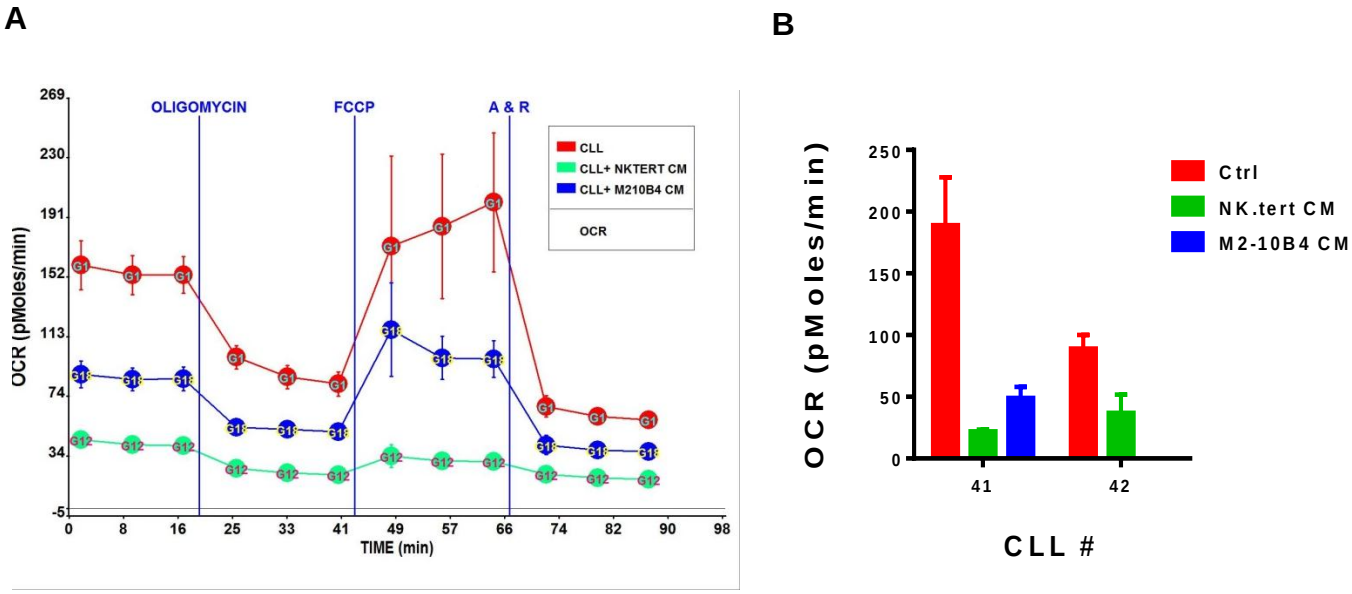

Figure 29. Effect of conditioned media culture on CLL OxPhos.

A. Basal OCR of CLL cells in suspension culture (red curve) was compared with CLL cells cultured in conditioning media (CM; media from stroma cultures was removed 24hr after its addition) from NK.Tert (green curve) or M2-10B4 cells (blue curve). B. Basal OCR of CLL cells (n=2) in suspension culture were compared to the cells in conditioning media; five technical replicates were used.

The possibility of growth factors secreted by stroma cells into media that could regulate oxygen consumption of CLL cells can be excluded.

Stroma derived factor-1 (SDF-1), is a chemokine that binds to the CXCR4 receptor on the CLL cell surface and helps the cells in chemotaxis towards the bone marrow. Exogenous SDF-1, which is secreted as a soluble protein that activates CLL cells and induces proliferation and differentiation, is incubated with CLL cells from (n=2). These cultures were then assayed for OCR (Figure 30A).

BAFF on the other hand, resulted in a decrease in CLL OCR (Figure 30B). SDF-1 and BAFF were added together to CLL suspension cultures to test if they complement in inducing oxygen consumption. But, both the cytokines taken together did not cause any effect on CLL oxygen consumption (Figure 30B).

These experiments with conditioning media and cytokines suggest that contact with stroma cells may be necessary to induce OCR. To test the possibility of cell adhesion causing the augmentation in OCR, experiments using fibronectin in place of stroma were performed.

Fibronectin is a glycoprotein that binds to integrins in the extracellular matrix (Pankov and Yamada 2002). It can also be secreted by stroma cells by which CLL cells adhere to bone marrow/lymph nodes *in vivo*. CLL cells were cultured on fibronectin coated XF96 plates in increasing concentrations (5, 10, 15, 20µg). After 24hr, these cells were assayed for OCR. Fibronectin decreased CLL OCR and therefore did not mimic stroma co-culture (Figure 31). Furthermore, CLL cells were incubated with IgM to activate the B-cell signaling pathway and assayed for OCR (n=5). IgM did not result in increase in oxygen consumption either (Figure 32A)

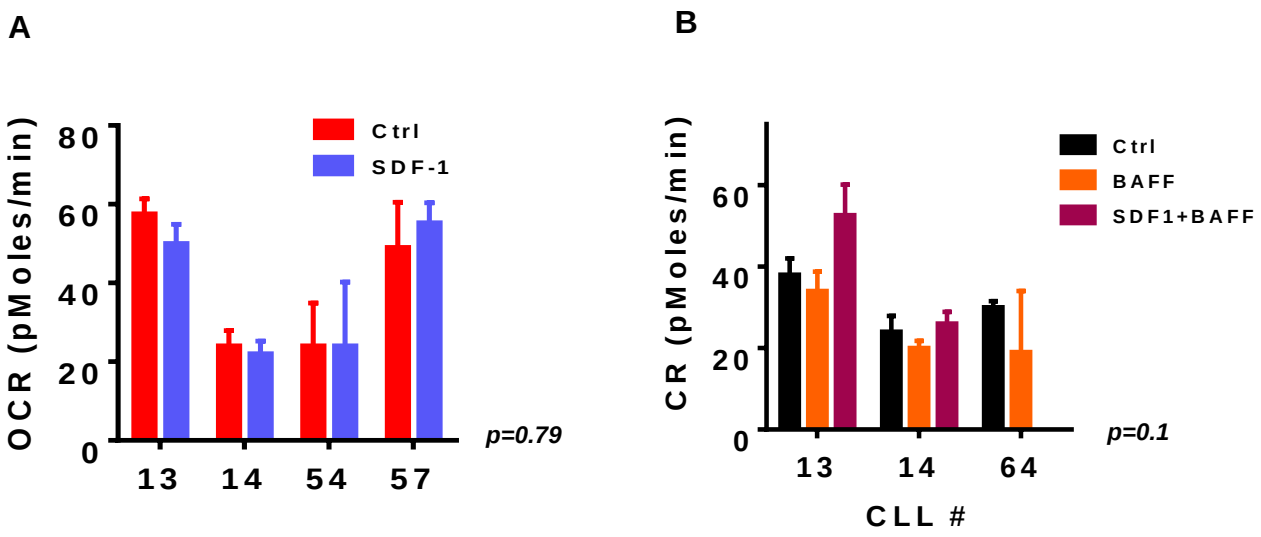

Figure 30. Effect of chemokines on CLL oxygen consumption.

A. CLL cells were assayed for OCR after incubation with SDF-1 (250 ng/mL) B. CLL cells were assayed for OCR after incubation with BAFF (150 ng/mL) or SDF-1 + BAFF for 24hr. Paired student's t-test was used to calculate statistical significance.

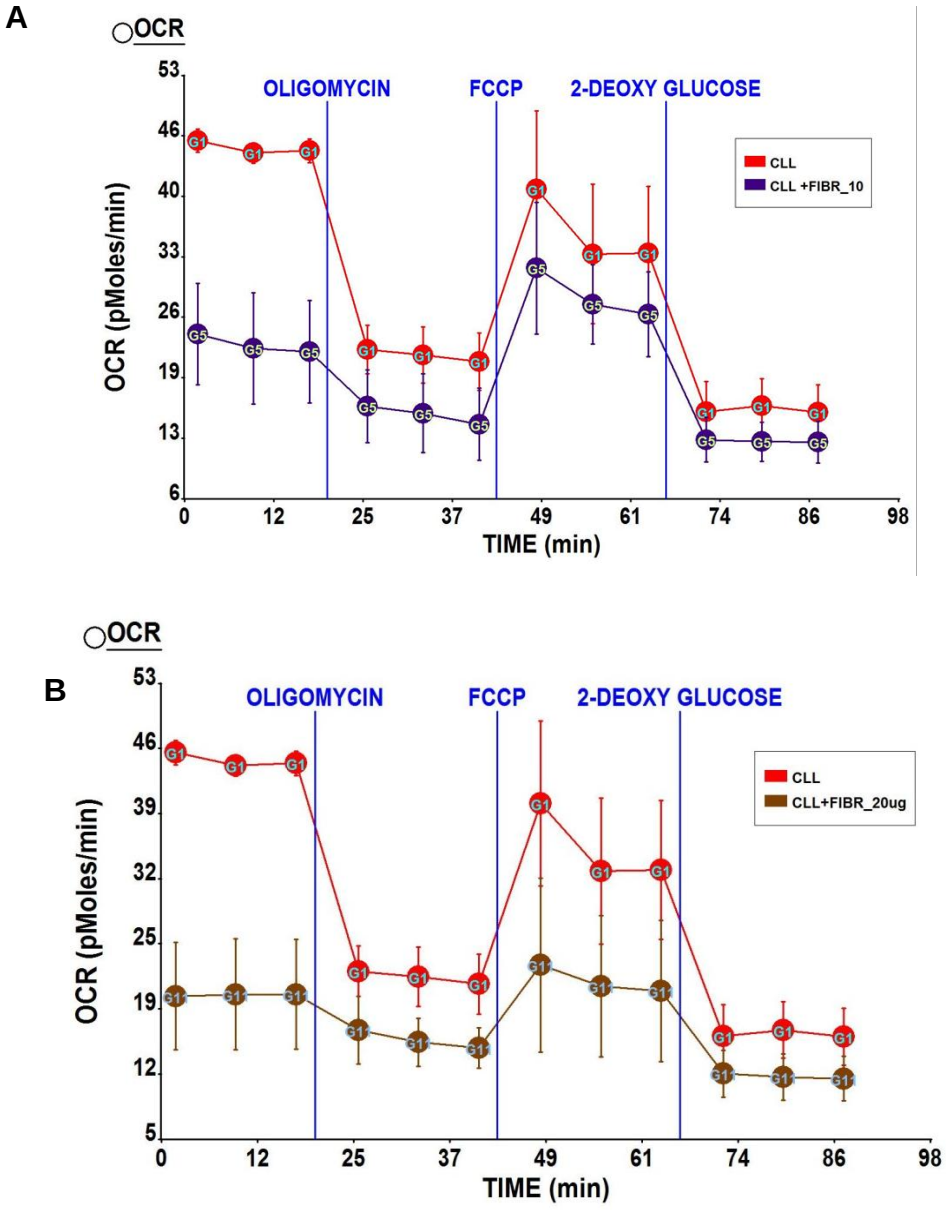

Figure 31. Impact of fibronectin culturing on CLL OxPhos.

CLL cells cultured on fibronectin coated XF96 plates for 24 hrs were assayed for OCR. A. CLL OCR in suspension (on cell tak) versus culture on 10 µg fibronectin. B. CLL OCR in suspension (on cell tak) versus culture on 20 µg fibronectin.

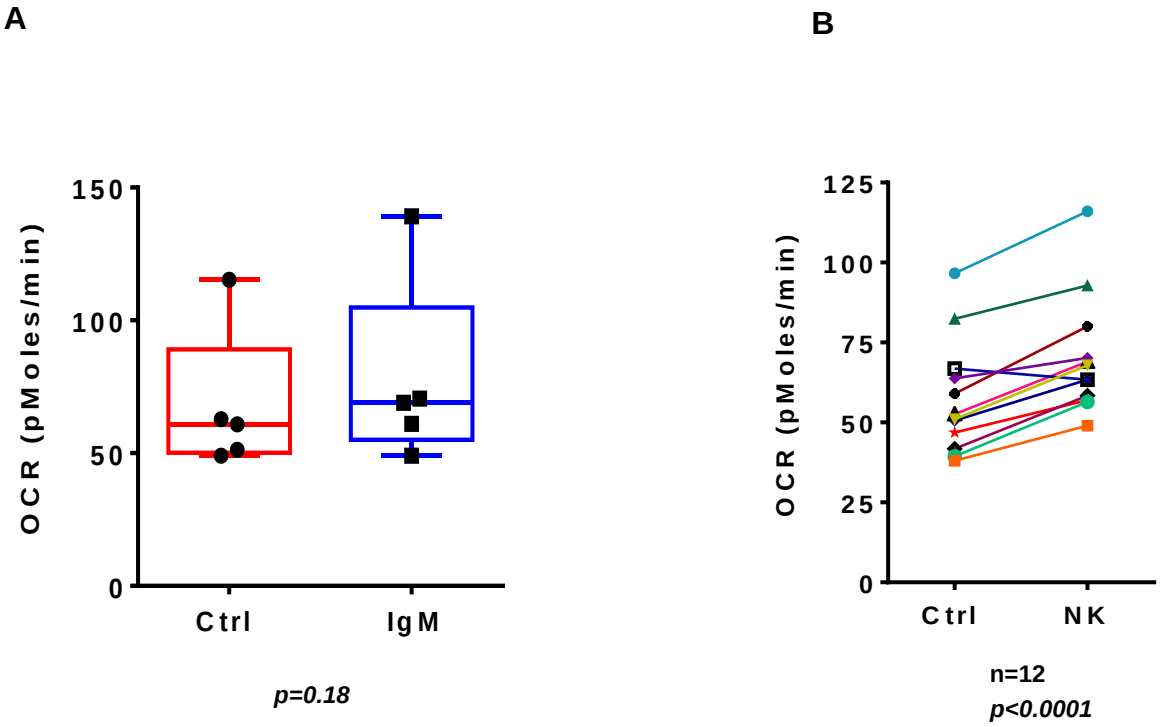

Figure 32. Effect of IgM stimulation or immediate stromal contact on CLL oxygen consumption.

A.CLL cells were assayed for OCR after incubation with IgM (10μg/mL) for 24hr. B. CLL basal OCR was compared after 2 hours of stromal co-cultures (NK) with corresponding suspension cultures (Ctrl) of 12 patient samples. Paired student's t-test was used to calculate statistical significance.

This underpins that stromal cell contact is necessary for induction of OCR. To confirm this, CLL cells were plated on top of NK.Tert cells, just before the beginning of the assay without any prior co-culture. The experimental set up takes about two hours, therefore CLL-stroma cells were in contact for 2hr before the assay. Induction of stromal-mediated CLL cell OCR increase was an early event; 11 of 12 CLL samples showed a statistically significant increase in basal OCR but not MRC when plated on stroma for 2 hours (Figure 32B).

Aim 2.3 Evaluate the impact of stroma co-culture on substrate uptake, ATP pools and mitochondrial biology, by CLL cells.

Effect of stroma co-culture on glucose and glutamine uptake by CLL cells

The most important building blocks necessary for cellular bioenergy and biosynthesis are carbon and nitrogen. Glucose is a major source of carbon, whereas glutamine provides nitrogen to the cell. Glucose and glutamine are also the most important substrates for ATP production along with fatty acids. Since, stroma promotes oxidative phosphorylation in CLL, it would be necessary to test if glucose or glutamine consumption to fuel OxPhos/TCA cycle would be enhanced as well.

In previous studies, it has been shown that stroma co-culture activates PI3K/AKT signaling pathway. Active AKT signaling is related to increase in glycolysis and glucose uptake. From experiments in Aim 2.1, it is clear that though AKT signaling is active (it was demonstrated in previous studies that stroma interaction promotes AKT activation in CLL), glycolysis in CLL cells was not promoted, atleast in terms of conversion of glucose to lactate. There is a possibility that glycolysis, is in fact upregulated in presence of stroma,

however, glucose is converted to pyruvate and fed into the TCA cycle, instead of getting converted to lactate.

To determine whether stroma co-culture may induce CLL cells to take up more glucose, its uptake was measured in CLL cells, 24hrs after co-culture with NK.Tert cells. The procedure for uptake of [H^3]-2-Deoxy-D-Glucose assay is described in materials and methods section. The results were quantitated based on cell number. It was surprising that glucose uptake was lower after stroma co-culture, in all 7 samples measured as compared to suspension culture (Figure 33A). In addition, I also tested the levels of glucose transporter GLUT4 (commonly expressed in CLL), in CLL cells after co-culture with stroma in 11 patient samples. There was slight increase in expression of GLUT4 in 2 of 11 samples (Figure 33B).

Many malignant cell types have been shown to increase the catabolism of glutamine to supplement their increased metabolic needs and also become addicted to it (Eagle 1955); It may be possible that CLL cells switch their carbon source preference upon interaction with stroma, and therefore an alternative carbon source could be utilized. Therefore, glutamine uptake in CLL cells with and without co-culture on stromal cells was measured. However, glutamine increase was heterogeneous, as cells obtained from only 3 of 7 samples, showed an increase on stromal interaction (Figure 33A). As controls, CLL samples were stimulated with insulin (obtained from bovine pancreas) or IgM half an hour before the glucose and glutamine experiments. This did not impact the outcome of the experiments significantly (data not shown).

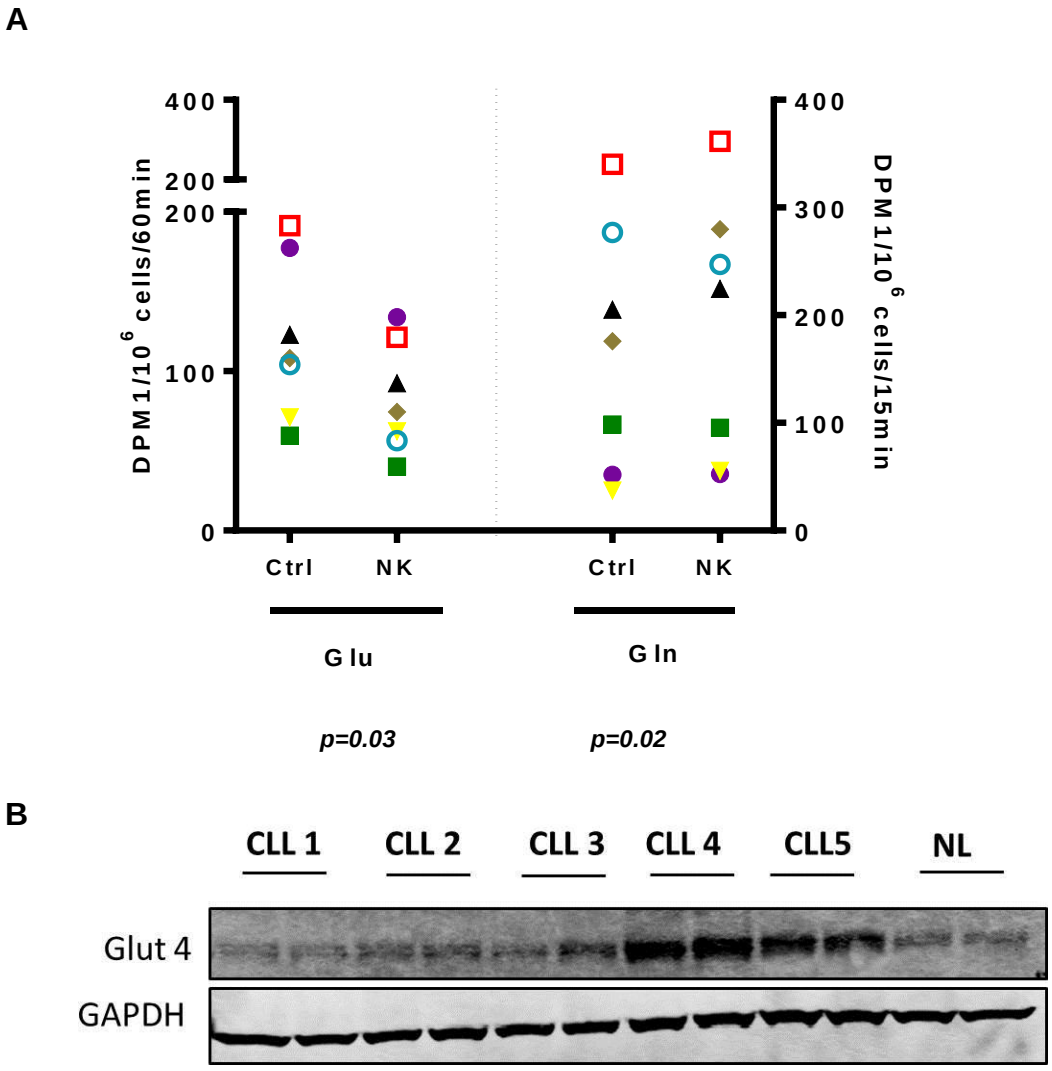

Figure 33. Effect of NK.Tert on substrate uptake and glucose transporter levels in CLL.

A. Effect of stroma on glucose (Glu) and glutamine (Gln) uptake in CLL cells. [^{3}H] 2-Deoxy-ɒ-glucose was used to determine the cellular uptake of the substrate in CLL cells (n=7) in suspension (Ctrl) or with (NK) co-culture, and analyzed for statistical significance. Three technical replicates were performed for suspension and co-culture. Disintegrations per minute (DPM)/60 min were normalized to 10^6 cells. Similarly, [^{3}H] glutamine was used to compare cellular uptake of the substrate in CLL cells (n=7), before and after co-culture; DPM/15 min were normalized to 10^6 cells. B. Immunoblot analysis of whole-cell extracts of control (C) and NK.tert co-culture (N) of CLL cells (n=5) and normal lymphocytes (NL). Proteins were extracted and analyzed using antibodies to detect protein levels of GLUT4. GAPDH serves as loading control.

Effect of stromal co-culture on ATP production in CLL

As OxPhos and energy production feed into nucleotide biosynthesis, levels of intracellular ribonucleotide pools were measured. CLL cells after 24 hr (n=12) and 48hrs (n=6) of co-culture with NK.Tert cells were assayed for changes in NTP pools levels. Of the 4 ribonucleotide triphosphates, ATP (adenosine triphosphate), GTP (Guanine triphosphosphate), and CTP (Cytosine triphosphate) pools showed 40% increase and the UTP (Uridine triphosphate) pool showed a 150% increase after interacting with NK.Tert cells at 24 and 48 hours (Figure 34A). Endogenous concentrations were normalized as 100%. In 6 out of 12 samples assayed post 24hrs, a significant increase in all NTP pools was observed, and in the rest of the samples, only a modest increase was detected. Cell viability, number and size were taken into consideration while calculating the NTP pools. Additionally, CLL cells were also co-cultured with M2-10B4 cells for 24hr and were assayed changes in NTP pools (Figure 34B). There was a significant increase in all NTP pools in 4 of 5 patient samples measured.

Although, an overall increase in NTP pools was not anticipated, augmentation of ATP pools consolidated the increase in oxidative phosphorylation of CLL after co-culture.

Effect of stromal co culture on mitochondrial functionalities of CLL

Since mitochondrial respiration increased in CLL in presence of stroma, it is likely that mitochondrial functionalities like generation of reactive oxygen species (ROS) and mitochondrial outer membrane potential (MOMP) also get affected. Therefore, changes in ROS and MOMP in CLL cells were measured 24 hours after co-culture by flow cytometry. Of the 8 patients measured for ROS, only one of them showed a significant downregulation

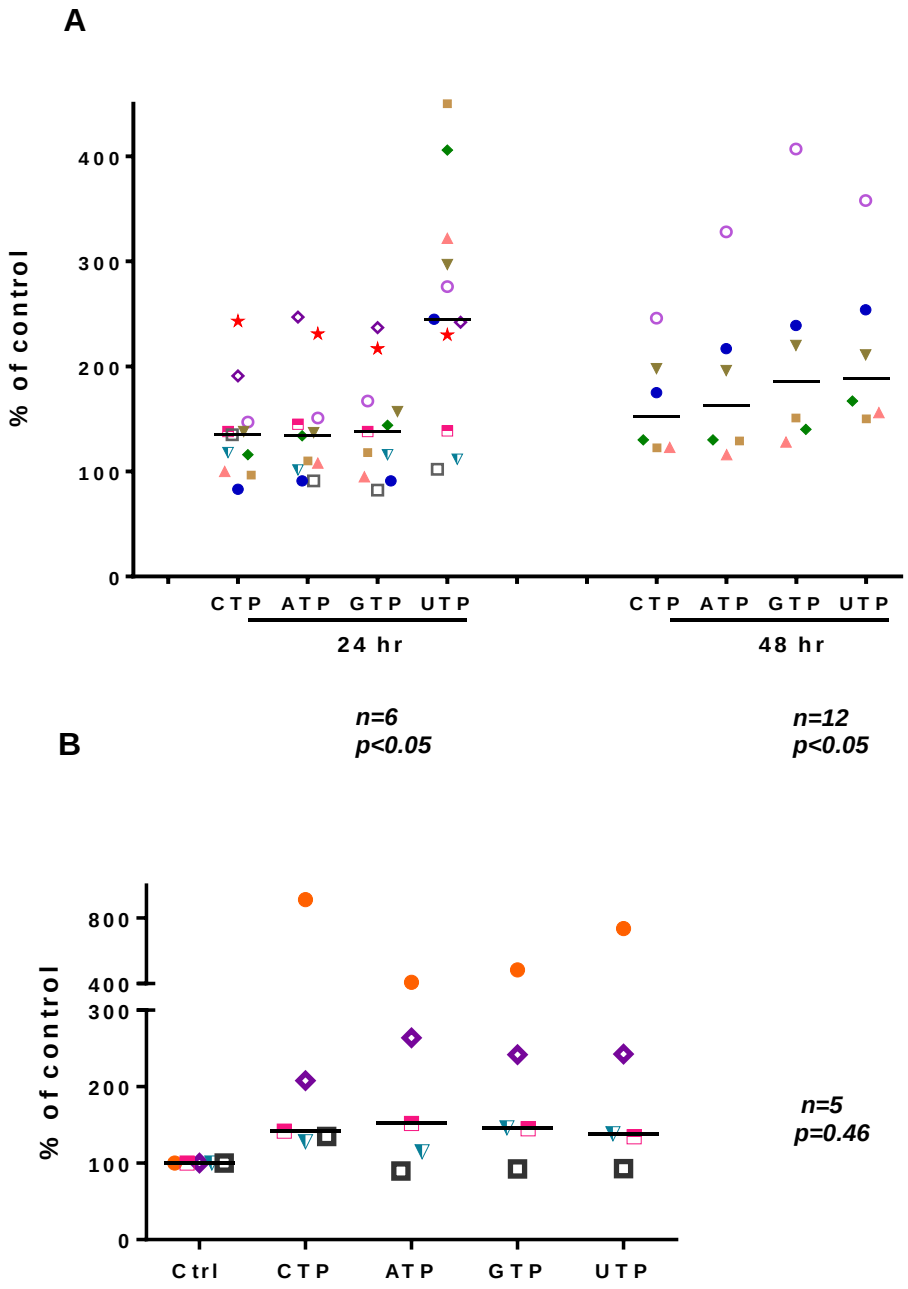

Figure 34. Effect of stroma co-culture on CLL intracellular nucleoside triphosphate pools.

A.NTP pools were extracted using perchloric acid from CLL cells after 24 (n=11) or 48(n=6) hours of co-culture with NK.Tert cells and analyzed using high performance liquid chromatography (HPLC). B. Similar to A, NTP pools were extracted from CLL cells in suspension and corresponding co-cultures with M2-10B4 cells (n=5) after 24hr. Statistical significance was analyzed by using one way ANOVA.

upon co-culture (Figure 35A); otherwise changes in ROS levels were sparing. Similarly, no significant changes were observed in MOMP in suspension version co-cultures (n= 3).

To test for the possibility of mitochondrial fission, changes in mitochondrial mass and mtDNA copy number in CLL cells upon coculture, all three were analyzed by flow cytometry. Mitochondrial mass was not affected after 24 hours after co-culture (n=3) (Figure 35A). Similarly, mtDNA copy number was analyzed in 4 patient samples (Figure 35B). In one sample, the copy number decreased contrary to what was expected, and rest of the samples recorded no major change.

Effect of stromal co-culture on CLL mitochondrial complexes function and activity.

Electron transport chain is the major physical component of oxidative phosphorylation. It consists of five major complexes inclusive of the ATP pump. It is necessary to probe for changes in the expression and activity of these five complexes. Whole cell extracts from CLL samples (n=6) were probed for NADH dehydrogenase (CI), succinate dehydrogenase (CII), (cytochrome c reductase) CIII, (cytochrome c oxidase) CIV and ATP synthase (CV) by immunoblotting. No major change was observed in the expression levels of these proteins (Figure 36A). Therefore, we next tested changes in activity of each of these complexes. Akin to their expression levels, there was no major change in the ETC complex activity in two patient samples analyzed (Figure 36B).

Effect of stromal co culture on mitochondrial biogenesis markers and uncoupling protein in CLL

Parallel to the measurement of mitochondrial functionalities, CLL cells in suspension

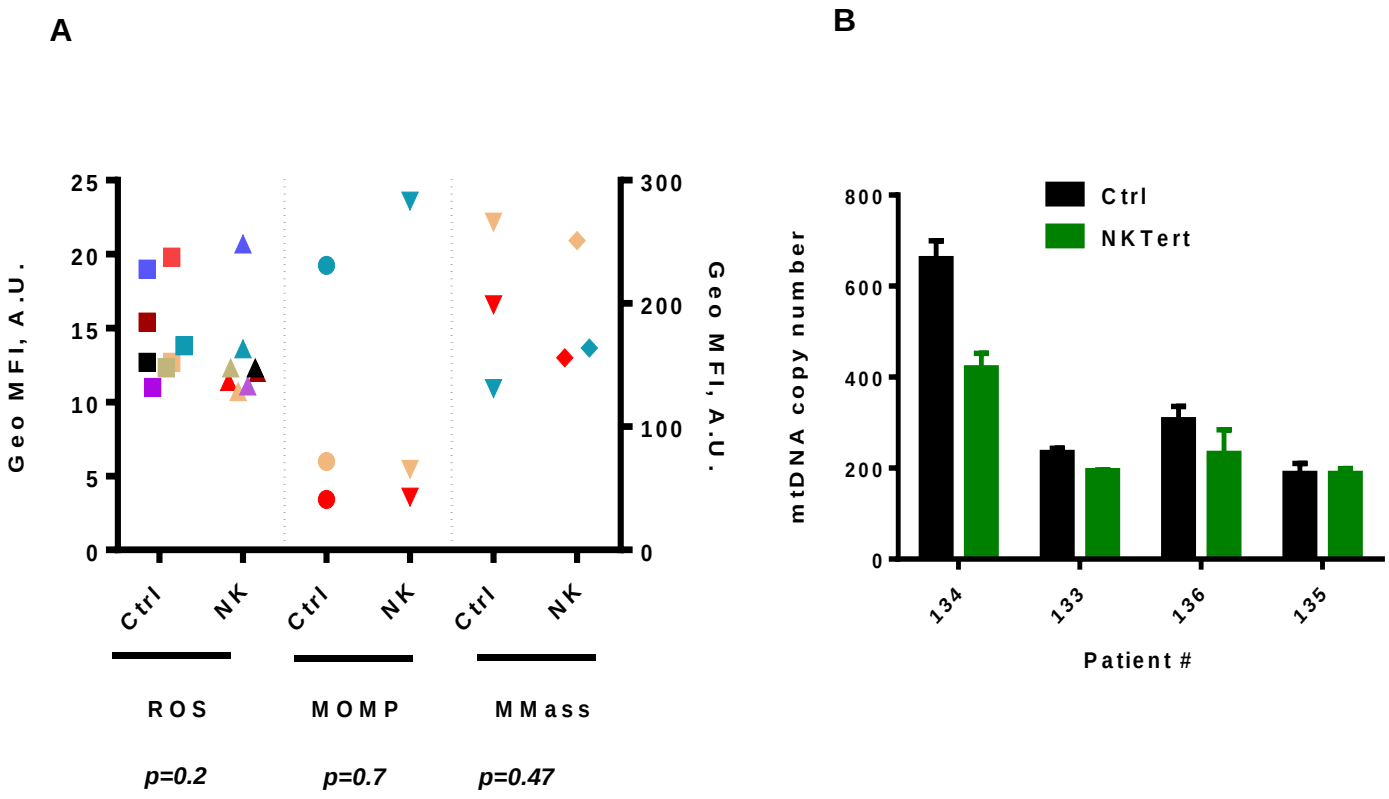

Figure 35. Effect of NK.Tert on CLL mitochondrial biology and functionalities.

A. Geometric means (from flow cytometry data) of CLL cells from 8 patient samples were analyzed to compare mitochondrial reactive oxygen species (ROS) (on left y-axis) before and after NK.tert co-culture. Similarly, 3 patient samples were analyzed for mitochondrial outer membrane potential (MOMP) and mitochondrial mass (on right y-axis), before and after co-culture. B. DNA was extracted from CLL cells from 4 patient samples that were co-cultured with NK.tert. qPCR analysis for CLL mtDNA from suspension culture (black bar), CLL mtDNA post co-culture with stroma (green bar) was performed in triplicate. The results were analyzed by a paired student's t –test p=0.192.

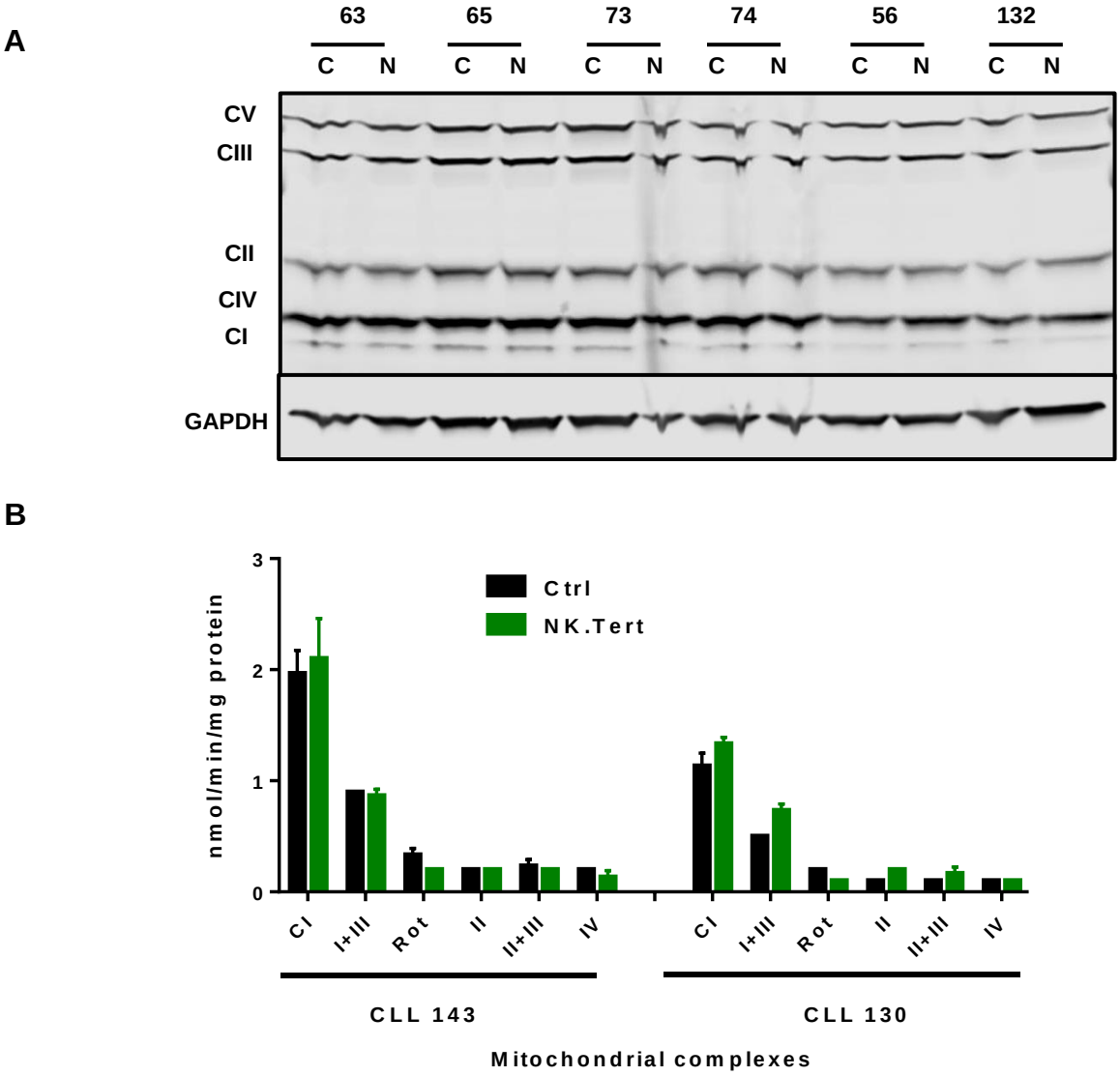

Figure 36. Effect of NK.Tert on CLL mitochondrial electron transport chain protein expression and function.

A. Immunoblot analysis of whole-cell extracts of control (C) and NK.tert co-culture (N) of CLL cells (n=6). Proteins were extracted and analyzed using antibodies to detect protein levels of all 5 mitochondrial respiratory chain complexes (I, II, III, IV, and V). GAPDH serves as loading control. B. Mitochondrial respiratory complexes activity comparison in suspension (Ctrl) and NK.Tert co-culture in two patient samples.

and co-culture were assayed for changes in expression of mitochondrial biogenesis markers like DNA polymerase γ (POLG) necessary for mitochondrial DNA replication and nuclear respiratory factor 1 (NRF1), which is a transcription factor required for mt DNA transcription and replication. However, immunoblot of these proteins did not depict detectable changes post co-culture (Figure 37A).

Since, oxygen consumption is enhanced, mitochondrial uncoupling protein 2 (UCP2) levels were also measured. Uncoupling proteins dissociate ATP synthesis from oxygen consumption in mitochondria (Andrews et al. 2005), therefore UCP2 (isoform majorly expressed in B cells) levels are expected to fluctuate after stroma co-culture, since OCR as well as ATP levels increased. However, there was no change in UCP2 protein levels (Figure 37B).

Effect of stromal co culture on PI3K, mTOR and STAT3 pathways in CLL

PI3K and mTOR are major players in regulating cell metabolism. Recently, the STAT3 pathway was implicated in affecting mitochondrial metabolism (Gough et al. 2009, Demaria et al. 2010). Therefore, it is required to test if these pathways are activated upon interaction with stroma. It is already known that PI3K/AKT pathway is activated after co-culture. CLL cells were co-cultured with NK.Tert cells for 24hrs and were harvested to perform immunoblot analysis to detect the phosphorylation of AKT on Ser473, phospho-S6 (downstream effector of mTORC1) and phosphorylation of STAT3 on Ser727. Although the results were heterogeneous, p-S6 levels were elevated in 6 of 11 patient samples tested (Figure 38).

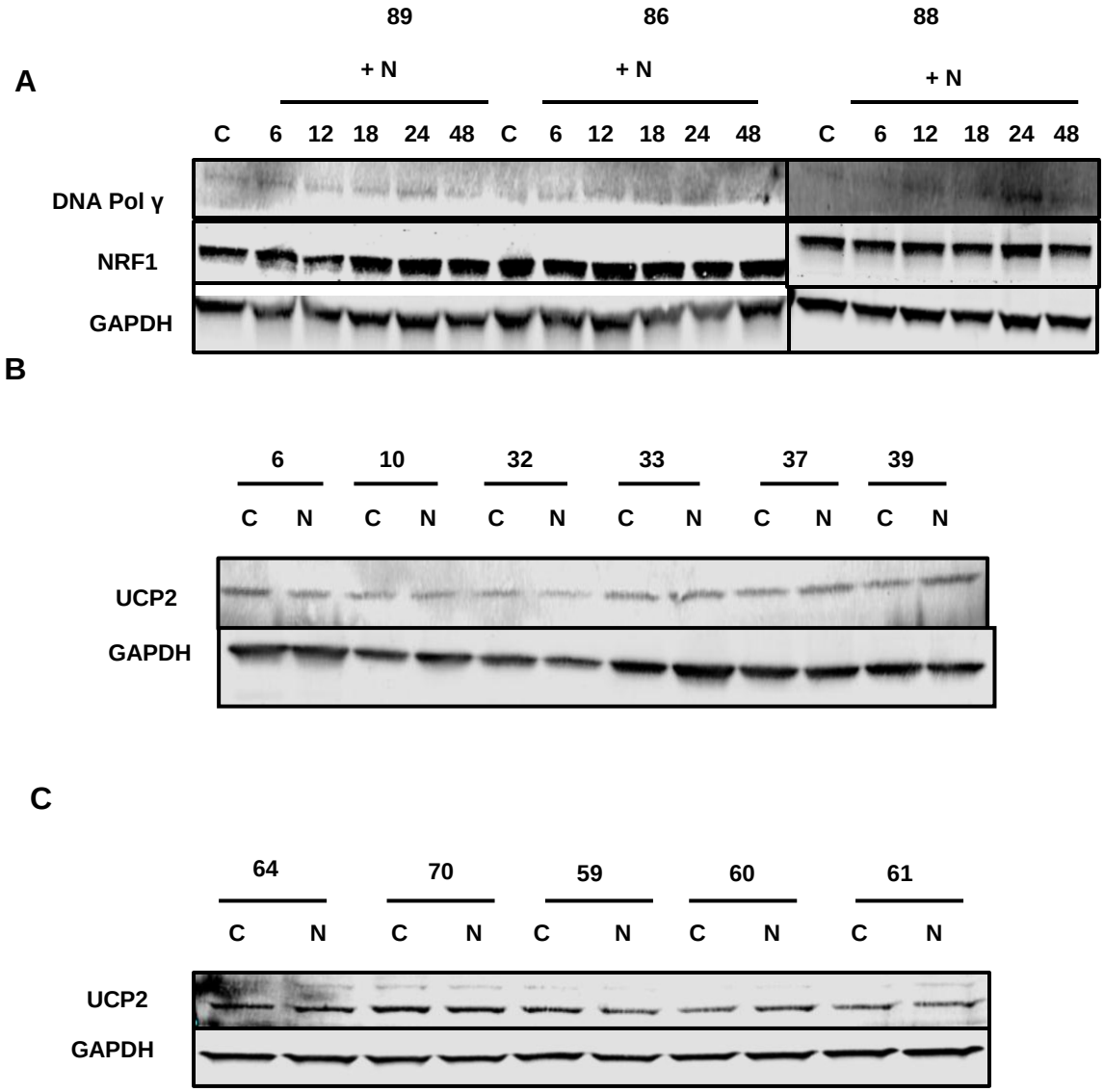

Figure 37. Effect of stroma on CLL mitochondrial biogenesis markers and uncoupling protein 2 expression.

A. Changes in mitochondrial biogenesis markers in CLL were probed for after stroma co-culture. CLL cells were cultured with NK.Tert (N) cells and were harvested indicated time points. Proteins lysates were extracted from cells and used for immunoblot analysis of control (C) and NK.Tert co-culture (N) to detect expression levels of DNA Pol γ and NRF1. B-C. CLL cells were cultured with NK.Tert cells (N) and were harvested at 24hr. Proteins lysates were extracted from cells and used for immunoblot analysis to detect expression levels of UCP2.

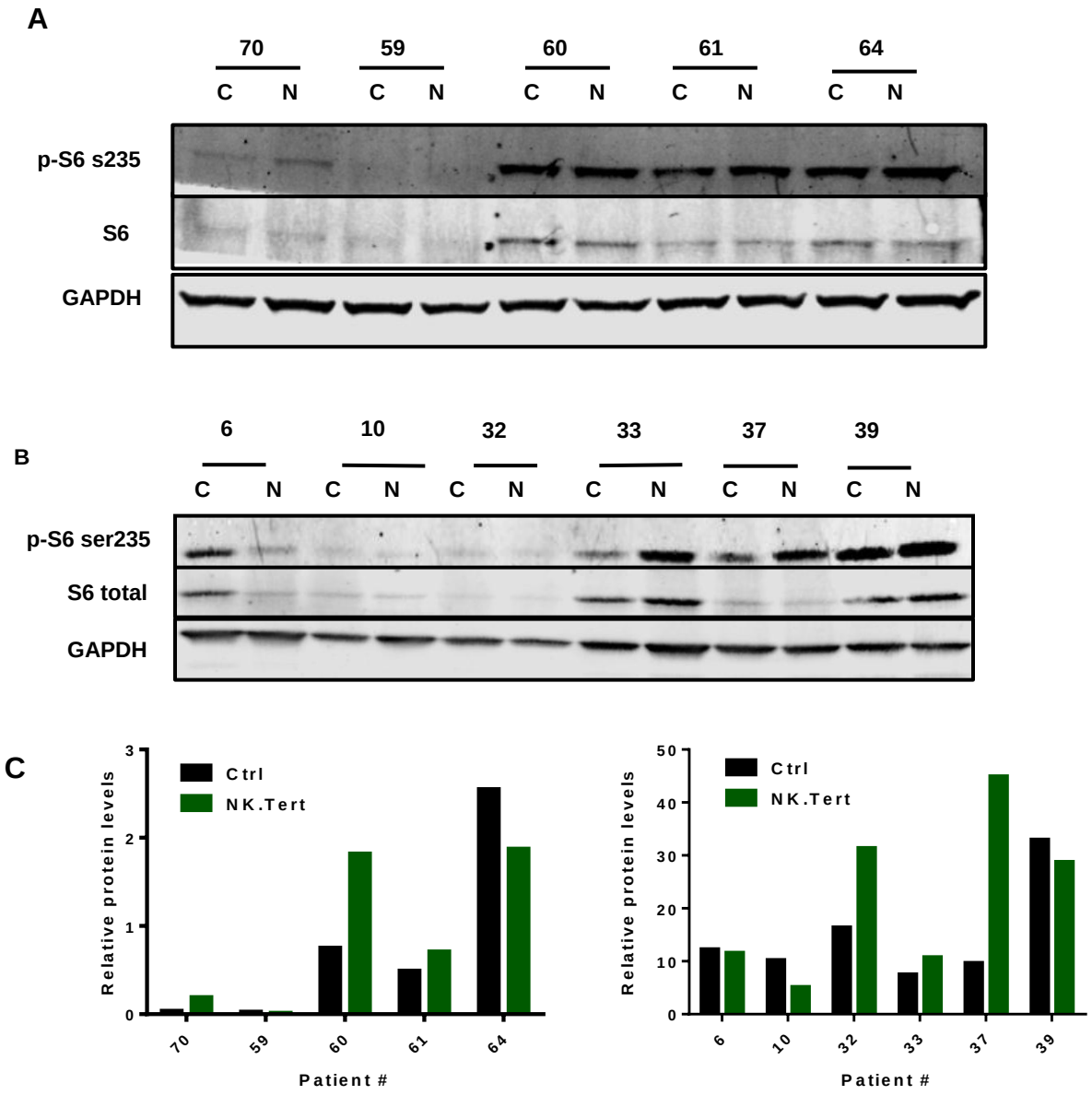

Figure 38. Effect of stroma on activation of mTOR pathway in CLL cells.

A-B. Immunoblot analysis of whole-cell extracts of control (C) and NK.tert co-culture (N) (24hr) of CLL cells (n=11). Proteins were extracted and analyzed using antibodies to detect activation of mTOR pathway by checking for phosphorylation of ribosomal S6 protein at Ser235 residue. C. Densitometry plot showing relative protein levels of p-S6/S6 protein.

Similarly, in spite of heterogeneity, STAT3 was activated after NK.Tert or M2-10B4 co-culture (Figure 39). This further implies that pathways regulating metabolism are indeed activated upon stroma co-culture.

As hypothesized, stroma affected oxidative metabolism in CLL cells, without causing major changes in glycolysis. Cell-to cell contact was necessary for this stroma-induced metabolic change in CLL and this phenomenon could not recapitulated by addition of cytokines to CLL. CLL cells saw an increase in ATP levels along with other ribonucleotide triphosphates upon 24hr co-culture with stroma cells. Major changes in mitochondrial biology were not observed in spite of increase in oxygen consumption.

Aim 3. Delineating the role of PI3K/AKT axis on CLL bioenergetics

Aim 3.1. Determine the role of PI3K pathway in regulating glycolysis and mitochondrial oxidative phosphorylation in CLL by pharmacologic inhibition.

Pharmacological inhibition of the PI3K/AKT pathway diminishes CLL mitochondrial OxPhos.

Prior investigations have established stroma-mediated survival benefit to CLL cells and induction of PI3K/AKT signaling. The PI3K axis is constitutively active in CLL cells in presence of the microenvironment, and many PI3K inhibitors have been developed that abrogate this pathway.

Effect of duvelisib on CLL metabolism

PI3K δ/γ inhibitor, duvelisib, is in Phase III clinical trials for CLL. I examined its ability to alter the OxPhos pathway in CLL cells with or without stroma.

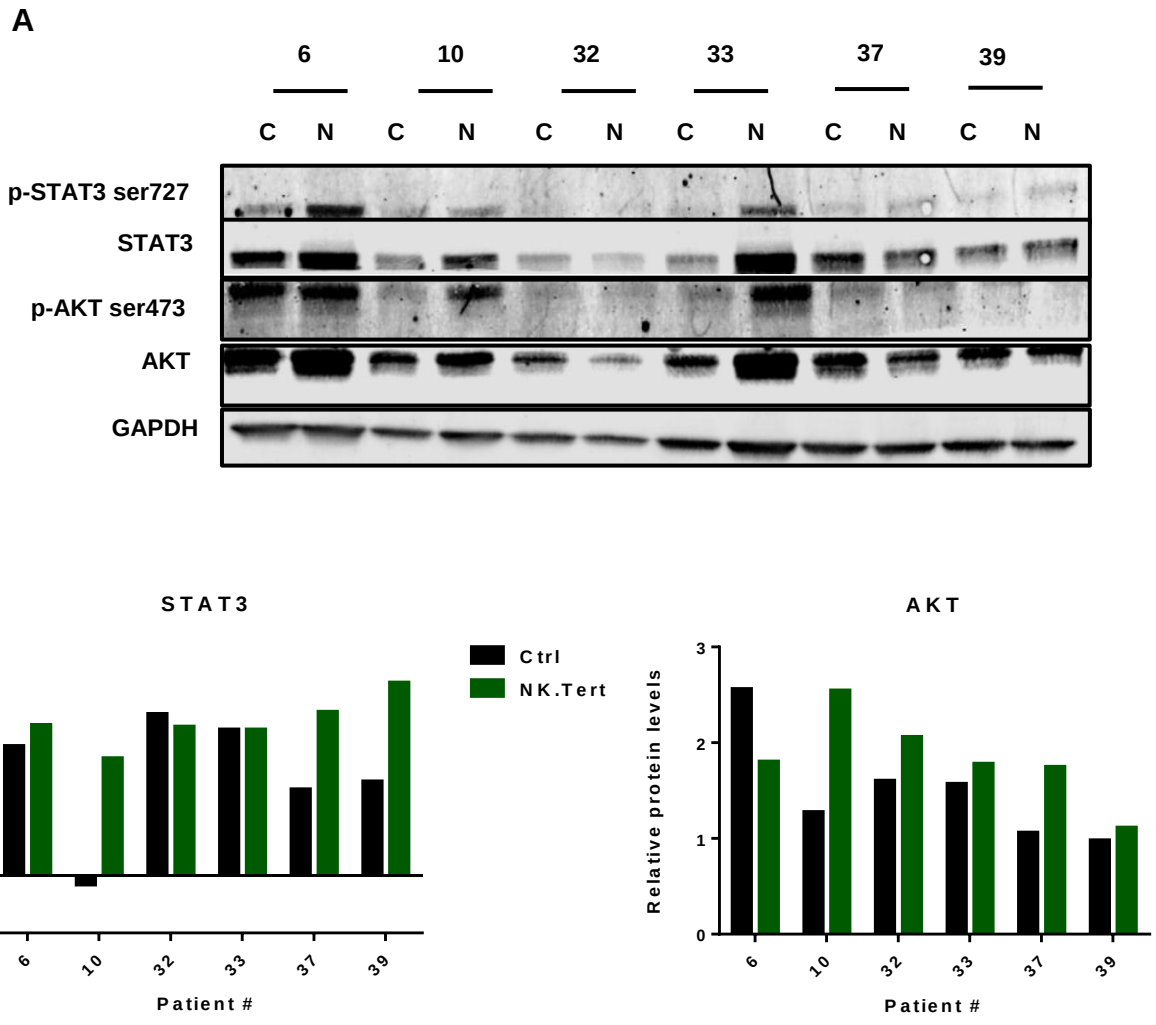
A
6
10
32
33
37
39
C N C N C N C N C N C N
p-STAT3 ser727
STAT3
p-AKT ser473
AKT
GAPDH
STAT3
Relative protein levels
2.0
1.5
1.0
0.5
0.0
-0.5
6 10 32 33 37 39
Patient #
Ctrl
NK.Tert
AKT
Relative protein levels
3
2
1
0
6 10 32 33 37 39
Patient #

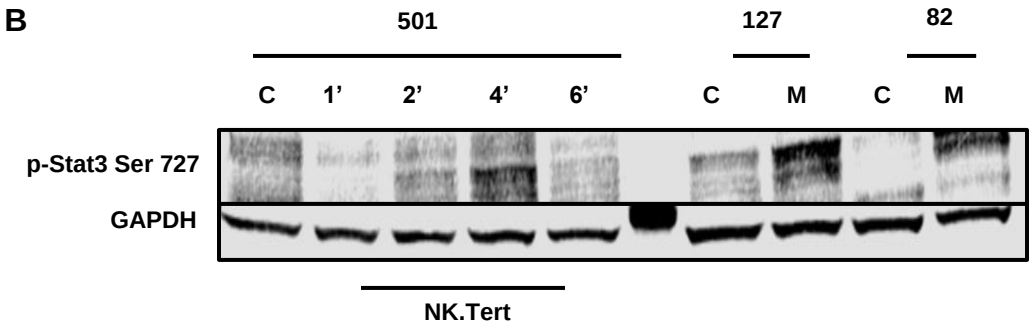
B
501
127
82
C 1' 2' 4' 6' C M C M
p-Stat3 Ser 727
GAPDH
NK.Tert

Figure 39. Effect of stroma on activation of AKT and STAT3 pathways in CLL cells. Immunoblot analysis of whole-cell extracts of control (C) and NK.tert co-culture (N) (24 hr) of CLL (n= 6). Proteins were extracted and analyzed using antibodies to detect activation of AKT pathway by probing for phosphorylation of AKT at Ser 473 residue and STAT3 by probing for phosphorylation of STAT3 at Ser 727 residue. Densitometry graph of p-STAT3/STAT3 and p-AKT/AKT B. CLL sample # 501 was co-cultured with NK.Tert and harvested at the indicated time points. CLL samples # 127 and 82 were co-cultured with M2-10B4 (M) cells for 24 hr.

CLL cells were incubated with duvelisib (1 μM) for 24hr and assayed for cell death using annexin –PI staining. Modest cell death was observed with duvelisib in 40 samples tested (Figure 40). Then, cells were counted and equal number of untreated and duvelisib treated cells were assayed for glycolysis and OxPhos. Duvelisib treatment mitigated both glycolysis and aerobic respiration (Figure 41-42). Although, there was heterogeneity in reduction of basal OCR, MRC was significantly reduced upon duvelisib treatment. Similar extents of decline in OCR were obtained, when CLL cells were co-cultured on stroma (Figure 43) in 3 of 5 samples tested.

Effect of idelalisib and MK2206 on CLL metabolism

Since, duvelisib inhibits both PI3K δ and ɣ, an inhibitor of single PI3K isoform or downstream AKT were employed to test if they can impact overall energy metabolism. Therefore the effects of a PI3K δ inhibitor, idelalisib was examined, whose signaling is more prominent in CLL cells, in context of microenvironment. Idelalisib is approved for CLL therapy by the FDA. To further test whether this inhibition of metabolic pathways is AKT dependent, an AKT inhibitor MK-2206, was used.

CLL cells were treated with DMSO or one of the drugs, idelalisib (1 μM) or MK2206 (2.5 μM). Both these drugs compromised glycolysis in all 5 samples tested, without being cytotoxic (Figure 44). Similarly they caused a significant decline in MRC, although their effect on basal OCR was heterogenous (Figure 45). This suggests that inhibition of the AKT pathway at least in part underlies the mitigation of glycolysis and OxPhos pathways.

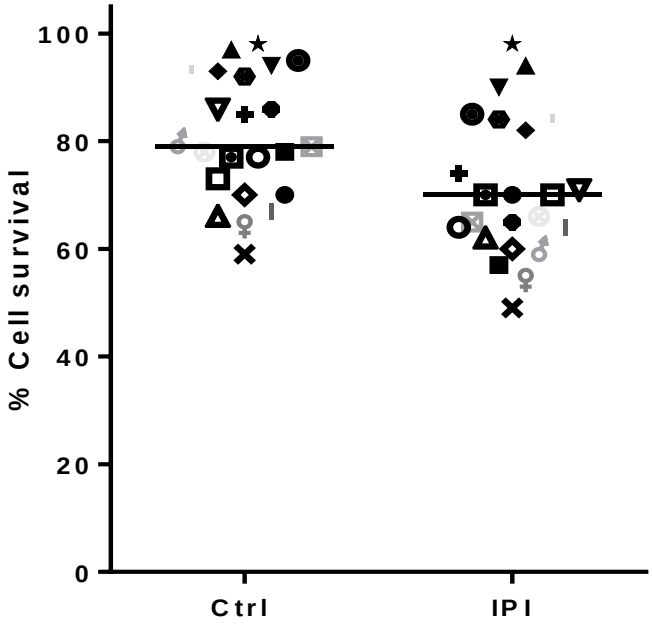

Figure 40.Effect of duvelisib treatment on survival of CLL cells *in vitro*.

CLL cells untreated (DMSO) and duvelisib treated (1 μM) were incubated for 24hr and stained with annexin- PI and analyzed by flow cytometry. The results were analyzed by a paired student's t –test (n=23, p=0.0081). Duvelisib causes minimal cell death (5-15%) at 1 μM concentration.

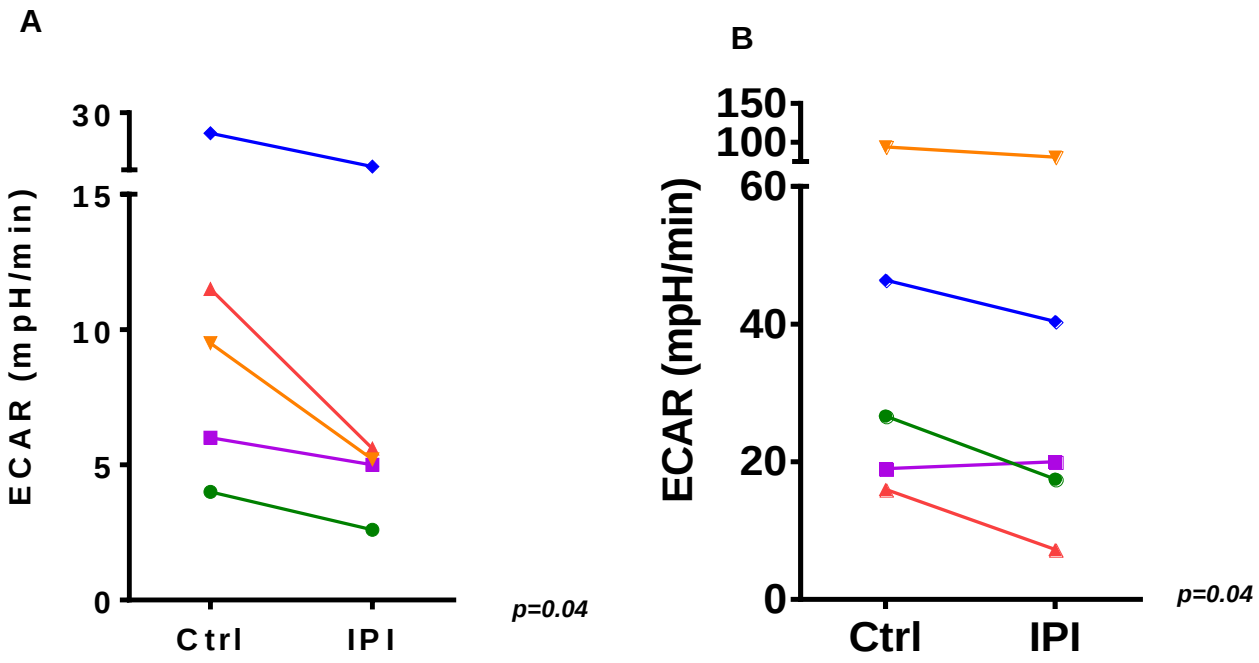

Figure 41.Effect of duvelisib on glycolysis in CLL.

A.CLL cells were treated with 1 µM duvelisib for 24hr (n=5) and assayed for glycolytic flux along with untreated controls. B. Duvelisib treated patient samples in A were analyzed for glycolytic capacity (n = 5). The results were analyzed by a paired student's t –test p=0.98.

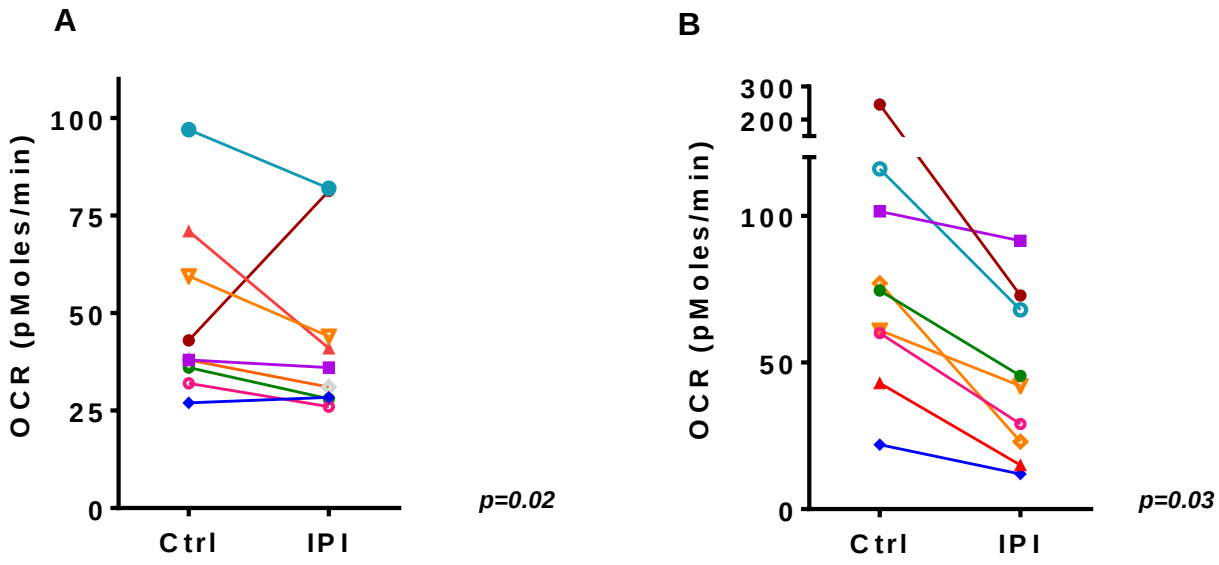

Figure 42. Effect of duvelisib on mitochondrial OxPhos in CLL cells in suspension culture.

CLL cells were either DMSO treated (Ctrl) or treated with 1 µM duvelisib (IPI) for 24hr and were assayed for OxPhos. A. Basal OCR and B. maximum respiration capacity were compared in control versus duvelisib treated CLL cells (n = 9). The results were analyzed by a paired student's t –test.

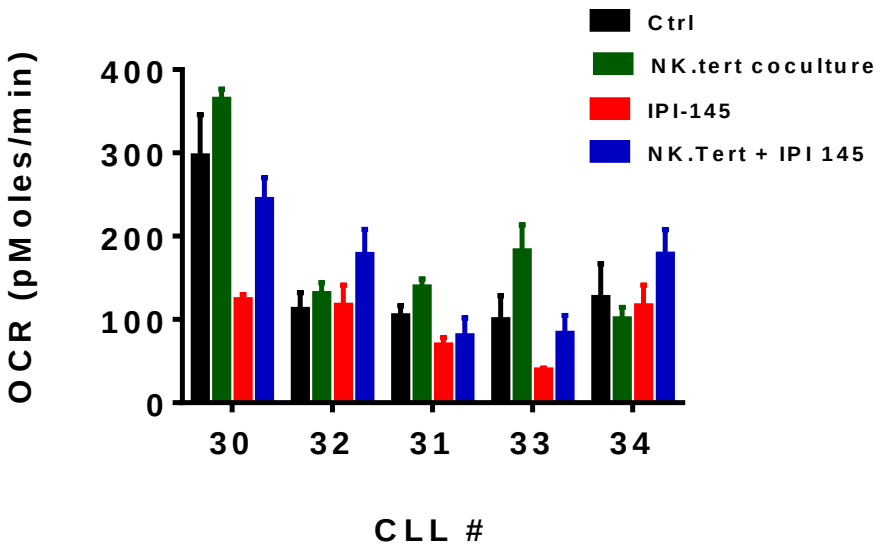

Figure 43. Effect of duvelisib treatment on CLL OxPhos in presence of stroma.

CLL lymphocytes from five patients were isolated and were either DMSO treated (Ctrl) or treated with 1µM duvelisib in suspension or in stroma co-culture for 24 hours and compared for changes in basal OCR. The results were analyzed by a paired student's t –test between Ctrl vs IPI-145 (p=0.15), NK.Tert vs NK.Tert + IPI-145 (p=0.48).

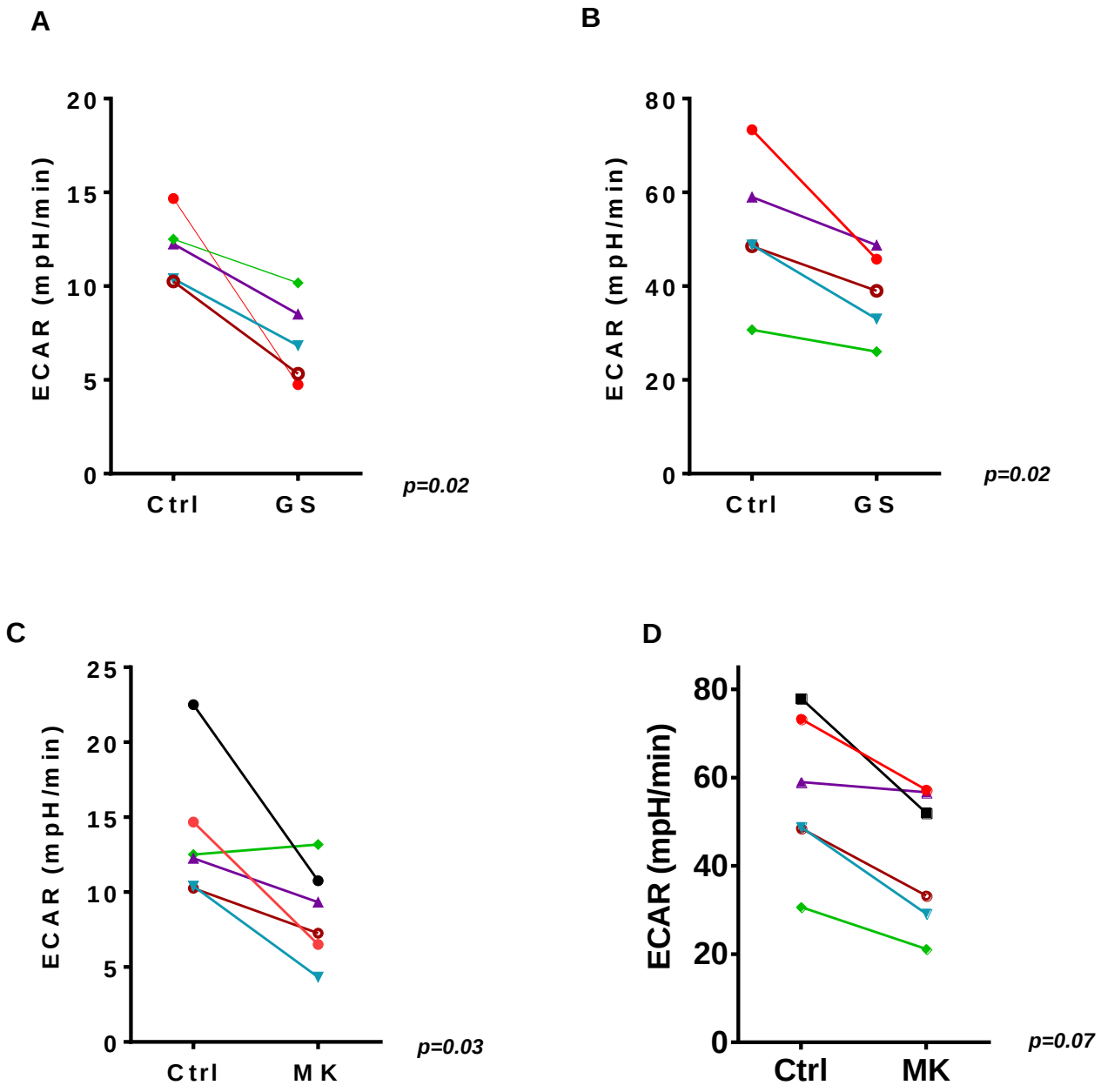

Figure 44.Effect of idelalisib and MK2206 on CLL glycolysis.

CLL cells untreated or treated for 24 hours with PI3K δ inhibitor idelalisib (GS, n = 5) and were compared for changes in glycolytic flux (A) and glycolytic capacity (B). CLL cells were treated with AKT inhibitor MK2206 (MK, n = 6) and compared with untreated controls for changes in glycolytic flux (C) and glycolytic capacity (D). The results were analyzed by a paired student's t –test p=0.98.

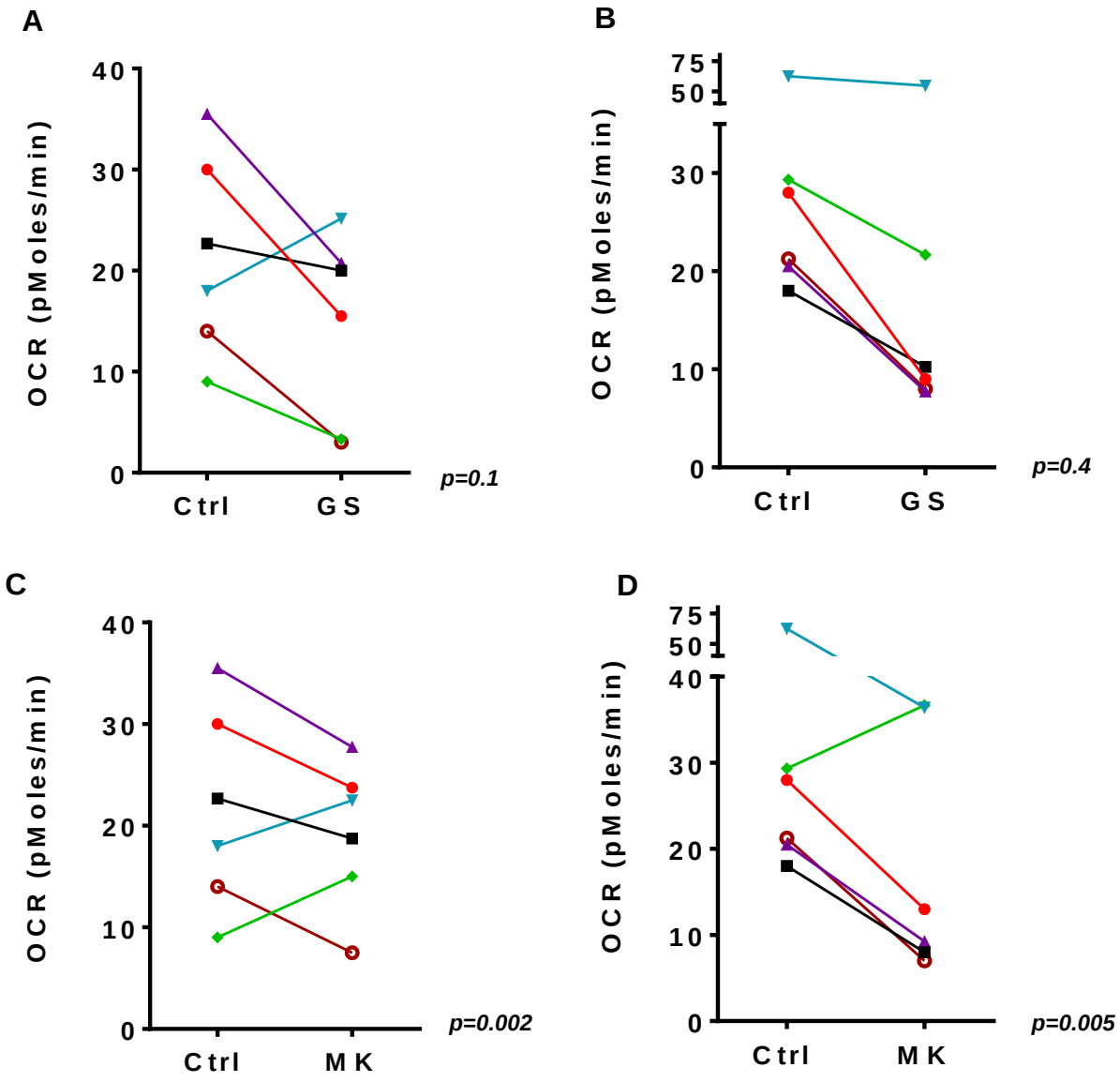

Figure 45.Effect of idelalisib and MK2206 on CLL mitochondrial OxPhos.

CLL cells untreated (Ctrl) or treated for 24 hours with PI3K δ inhibitor idelalisib (GS, n = 6) and were compared for changes in basal OCR **(A)** and maximum respiratory capacity **(B)** Similarly, CLL cells, untreated (Ctrl) or treated for 24 hours with AKT inhibitor MK-2206 (MK, n = 6) compared for changes in basal OCR **(C)** and maximum respiratory capacity **(D)**. The results were analyzed by a paired student's t –test.

Aim 3.2. Determine the impact of PI3K/AKT inhibition on substrate uptake, ATP ribonucleotide pools and mitochondrial biology in CLL.

Effect of duvelisib on glucose and glutamine uptake by CLL cells

Because glycolysis is hampered by inhibition of AKT, whose role in glucose uptake and utilization is well established, we hypothesized that duvelisib treatment would inhibit glucose uptake. Surprisingly, an assessment of the uptake of [^{3}H] 2-deoxy-D-glucose demonstrated that glucose uptake was not significantly impacted by duvelisib treatment (Figure 46), which might mean, although, glucose uptake did not change, there is a possibility that its utilization maybe encumbered. Furthermore, glutamine uptake was not affected as well (Figure 46). As controls for these experiments, glucose incubated with duvelisib for a minimum of 4 hr (by which time, it should block the PI3K/AKT pathway) and stimulated with IgM or insulin for 30 minutes before addition of the radioactive compounds. However, this did not induce any change in glucose/glutamine uptake.

Effect of duvelisib on Acetyl coA Carboxylase and fatty acid metabolism

To test if duvelisib affects metabolism of fatty acids, which in turn, may fuel CLL OxPhos, Acetyl CoA Carboxylase (ACC1) were probed for phosphorylation. ACC1 is enzyme necessary for fatty acid synthesis. However, no significant changes were detected (Figure 47A). CLL cells were cultured in glucose and glutamine free media and with L-carnitine (which helps utilize fatty acids for energy production in the cell) for 24hr ± duvelisib to assay for OCR.

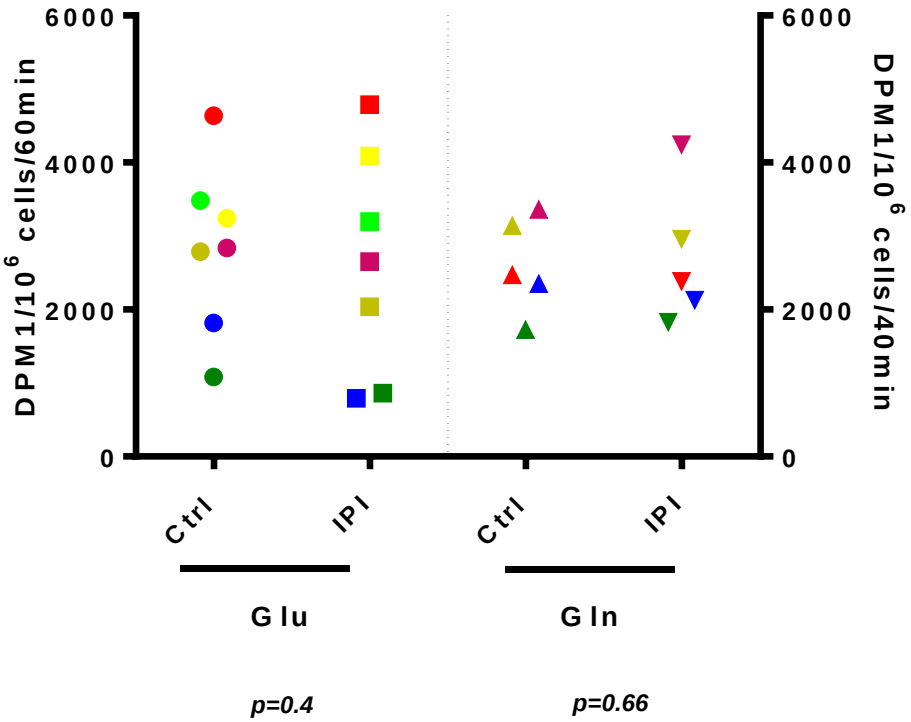

Figure 46.Effect of duvelisib on glucose (Glu) and glutamine (Gln) uptake in CLL cells.

Uptake of [^{3}H] 2-deoxy-D-glucose was compared in 7 CLL patient samples, either untreated or duvelisib treated. Three technical replicates were performed for control and drug treatment. Disintegrations per minute (DPM)/60 min counted using a scintillation counter and the values were normalized to 10^6 cells. Similarly, [^{3}H] glutamine uptake was compared in 5 CLL patient samples, untreated and duvelisib treated; DPM/40 min were normalized to 10^6 cells. The results were analyzed by a paired student's t –test.

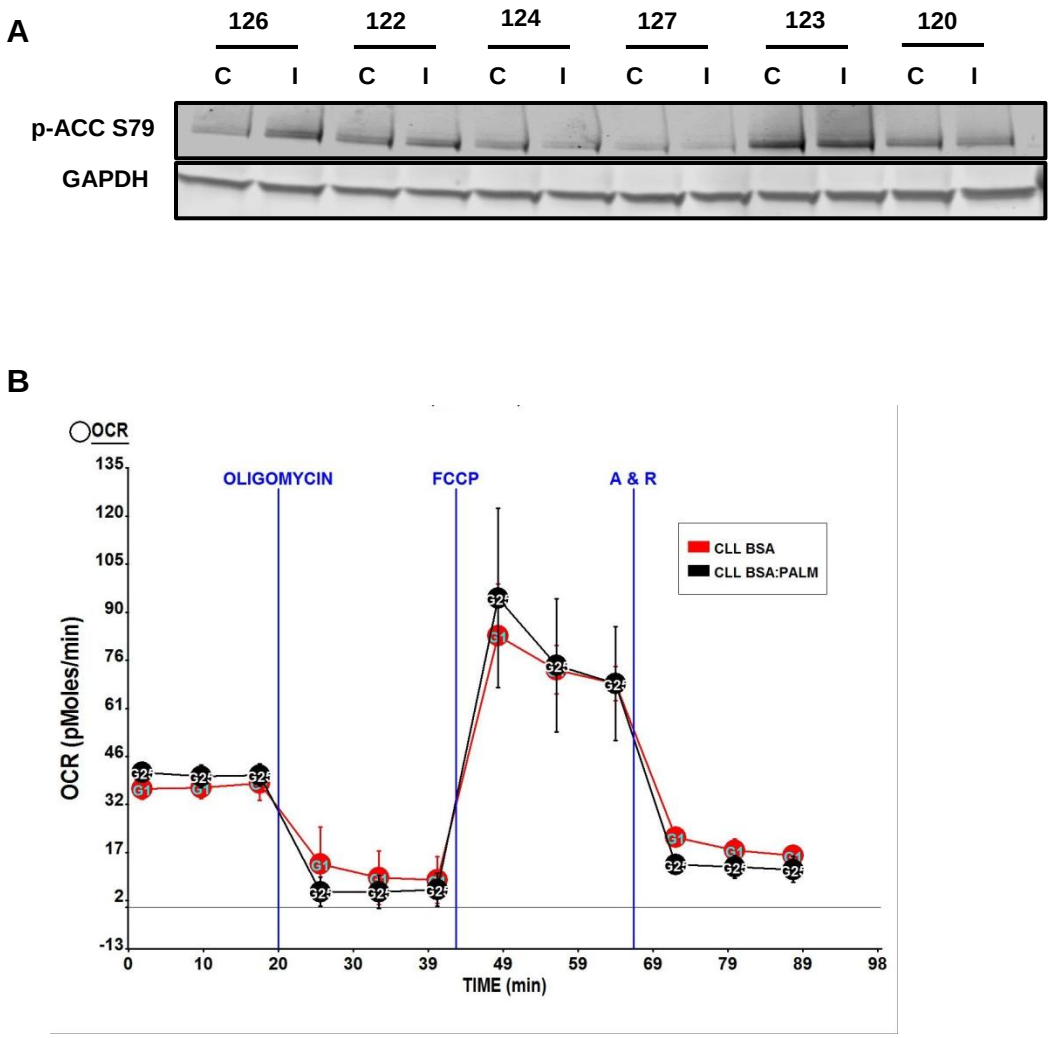

Figure 47. Influence of duvelisib on fatty acid oxidation in CLL.

A. Immunoblot analysis of whole-cell extracts of control (C) and duvelisib treated (I) CLL (n= 6). Proteins were extracted and analyzed using antibodies to detect phosphorylation of Acetyl COA Carboxylase on Ser79. B. CLL cells analyzed for OCR in control : BSA supplemented media (red curve) versus BSA conjugated palmitate supplemented media.

CLL cells were assayed for OCR using palmitate conjugated to bovine serum albumin (BSA) as the substrate (Figure 47B). CLL cells (n= 4) did not exhibit higher OCR with palmitate when compared to BSA only control indicating that CLL cells were not able to utilize extrinsic fatty acids as substrate to fuel OxPhos.

Effect of duvelisib on ATP production in CLL

Since, PI3K δ/ɣ inhibition resulted in decline in OxPhos. I next tested the effect of duvelisib on NTP pools. CLL cells from 7 patients were treated with duvelisib for 24hrs and later harvested for perchloric acid extraction. These samples were assayed for NTP pools by HPLC. A 25% to 50% decrease in intracellular ribonucleotide triphosphate pools was observed (Figure 48). Endogenous intracellular concentrations of NTP were normalized as 100%. Decline in ATP is consistent with mitigation of OxPhos by the drug. Decrease in other NTP pools suggest that overall energy metabolism is affected by inhibiting PI3K pathway.

Effect of duvelisib on mitochondrial functionalities and biology of CLL

As with stroma co-cultures, mitochondrial ROS, membrane potential, mitochondrial mass (Figure 49A) and mitochondrial DNA copy number (Figure 49B) were assayed after drug treatment. None of these parameters were affected in contrast to decrease in OCR and ATP pools. No significant changes were observed in the protein levels or enzyme activity of respiratory chain complexes (I-V) after duvelisib treatment (Figure 50A-B).

.

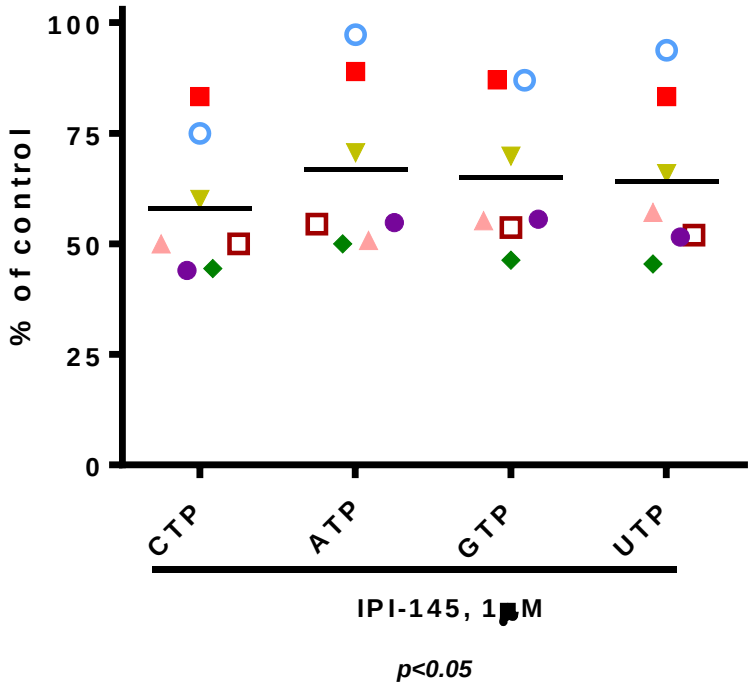

Figure 48. Influence of duvelisib treatment on the intracellular nucleotide pools in CLL lymphocytes.

NTP pools were extracted from CLL cells from blood of patients (n = 7) that were either untreated or treated with 1μM duvelisib for 24 hours and analyzed using HPLC. Each symbol represents a patient sample. The p-value is determined by one way ANOVA and dunnett's multiple comparisons t-test of Ctrl versus each NTP pool.

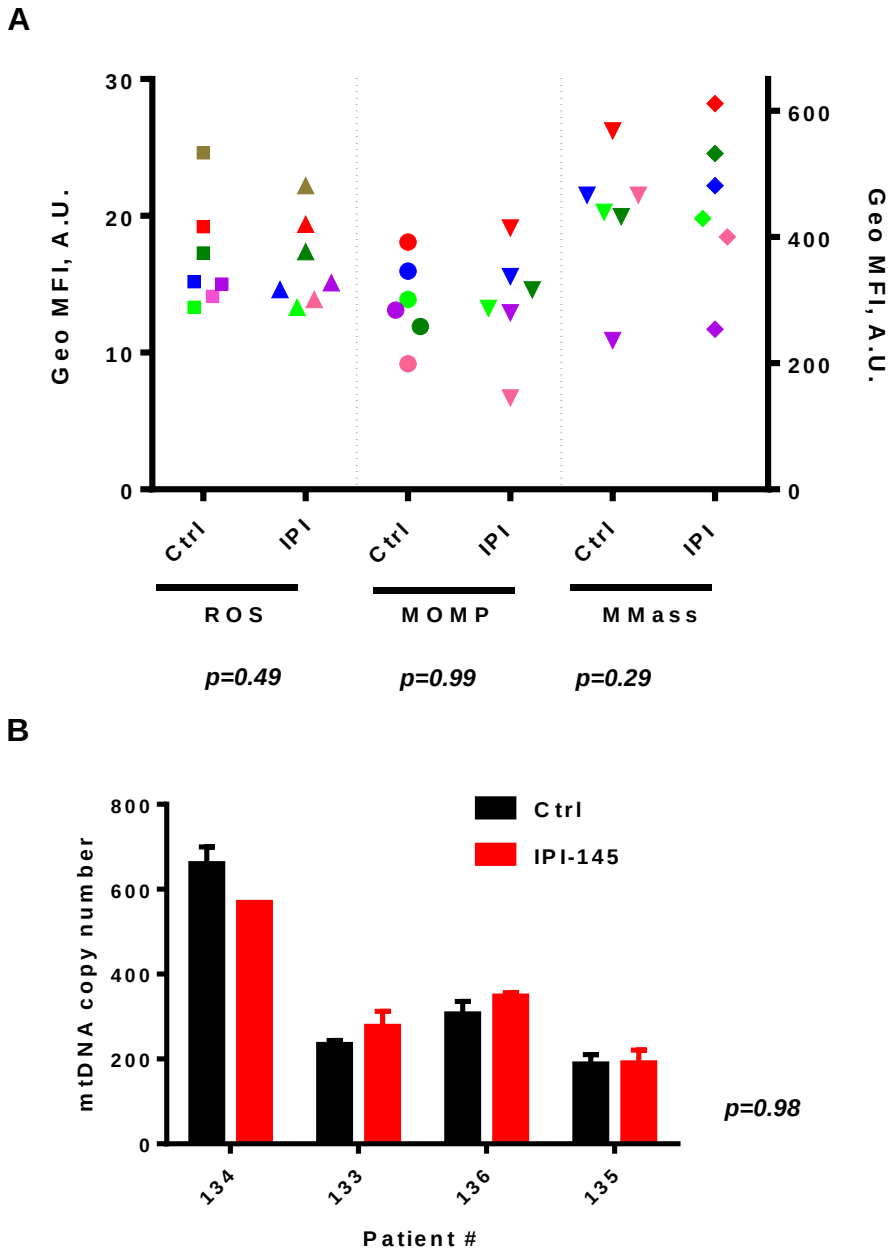

Figure 49. Effect of duvelisib on CLL mitochondrial biology and functionalities.

A. Geometric means of CLL cells (obtained by Flow Jo software analysis) from 7 patient samples were analyzed to compare mitochondrial reactive oxygen species (ROS, left *y*-axis) before and after duvelisib treatment. Similarly, 6 patient samples were analyzed for mitochondrial outer membrane potential (MOMP, right *y*-axis) and mitochondrial mass (right *y*-axis) before and after drug treatment. B. DNA was extracted from CLL cells obtained from 4 patient samples , and were treated with 1 μM duvelisib for 24hr. qPCR analysis for CLL mtDNA from suspension culture (black bar), and post duvelisib treatment (red bar) was performed in triplicate. The results were analyzed by a paired student's t –test p=0.98.

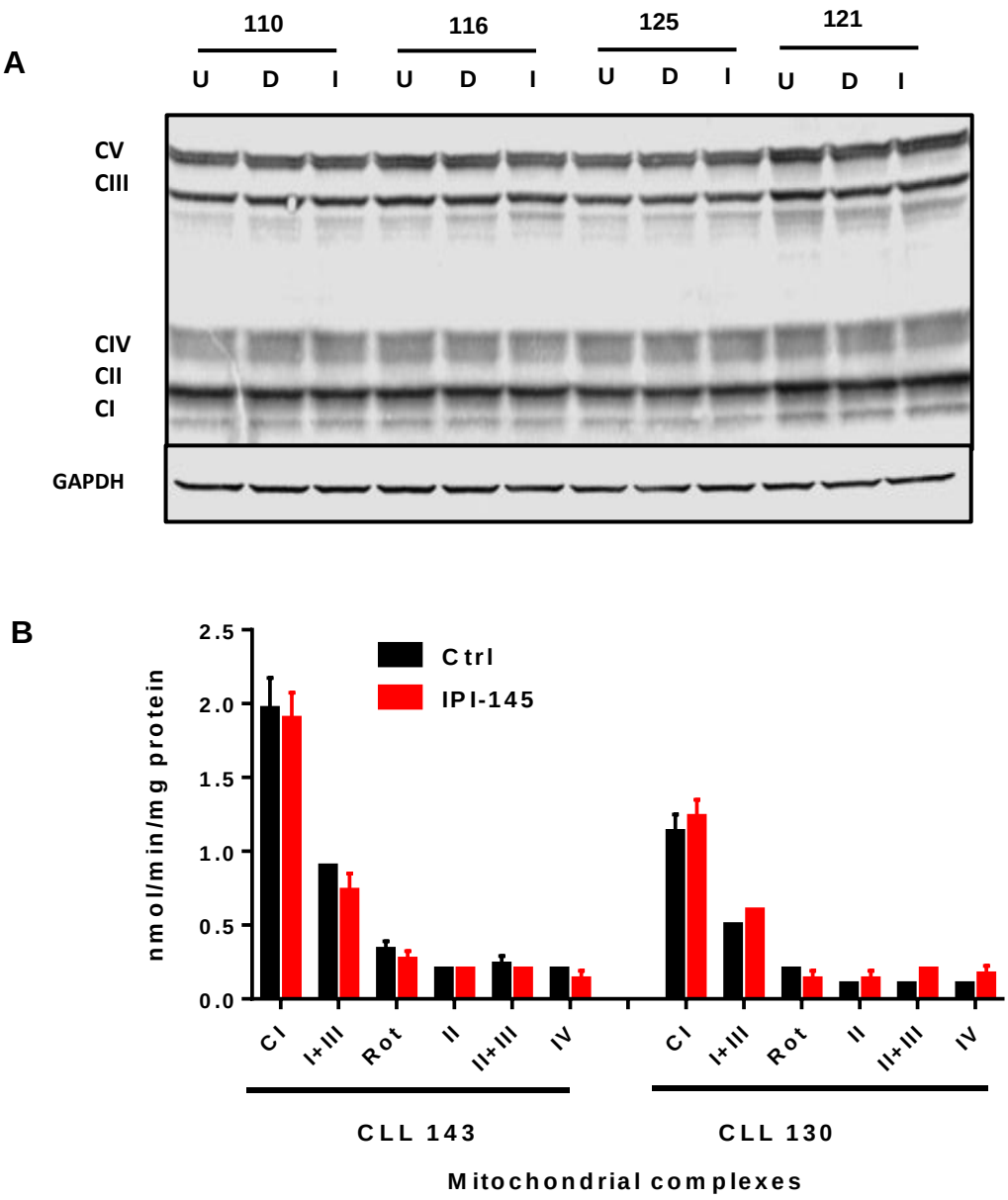

Figure 50. Effect of duvelisib on CLL mitochondrial electron transport chain protein expression and function.

A. Immunoblot analysis of whole-cell extracts of untreated (U), DMSO (D), and duvelisib–treated (I) CLL cells from patients (n=4) to detect protein levels of all 5 mitochondrial respiratory chain complexes (I, II, III, IV, and V). GAPDH serves as loading control. B. Mitochondrial respiratory complexes activity comparison in suspension (Ctrl) and duvelisib (IPI-145) treated samples**.**

Aim 3.3. Determine the impact of genetic ablation of PIK3CD in malignant B cell lines

Since, pharmacologic inhibition of PI3K signaling lowered OCR, genetic ablation of PI3K δ should cause a similar effect on cellular metabolism. Firstly, MCL cell lines, JeKo-1 and Sp53 were assayed for glycolysis and OxPhos to evaluate if they mimic CLL cells, after they are co-cultured with stroma (NK.Tert) and treated with duvelisib (10 μM). Similar to CLL, MCL cells also displayed increased OxPhos when co-cultured with stroma and reverse impact was observed when treated with duvelisib (Figure 51).

JeKo-1 was employed to obtain a genetic knockout (KO) of PIK3CD (coding for catalytic subunit p110δ). To establish a knockout cell line, JeKo-1 cells were co-transfected with a plasmid expressing Cas9 and a PIK3CD-targeting guide RNA for KO of PIK3CD, along with a plasmid for knock-in of Green Fluorescent Protein (GFP) in its position. GFP-positive (PIK3CD KO) cells were sorted by FACS after the 3rd day after transfection and expanded in cell culture for a week. They were analyzed for OxPhos and glycolysis, along with unmodified cells (WT) from a parallel culture. The PIK3CD KO cells displayed reduced glycolysis (Figure 52) and respiration levels (basal OCR and spare respiratory capacity) as compared to the WT (Figure 53; n=3,p=<0.0001).The PIK3CD KO did not result in decrease in cell proliferation rate or size as compared to WT (Figure 54). The PIK3CD KO cell line was further validated for KO by RT-PCR.

PI3K signaling is very critical for survival of cells as another cell line Ly19 (diffuse large B cell lymphoma employed for PIK3CD KO did not proliferate after FACS and thereby the cells did not survive in culture for more than 4 days.

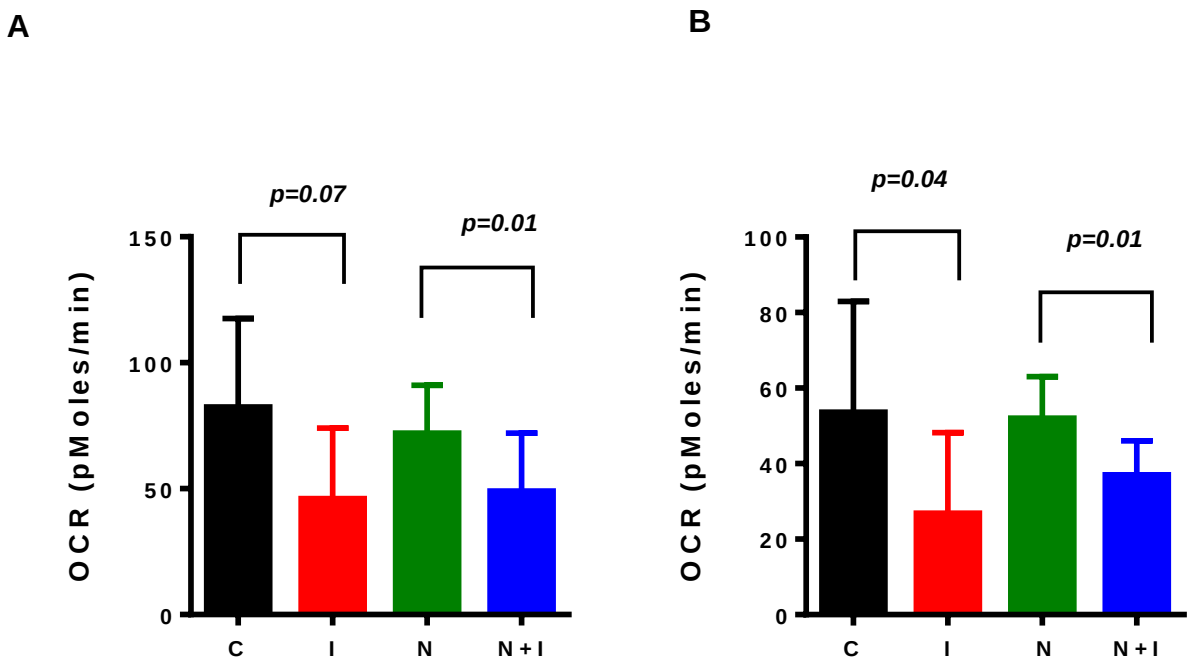

Figure 51. Effect of stroma and duvelisib on OxPhos in mantle cell lymphoma cell lines.

A. JeKo-1 cells which were co-cultured with NK.Tert (N) or treated with duvelisib (I) in presence or absence of NK.Tert, were assayed for OxPhos along with untreated controls (C). B. Sp53 cells, co-cultured with stroma or treated with duvelisib (I) in presence or absence of NK.Tert, were assayed for OxPhos along with untreated controls (C). n=3 biological replicates for each treatment with both cell lines. Statistical significance was calculated using paired student's t test between the specified groups.

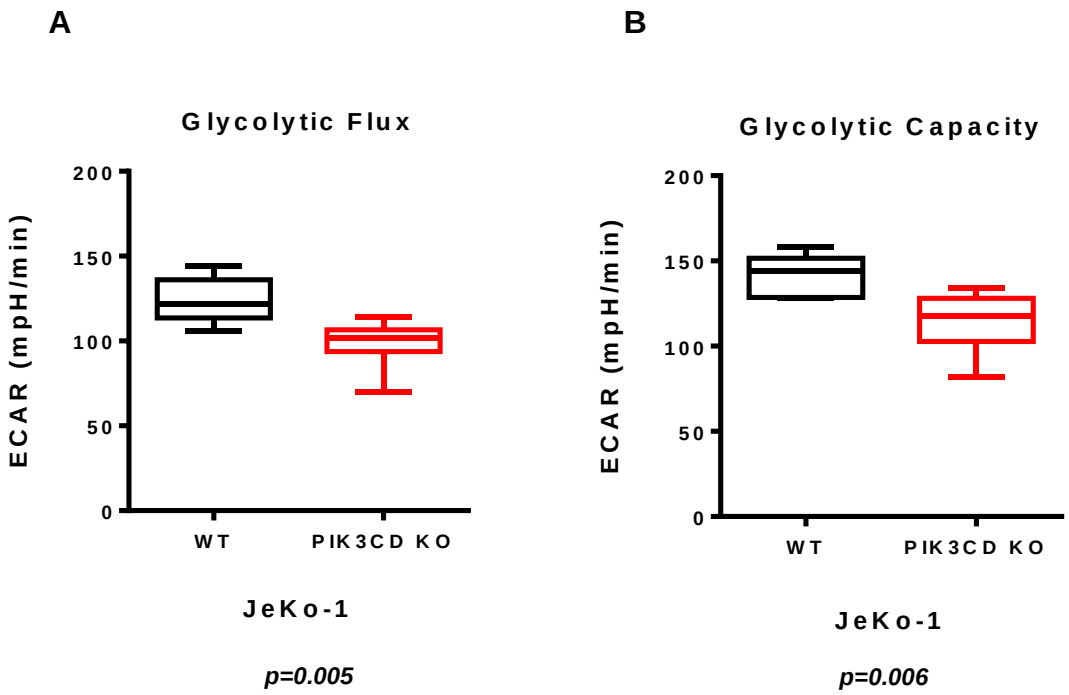

Figure 52. Impact of PIK3CD knockout on glycolysis in mantle cell lymphoma cell line.

JeKo-1 wild –type (WT) and PIK3CD KO cells were analyzed for (A) glycolytic flux and (B) glycolytic capacity (n=4 technical replicates and biological triplicate). Student's paired t-test was used in the statistical analysis.

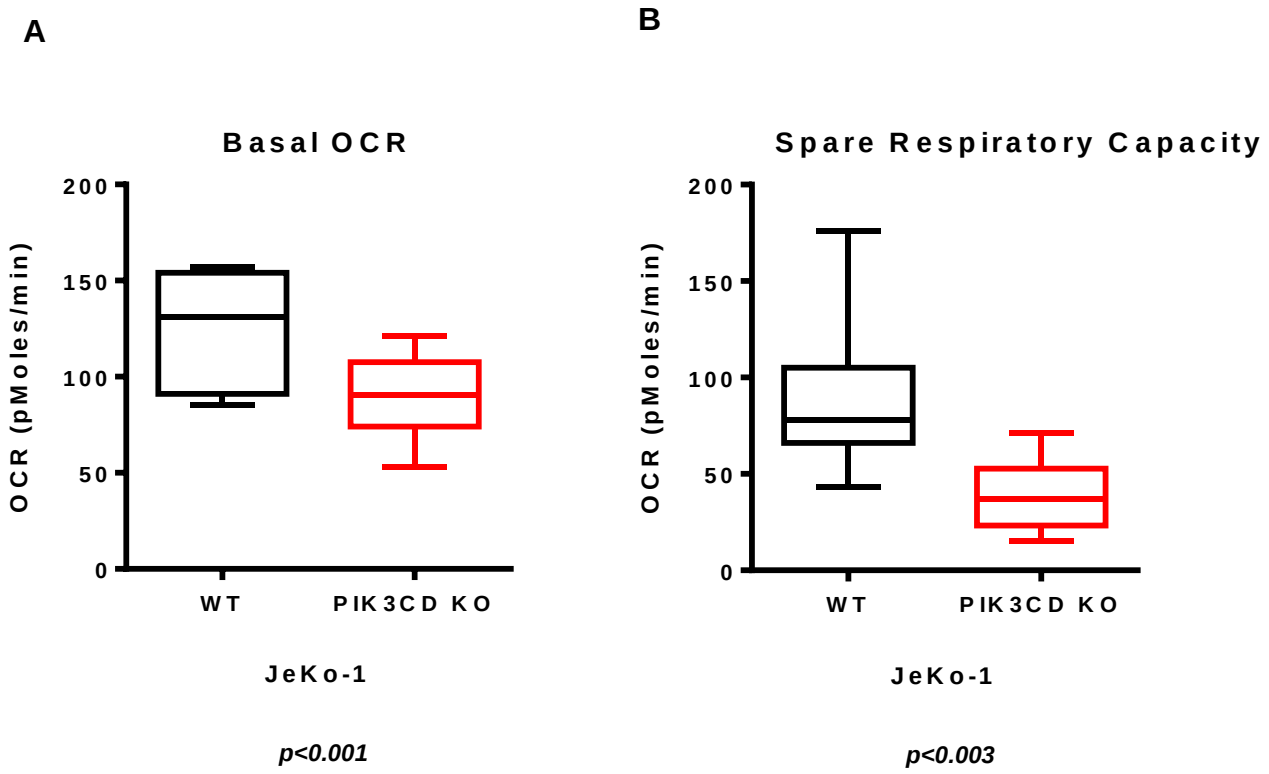

Figure 53.Impact of PIK3CD knockout on mitochondrial OxPhos in mantle cell lymphoma.

JeKo-1 wild –type (WT) and PIK3CD KO cells were analyzed for (A) basal OCR and (B) spare respiratory capacity (n=4 technical replicates and biological triplicate. Student's paired t-test was used in the statistical analysis.

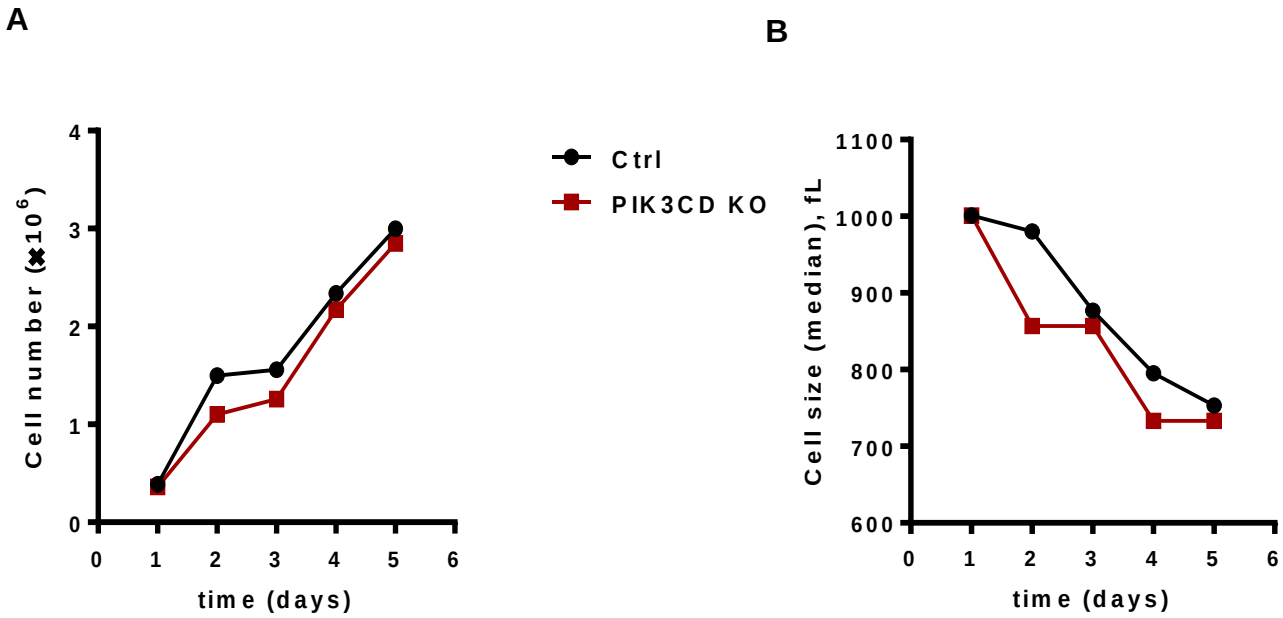

Figure 54. Comparison of cell proliferation and cell size of JeKo-1 wild type versus PIK3CD knock out cells.

A.WT and PIK3CD KO JeKo-1 clones were plated at a concentration of (2×10^5)/mL in RPMI 1640 media supplemented with 10% FBS and 1% penicillin-streptomycin solution on day 1 and the cell numbers were measured on days 2, 3, 4 and 5. B. Under similar conditions to A, median cell size was recorded on days 2, 3, 4, 5.

To elucidate the impact of B cell receptor signaling in regulating CLL metabolism, JeKo-1 cell line was employed to create BCR KO (CH_2 region of heavy chain IgM). Three clones of BCR KO, MC4, MC5 and MC6 were generated. BCR KO along with WT cells were tested for OCR. BCR KO clones similar to PI3KCD KO cells displayed reduced OxPhos levels (Figure 55). They did not differ from wild type JeKo-1 cells in proliferation rate or cell size (Figure 56).Immunoblotting further confirmed that AKT signaling (p-AKT Ser 727) and MAPK signaling (p-MAPK 44/were mitigated upon serum starvation and stimulation with IgM (Figure 57). These results substantiate the importance of B cell receptor pathway and PI3K signaling in regulating CLL metabolism.

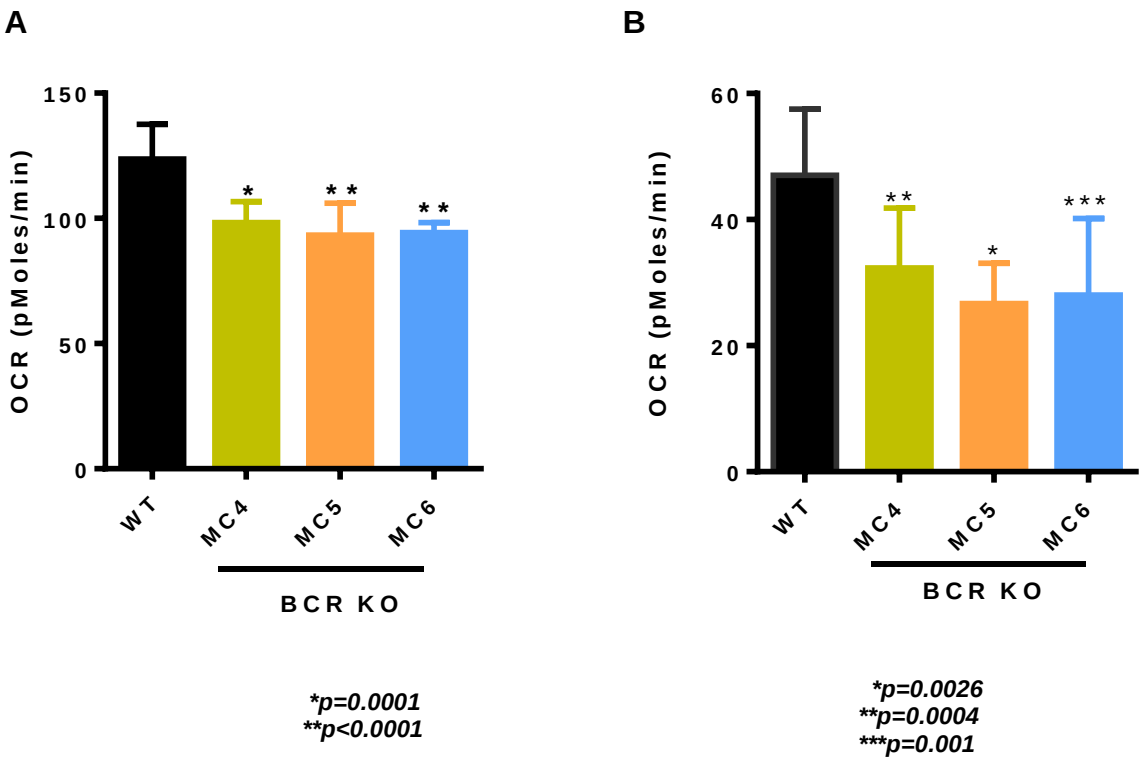

Figure 55. Impact of BCR knockout on mitochondrial OxPhos in mantle cell lymphoma.

JeKo-1wild –type (WT) and BCR KO clones (MC4, MC5, MC6) were analyzed for basal OCR (A) and spare respiratory capacity (B) using extracellular flux analyzer (n=6) technical replicates and biological triplicate). One-way ANOVA with multiple comparisons was used to compare control values with that of KO.

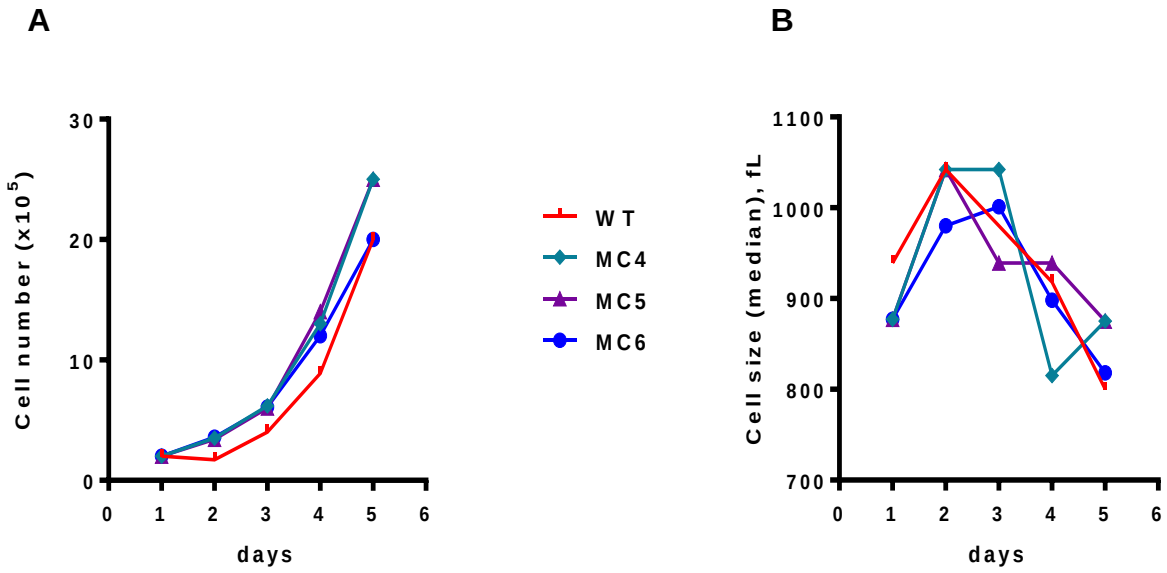

Figure 56. Comparison of cell proliferation and cell size of JeKo-1 wild type versus BCR knock out clones.

BCR wild type (WT) and three BCR KO JeKo-1 clones (MC4, MC5, MC6) were plated at a concentration of (2×10^5)/mL in RPMI 1640 media supplemented with 10% FBS on day 1 and the cell number (A) and median cell volume (B) were measured on days 2, 3, 4 and 5.

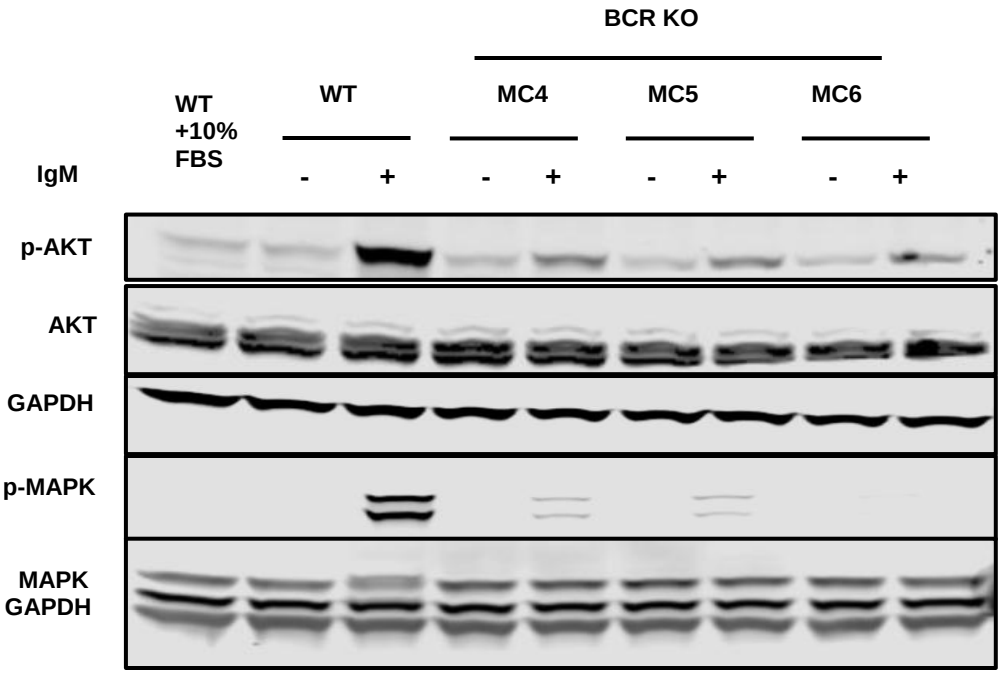

Figure 57. Impact of BCR knockout on BCR signaling in mantle cell lymphoma cell line.

Immunoblot analysis of BCR pathway proteins from whole-cell extracts of JeKo-1 WT and three BCR KO clones ± IgM stimulation. WT and BCR clones were serum starved (RPMI 1640 media supplemented with 0.5% serum) for 2 hr followed by addition of 10 μM IgM for 20 min. The p-AKT Thr308 and total AKT were probed using antibodies from two different species. The p-MAPK p(44/42) Thr202/Tyr204 and total MAPK were probed using antibodies from two different species followed by GAPDH immunogenicity.

CHAPTER 4. DISCUSSION

Cancer cells have high energy demands owing to their rapid proliferation rates. However, in CLL, the malignant B cells are mature and arrested in the G_0 stage of the cell cycle. In some cases, stimulus from the microenvironment (lymph node) may lead to their proliferation, otherwise, they remain quiescent. As a result, CLL is not an attractive model to study the rewiring of metabolism in malignant neoplasms. Not many studies have been conducted to decipher the bioenergetic profile of CLL B cells. Although, CLL cells may not actively proliferate, they need bioenergy for survival and sustenance.

CLL vs normal lymphocytes metabolism

CLL literature may not be replete with studies on metabolism, however, there were a few reports in 60s and 70s that showed glucose uptake is reduced in CLL when compared to normal B cells, indicating that glycolysis is not a major pathway in CLL cell metabolism (Brody et al. 1969, Brody and Merlie 1970). In contrast to what was reported earlier, recent findings demonstrated an increase in glycolytic intermediates, 2-phosphoglycerate and lactic acid along with increase in glutamine metabolism and TCA cycle intermediates in indolent and aggressive CLL cases in which miR-125b is overexpressed (Tili et al. 2012). Another study characterized the transcriptome of CLL cells and found that genes involved in metabolic pathways were upregulated in CLL cells compared with normal lymphocytes in a cohort of 98 patients (Ferreira et al. 2014). Ingenuity pathway analysis of this study's data revealed that activity of mTOR and PI3K/AKT signaling pathways are elevated in CLL cells compared to normal B cells. Jitschin *et al*, demonstrated that CLL cells compared to normal B cells displayed increase in mitochondrial respiration in 4 samples (Jitschin et al. 2014). The

above studies indicate the upregulation of energy generating pathways in malignant B lymphocytes compared to normal lymphocytes.

I performed a comprehensive study, encompassing the metabolic phenotype of CLL cells, its association with prognostic features, the effect of stroma and role of PI3 kinase.

The present study evaluates the metabolic characteristic of freshly isolated malignant lymphocytes from peripheral blood of 41 CLL patients. Glycolysis and Oxidative Phosphorylation, the two major pathways contributing to cellular bioenergy (ATP) have been measured. These malignant B lymphocytes are oxidative in their phenotype and overall metabolically less active than normal B cells (Figure 1). Metabolic activities reported in CLL cells are synchronized as all the cells are arrested in G_0 phase of cell cycle.

Mitochondria in CLL

Mitochondria play a significant role in energy metabolism. Mitochondrial genome in CLL is very stable with hardly any mutations detected (Cerezo et al. 2009). Mitochondrial DNA (mtDNA) is more vulnerable to DNA damage than nuclear DNA, due to the lack of histone proteins (Caron et al. 1979, DeFrancesco and Attardi 1981). In CLL, heteroplasmic mutations were detected in mtDNA post chemotherapy, esp. with the use of alkylating agents. A study reported that patients who did not respond to chemotherapy had higher number of mtDNA mutations (in cytochrome c oxidase) resulting in excess ROS generation, than patients that responded to therapy (Carew et al. 2003). ROS is a byproduct of mitochondria ETC; therefore it becomes necessary to study changes in ETC in a complex disease like cancer.

A recent study reported increase in expression of molecules involved in mitochondrial biogenesis; e.g., TFAM was upregulated in CLL cells compared to normal B cells along with mitochondrial respiration (Jitschin et al. 2014). The same study also reported that ROS is overproduced in CLL as result of increased mitochondrial activity, suppressing the activity of T cells. Additionally, another group reported that free oxygen radicals in cells are heterogeneous among patients with CLL but significantly higher in CLL cells from patients with prior chemotherapy (Zhou et al. 2003). Also, increase in mtDNA copy numbers was associated with increased risk of CLL (Hosnijeh et al. 2014).

However, I did not find significant change in mitochondrial ROS levels post co-culture with stroma or treatment with PI3K inhibitor, duvelisib (Figure 35, 49). I tested for changes in mtDNA copy number and mitochondrial mass; however, no major changes were found in either (Figure 35, 49). Also, no changes were found in mitochondrial biogenesis markers like NRF1 and DNA pol γ in CLL post co-culture with stroma.

CLL metabolism correlates with prognostic factors of the disease

According to a recent meta-analysis to come up with suitable prognostic markers for CLL globally; in which a comprehensive analysis of 26 prognostic factors in 845 patients was evaluated. IgVH mutation status, Rai stage, age and β2M and cytogenetic deletions – TP53 were considered independent prognostic markers.

ZAP 70 and CLL OCR

ZAP 70 is present on T cells and is involved in signaling and activation. ZAP 70 has two SH2 containing domains and a carboxyl terminal domain. ZAP 70 is recruited by

immunoreceptor tyrosine-based activation motif (ITAM) after T cell receptor encounters an antigen. Multiple tyrosine residues in ZAP 70 are phosphorylated upon recruitment that acts as docking sites for downstream signaling molecules. One among them is PI3K regulatory subunit p85 (Moon et al. 2005). However, the mechanism by which ZAP 70 activates B cell receptor signaling is still unclear; even when ZAP 70 is insufficiently phosphorylated in CLL cells, it still recruits and activates its downstream effectors. CLL cells that express high levels of ZAP 70 are reported to have increase in tyrosine phosphorylation in the BCR complex after BCR crosslinking (Chen et al. 2002). CLL cells from different patients differ in their ability to respond to BCR crosslinking and this is said to be related to ZAP 70 expression (Gobessi et al. 2007). However, it is to be noted that ZAP 70 is not present on normal B cells and their B cell signaling is intact. A study reported that ZAP 70's role in malignant B cell signaling is different from T cell signaling, as its activation in CLL cells upon B cell stimulation is inefficient. However, it was reported to amplify BCR signaling for a long time (Gobessi et al. 2007). It is postulated that it may act as an adaptor protein, recruiting the proteins necessary for formation of signalosome. ZAP 70 activates BCR complex even in the absence of SYK, which is another tyrosine kinase that serves a similar function. IgM ligation of BCR complex in ZAP 70 positive patients' results increased phosphorylation of in SYK, BLNK, and phospholipase-C γ and boost calcium flux (Chen et al. 2005).

Induction of calcium levels in the mitochondrial matrix is linked to the increase in ATP production by OxPhos (Jouaville et al. 1999). In the present study, OxPhos is higher in the ZAP 70 positive cohort as compared to the negative cohort. This can be linked to amplified BCR signaling leading to increased cell metabolism as the BCR knockout cells

displayed lower mitochondrial respiration when compared to wild type cells of mantle cell lymphoma cell line.

Gene expression profiling of CLL identified an upregulation of lipoprotein lipase (LPL) levels, an enzyme central to lipid metabolism (Klein et al. 2001). A follow up study revealed the correlation between LPL and ZAP 70 expression and IgVH status (Heintel et al. 2005), proposing it as a diagnostic target in CLL. High levels of LPL correlated with shorter progression free survival.

IgVH and CLL OCR

Among the molecular markers that are employed in risk stratification analysis for CLL is the mutational status of immunoglobulin heavy chain (IgVH) (Pflug et al. 2014). Earlier studies established that unmutated IgVH was associated with more aggressive disease (Hamblin et al. 1999), high CD38 expression (Damle et al. 1999) and correlated with ZAP 70 expression (Figure 58) (Wiestner et al. 2003, Rassenti et al. 2004). Patients with unmutated IgVH genes had far inferior median survival than patients with mutated IgVH genes (Oscier et al. 2002).

The heavy chain of the antibody is encoded by genetic elements that are rearranged during B-cell development (Tonegawa 1983, Yancopoulos and Alt 1986). One of several diversity (D) segments combines with one of six joining (JH) gene segments to form a novel DJH segment. Rearrangement of this DJH segment with one of several immunoglobulin heavy chain variable region (VH) genes generates a VHDJH gene complex that encodes the variable (V) region of the immunoglobulin (Ig) heavy chain.

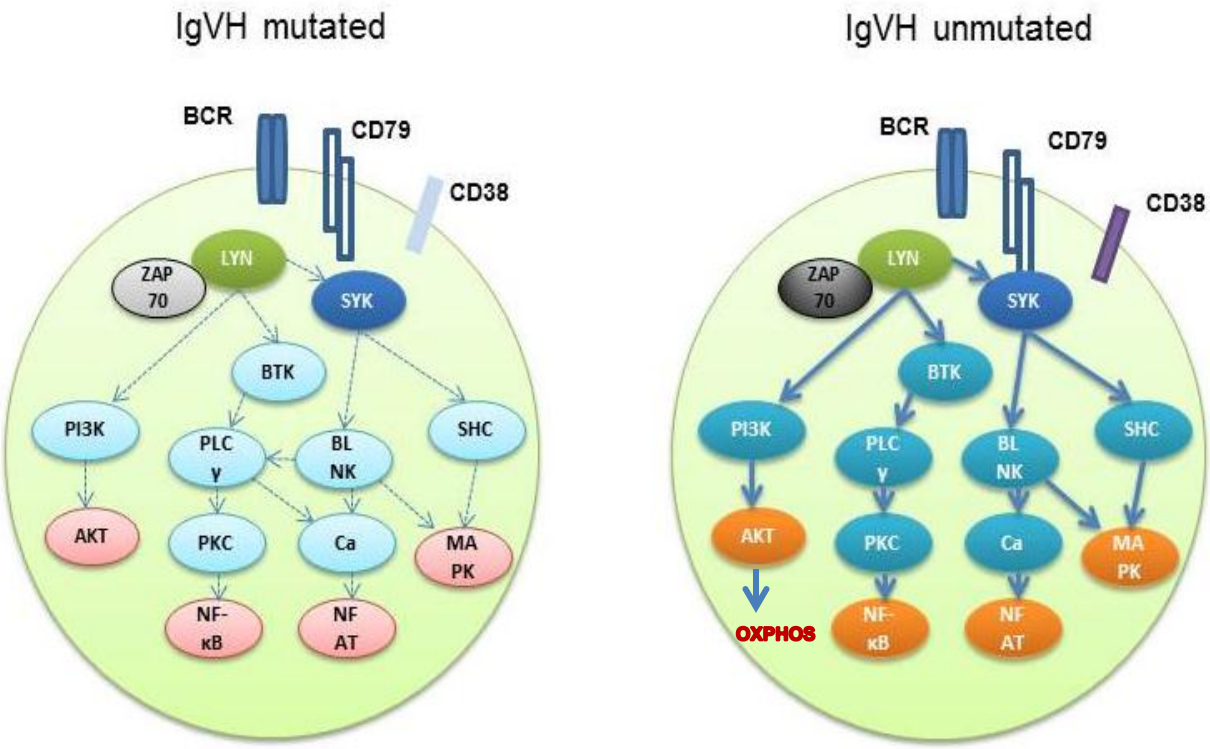

Figure 58. Signaling in CLL cell based on IgVH mutation status and ZAP 70 expression.
CLL cells that do not undergo gene rearrangements leading to IgVH mutations commonly express high ZAP 70 levels and therefore are classified as IgVH unmutated and ZAP 70 positive. They have enhanced BCR signaling compared to their counterpart (depicted on the left), along with expression of CD38.

The combination of VH, D JH is said to be a non-random process in CLL. It was discovered that the VH regions expressed in CLL are attained from a restricted reservoir (of VH genes) used during B cell development (Kipps et al. 1989). Along with co-stimulatory molecules, IgVH impacts cell survival, proliferation and differentiation through signaling. Somatic mutations indicate the antigen exposure of B cells. Mutations occur in the antigen binding site of the variable region. High rates of somatic mutations are said to occur in B cells in germinal centers as clonal evolution occurs within these centers. Once the cells leave the germinal centers the VH expression is reported to be relatively stable. IgVH mutations give an insight into the ontology and pathogenesis of the malignant B cells and therefore, the study of IgVH is of importance (Schroder et al. 1996). Gene expression profiling in IgVH unmutated versus mutated patients, identified many genes that differentially expressed in these 2 subsets of CLL. The expression of genes involved in metabolism like glutathione synthase, HPRT, and nucleotide phosphorylases and translocators was markedly upregulated in Ig unmutated cases (Rosenwald et al. 2001). Additionally, PI3K and CCND2 (cyclin D2) genes were overexpressed in the unmutated cohort (Kienle et al. 2006).

In the current study, cells from IgVH unmutated CLL cases displayed higher OCR than unmutated cases (Figure 13C). Unmutated IgVH usually co-occurs with high expression of ZAP 70 and CD38 markers (Wiestner et al. 2003, Rassenti et al. 2004). Patients with these markers have markedly decreased progression free survival. IgVH unmutated samples displaying significantly higher OCR, which may reflect on its association with ZAP 70 expression as ZAP 70 positive CLL cases also displayed high OCR aggressiveness of this

subtype of CLL. This observation is also in concert with increased expression of enzymes involved in metabolic activity in IgVH unmutated CLL.

Rai stage and CLL OCR

Rai is the most commonly used grading system for CLL progression. This system considers lymphadenopathy, organomegaly, anemia, and thrombocytopenia to classify patients into one of five stages, stage 0, I, II, III and IV. Median survival for stage 0 is around 12 years and for advanced stages III-IV is 19 months. Treatment plan for patients are decided based on staging.

CLL patients were classified as stage 0 if they harbored high lymphocyte counts, stage I- lymphomegaly, stage II enlargement of spleen or liver, stage III – anemia and stage IV thrombocytopenia. Advanced disease also has neovasculature in bone marrow and lymph nodes along with increased secretion of VEGF and bFGF (Menzel et al. 1996, Kini et al. 2000). A previous study reported that metabolic responses of CLL to hypoxia and glucose consumption correlated with the stage of disease (Koczula et al. 2015). This group also found that CLL cells from patients' samples (n=6) that were in early stage of the disease (Binet A0) were marked by low glucose and glutamine consumption and similarly, low lactate production.

In the present study, increased mitochondrial respiration (OCR) was observed at higher Rai stage in a pool of 51 patients (Figure 14A). Since, higher OCR was corresponding with markers of aggressive disease; therefore, increased oxygen consumption rates can act as a surrogate for aggressive disease.

A caveat of working with primary CLL cells is that, in suspension cultures, these cells are not supported by the microenvironment, as in the human body; therefore, the extent to which the their cell metabolism would represent that of the cells in the original state (human body) is in question. Although cell death was measured and only samples with highest percentage of live cells were incorporated in the study, the fact that these cells are on the path to apoptosis cannot be discounted. The time transpired between collection of blood from the patients and isolation of the CLL lymphocytes would also likely affect the cell survival and behavior.

Correlation between CLL patients' age and glycolysis

According to the study by Rai *et al*, age differences among patients with different stages of disease was statistically significant with stage 0-II patients younger than stage III patients. This is relatable as CLL progresses with time. Also, chances of survival post therapy declined with age. Therefore, when CLL glycolysis and OxPhos were analyzed for correlation with age, glycolysis (ECAR) displayed a significant increase in patients of older age (Figure 16B). This observation could be further elaborated by selecting patients from different age groups (early stage and comparatively young patient and advanced stage and older patients) and test how they would respond to insulin stimulation and glycolysis inhibition.

Lactate dehydrogenase (LDH) is a glycolytic enzyme that converts lactate to pyruvate. High levels of LDH in serum are an indicator of tissue damage. Studies demonstrated that high LDH levels correlated with CLL patients with shorter median survival (Itoyama et al. 2001). Tumor aggressiveness is directly proportional to serum LDH levels (Dumontet et al. 1999). LDH levels greater than 500 µg/mL correspond with poor

prognosis in CLL. However, a recent study reported that LDH levels may not be reliable surrogate marker for disease prediction (Bergmann et al. 2007). In the present study, CLL oxygen consumption rates did not vary significantly between patients in with normal and high LDH groups.

Beta-2-microglobulin (β2M) is a membrane protein (12 kDa) associated with the heavy chains of class I major histocompatibility complex proteins. It belongs to immunoglobulin superfamily. β2M is implicated in chemotaxis and suppresses immune response from T cells (Bernier 1980). However not much is known in term of its signaling and function. The presence of high levels of β2M, another poor prognostic feature (Hallek et al. 1996, Pflug et al. 2014), also showed a trend for increased OCR (Figure 15A).

Gender is also considered for prognosis in CLL. Previous studies showed that females fared better in response to therapy than male counterparts (Berger et al. 1978, Kelly et al. 2011, Robitaille et al. 2013). However, the reason behind the better prognosis of females remains unclear. CLL is also more common in men than women. In fact, a gender based score system was developed by GIMEMA, since, changes in progression free survival for CLL patients correlated only with gender (Kienle et al. 2006). This group also reported that females had an indolent disease course as IgVH mutations were frequent in this cohort and 17p and 11q deletions was less frequent this subgroup. CLL OxPhos did not vary in both male and female subsets of CLL.

CD38 is an ectoenzyme, present on the cell surface. It is also known as cyclic ADP ribose hydrolase that hydrolysis of cyclic ADP-ribose from NAD+ to ADP-ribose. It

regulates cell adhesion, signal transduction, and calcium regulation (Malavasi et al. 1994). CD38 is able to metabolize extracellular nucleotides, e.g., ATP and NAD, into nucleosides that can be taken up by cells (Aarhus et al. 1995). Increased CD38 expression, along with increased vascular density in lymph nodes, correlates with increased lymphocyte proliferation and disease progression. CD38 is used to distinguish B cells at various stages of differentiation (Shaik et al. 2008). As a result, CD38 expression inversely correlates with mutational status of IgVH, i.e., CLL B cells with elevated expression of CD38 (>20%) have unmutated IgVH. CD38 data was not available for most of the patients used in the present study. Out of the available patients' samples, 13 had low levels of CD38 (negative) and 8 had high levels (positive). Due to the limited sample size, not much variation in OCR was seen between the two groups (Figure 17A).

CLL cytogenetics and metabolism

Genetic mutations, indels and rearrangements also dictate the course of treatment. Deletion of TP53 (tumor suppressor 53) located on chromosome 17q and ATM (Ataxia – telangiectasia mutated) are related with poor clinical response of the disease. While, TP53 is the master tumor suppressor which regulates cell cycle progression and apoptosis, ATM functions primarily in DNA repair (Banin et al. 1998, Canman and Lim 1998). Trisomy 12 is another common genomic aberration in CLL. These deletions are not common in untreated CLL, but arise as a result of chemotherapy. Therefore, treatment for CLL after its first onset and reoccurrence would be based on the percent lymphocytosis and genetic aberrations. Clonal evolution does take place in CLL, to sustain activated signaling and become refractory to therapy. Mutations in SF3B1 (splicing factor 3B subunit 1) and XPO1 (exportin

1) are other new markers identified by exome sequencing that result in diminished response to therapy (Dohner et al. 2000, Landau et al. 2013, Ferreira et al. 2014).

TP53 negatively regulates cancer cell metabolism, therefore deletion of this gene, should alleviate the negative regulation on metabolic targets. However, the deletion of this genetic locus occurs least frequently (Dohner et al. 2000). Genetic deletion on chromosome 13q harboring retinoblastoma (RB) gene has very good clinical outcome, although patients with a higher percentage of nuclei exhibiting a 13q deletion had short survival (Cerezo et al. 2009). It is also the most common cytogenetic anomaly in CLL. Not many patient samples were available for the present study to evaluate the effect of a single genomic aberration on CLL OxPhos. Four patients harboring one or more of these cytogenetic abnormalities have relatively high OCR, but it is difficult to arrive at a conclusion in cases, as in most other patients the mutations are relatively insignificant or unknown (Figure 17B).

Microenvironment and CLL metabolism

Relapse rates for CLL are high in spite of promising targeted therapies (Ding et al. 2014). The primary reason for relapse is due to the residual disease in the bone marrow and lymph node compartments. Microenvironment confers protection to CLL by activating the signaling pathways in CLL and helps in survival, proliferation, chemotaxis, metabolism and angiogenesis. Microenvironment in CLL is diverse and contextual in different compartments, mainly, bone marrow (BM), lymph node (LN) and peripheral blood (PB). As discussed in the introduction, several cell types offer protection to CLL cells namely, bone marrow stroma cells, nurse-like cells, macrophages and T cells. Crosstalk between CLL cells and adjacent

cells take place by direct contact (adhesion molecules) or by secretion of cytokines into the extracellular matrix (ECM). Studies reported that CLL gene expression varies in depending on their location. CLL cells also proliferate in the germinal centers of BM and LN not in PB. CCL3 and CCL4 are secreted by CLL upon activation of BCR pathway which homes monocytes and T lymphocytes. High levels of CCL3 correlate with prognostic markers of the disease. Activation of BCR pathway leads to raised CCL3 and CCL4 levels (Burger et al. 2009, Herishanu et al. 2011).

A number of cell lines derived from human bone marrow as well as mouse bone marrow are employed for studying CLL- stroma interactions *in vitro*. These are NK.Tert, HS-5 (human), M2-10B4, KUSA-H1, KUSA (mouse). These cells mimic the stroma cells *in vivo* and provide survival advantage to CLL cells. Integrins α, β are adhesion molecules that mediate cell to cell interactions. Intergrin CD49d is a receptor for fibronectin and vascular cell adhesion molecule 1 (VCAM1). These integrins are expressed on most lymphocytes and mediate lymphocyte trafficking and immune surveillance (Butcher and Picker 1996). CLL B cells also adhere to bone marrow or lymph nodes via these integrins.

There is minimal understanding of interactions between CLL and its microenvironment in terms of metabolism. Therefore, studying the metabolic characteristics of CLL cells in context of microenvironment is critical. With exception of studies conducted by Huang's group (Zhang et al. 2012) and Mougiakakos's group (Jitschin et al. 2015), not many studies have been conducted to elucidate the metabolic responses and rewiring in CLL cells with context with microenvironment. Jitschin *et al.* reported that stroma cells modulate

CLL metabolism by upregulating glycolysis and genes involved in glycolytic pathway in a NOTCH- MYC dependent manner (Jitschin et al. 2015). They found overexpression of GLUT3 transporters on CLL cell surface, followed by increased ECAR post 6 day co-culture of 4 CLL samples with HS-5 (bone marrow derived stroma cells).However, ECAR levels observed in the CLL cells co-cultured with stromal cell lines and mesenchymal stroma cells obtained from patient biospies varied significantly. Although, glycolysis in the CLL cells increased with stroma in both the cases, the ECAR levels of CLL cells co-cultured with patient stromal cells was 10 fold lower as compared with cell lines. Furthermore, prolonged co-culture with stroma cells will generate nurse like cells and therefore changes the dynamics of CLL-stroma interaction (Burger et al. 2000). And with such few patients' samples, that were used in the Jitschin *et al*. study, it is hard to discern if glycolysis is upregulated in CLL cells upon stromal co-culture.

Zhang et al. demonstrated that CLL cells were dependent on stromal cells to import cysteine and synthesize glutathione, an antioxidant to relieve endogenous oxidative stress. The CLL cells have limited ability to take up cystine. After stroma cells take up cystine and convert to cysteine, CLL cell utilize the cysteine and synthesize glutathione (Zhang et al. 2012). These studies demonstrate the dependence of CLL cells on stroma for survival.

Several approaches used in the current study demonstrate that stroma interaction elevates mitochondrial respiration in CLL cells. Almost all samples displayed an increase in the OCR after 24-hour co-culture with NK.Tert cells. However, changes in glycolytic flux were variable when CLL were co-cultured with stroma and overall not significantly induced.

Co-culture with two other stromal cell lines recapitulated the effect on CLL the OCR and ECAR.

I also tested the impact of prognostic factors on stroma induced OCR. Owing to the overall increase in OCR across the patient samples tested, no differential impact on OCR was observed based on the expression levels of prognostic factors (Figures 25-28). Nonetheless, patients with low and high LDH levels did not display a significant increase in OCR upon stroma co-culture, in contrast to patients with medium LDH levels (Figures 26C). Similarly, patients of ages 60 to 69 did not exhibit significant increase in oxygen consumption (Figures 27B).

One of the main axes that is studied in bone marrow-CLL interactions is of CXCR4-CXCL12. Stroma derived factor 1(SDF-1/CXCL 12) is secreted by stromal cells and interacts with the CXCR4 receptor overexpressed on the CLL cell surface. ZAP 70 positive cells respond better to SDF-1 signaling which mediates chemotaxis towards BM/LN. This also results in migration of CLL cells beneath the stromal cell known as 'pseudoemperipolesis' (Burger et al. 1999). Additionally, SDF-1 protects CLL cells from undergoing spontaneous apoptosis. SDF-1 activates AKT and MAPK signaling pathways in CLL. Since, contact with bone marrow stroma cells upregulated OCR; I also tested if incubation with SDF-1 will recapitulate the response. Nevertheless, SDF-1 treatment did not augment CLL metabolism.

Similarly, the effect of B cell activating factor (BAFF) was also tested in inducing CLL OxPhos. BAFF is secreted by nurse like cells and promote CLL survival via paracrine signaling. BAFF-R, BCMA and TACI are the receptors for BAFF expressed on CLL. BAFF

belongs to the tumor necrosis family (TNF). It activates NF-κB and increases the expression of anti-apoptotic protein MCL-1 and promotes CLL cell survival. Incubation with BAFF for 24 hrs had a negative impact on oxygen consumption, contrary to what was expected. BAFF decreased CLL OCR, even in combination with SDF-1. The reason behind the decrease is unknown. These experiments further indicate the necessity of cell to cell contact for augmentation of OxPhos. This phenomenon of stroma induced CLL OCR is relatively quick, happens within 2 hrs of co-culture with stroma (Figure 32B). Nevertheless, CLL cells from two patient samples tested displayed higher levels of spare respiratory capacity after 24hr co-culture with stroma as compared to 2hr co-culture. And this may mean longer exposure to stromal cells may be necessary for CLL for mitochondrial respiration to be further elevated.

PI3K/AKT pathway regulates CLL metabolism

In concert with many previous studies, co-culture with stroma activated PI3K/AKT pathway, identified by phosphorylation of AKT (Figure 39A). Similarly, mTOR signaling pathway was also active determined by the phosphorylation of ribosomal S6 protein (Figure 38). PI3K is a lipid kinase that is most commonly activated in CLL. Mutations in the genes coding for PI3K isoforms are rare in CLL. Although infrequent, PIK3CA mutations (gene amplifications) are identified in 3.5% CLL cases (Brown et al. 2012). However, PI3K α is not the major player, when it comes to hematological malignancies; the delta isoform is the predominant active signaling molecule of this family.

PI3K/AKT/mTOR is a crucial regulatory pathways of cellular metabolism. In addition, PI3K can regulate metabolism in an AKT independent manner by activating MAPK (Mitogen activated protein kinase). MAPK is activated in CLL cells upon stromal interaction

by phosphorylation at Thr 44/42 residue (Balakrishnan et al. 2014). MAPK further activates p90RSK which in turn phosphorylates ribosomal S6 protein which regulates translation. MAPK can activate early response genes like c-MYC and c-FOS and thereby regulates transcription as well. c-MYC regulates glutamine uptake and genes involved in pyrimidine de novo synthesis (Huang and Graves 2003), cell cycle transition, e.g., E2F1. To be completely activated, AKT needs to be phosphorylated on Ser 473 by mTOR after initial activation by PDK1 on Thr 308. After both these sites are phosphorylated, AKT affects its downstream molecules.

The most well studied mode of PI3K signaling is through its ability to activate AKT. To be completely activated, AKT needs to be phosphorylated on Ser 273 473 by mTOR after initial activation by PDK1 on Thr 308. After both these sites are phosphorylated, AKT affects its downstream molecules. AKT plays an important role in cell proliferation by modulating numerous factors affecting cell growth. First, it regulates glycogen synthase kinase β (GSK3β) and cyclin dependent kinase (CDK) inhibitors. AKT can also directly boost ribosome biogenesis independent of TOR, thus promoting growth and proliferation (Chan et al. 2011). As mentioned in the introduction, AKT regulates insulin mediated glucose uptake and metabolism by trafficking glucose transporters to the cell membrane (GLUT1, GLUT4) and influencing the activity of the key enzymes of the glycolytic pathway including hexokinase and phosphofructokinase.

In the present study, neither glucose uptake nor the expression levels of the transporter, GLUT4 were augmented in CLL cells after stromal interactions. In fact, glucose uptake was markedly reduced in all samples, implying decreased dependence on glucose in CLL in context of microenvironment. However, additional studies need to be performed to

verify the reason behind decreased metabolic flux. Likewise, glutamine uptake was not particularly elevated in CLL cells post co-culture, although there was heterogeneity.

AKT was also shown to regulate the activity of mitochondrial electron chain complexes via 4E-BP-1. Downregulation of 4E-BP-1 activity by AKT increased the activity of all the respiratory complexes (Goo et al. 2012). Increase in the expression or activity was not found in CLL cells post co-culture, indicating that increased respiration is not due to amplification of ETC expression and activity (Figure 36).

AKT and nucleotide biosynthesis

AKT also regulates purine nucleotide biosynthesis. There are very few studies that evaluated nucleotide metabolism in CLL cells in comparison with normal cells (Henderson et al. 1974, Carlucci et al. 1997). Nucleotide metabolism provides precursors for both RNA and DNA synthesis. Therefore, it important to determine how the pathways of their synthesis are regulated. In case of CLL, the nucleotide pools are not directed towards DNA synthesis, as the latter does not take place as the cells are in a resting phase (Berger et al. 1978). In contrast, precursors for RNA synthesis are expected to increase, as RNA synthesis increases in CLL upon co-culture with stroma. AKT regulates phosphoribosylpyrophosphate (PRPP) production by the non-oxidative pentose phosphate pathway and also modulates the activity of aminoimidazole-carboxamide ribonucleotide transformylase (AICAR Transformylase), and inositide mono phosphate cyclohydrase (IMP cyclohydrase). IMP is center point of the de novo and salvage pathway of purine synthesis. Metabolite analysis has revealed that inosine levels increased in CLL cells after CLL co-culture with stromal cells, implying a increase in the metabolic flux of purine synthesis. In concordance, the rise in adenosine

monophosphate (AMP) and guandine monophosphate levels (GMP) signifies that purine synthesis is augmented in presence of stroma. IMP directly feeds into AMP synthesis and IMP is converted to xanthosine monophosphate before conversion to GMP (Henderson and Paterson 1973).

On the basis of the augmentation of the OCR after co-culturing with stroma, the cellular ATP pool in CLL lymphocytes might increase. As expected, in concert with increased OxPhos, ATP pools increased as well. Increase in the other nucleotide pools (CTP, GTP and UTP can be explained by altered enzymatic activity of purine and pyrimidine biosynthesis pathways.

Pyrimidine synthesis on the other hand is linked to mitochondrial ETC, by the enzyme dihydro orotate dehydrogenase (DHODH) that resides in the inner mitochondrial membrane, the only enzyme in that pathway that is located in the mitochondria (Figure 59). It reduces ubiquinone to ubiquitol and converts dihydroorotate to orotate (Jones 1980). Marginal increase in cellular orotate levels indicates the induction of DHODH activity along with OxPhos. Furthermore, UTP is converted to CTP directly by CTP synthase (Evans and Guy 2004). Additionally, mTOR signaling has recently been implicated in pyrimidine synthesis by phosphorylating carbamoyl-phosphate synthetase 2, aspartate transcarbamylase, dihydroorotase (CAD) (Ben-Sahra et al. 2013, Robitaille et al. 2013). However, this has not been tested in present study. CAD phosphorylation can be tested in CLL cells co-cultured with stroma by immunoblotting.

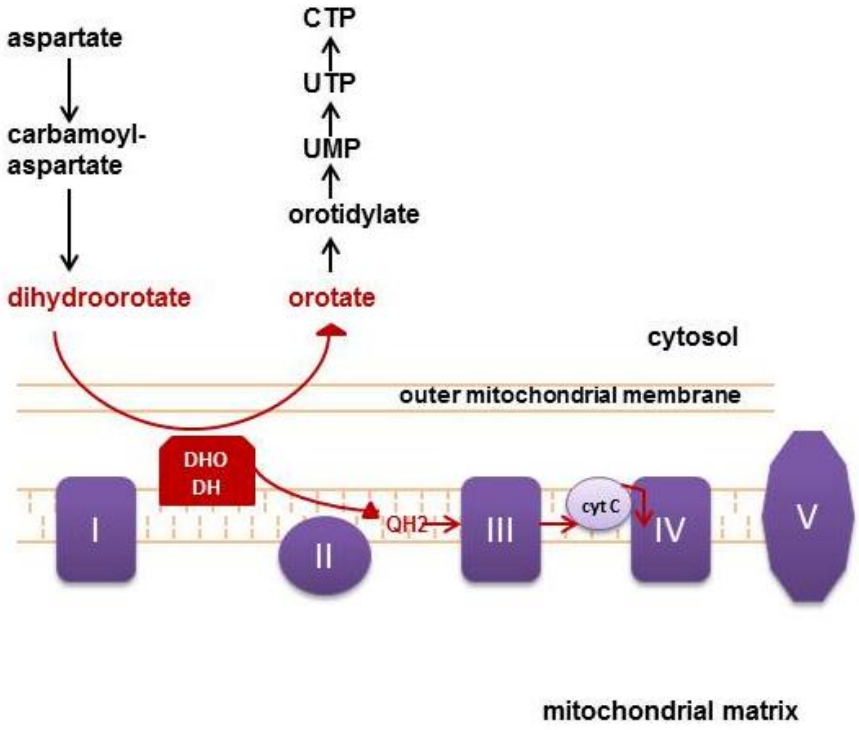

Figure 59. De novo pyrimidine synthesis pathway in the cell.

Cytidine triphosphate and Uridine triphosphate are the end products of the de novo pyrimidine synthesis pathway. One of critical steps in the pathway is catalyzed by the enzyme dihydroorotate dehydrogenase (DHODH) that resides in the inner mitochondrial membrane. It converts dihydroorotate to orotate. Broken red arrows depict the flow of electrons.

PI3K inhibitors in CLL

CLL bioenergetic rewiring is also associated with kinase sensitivity; for example, CLL was classified into subsets based on the dasatinib-induced differential dependency on mitochondrial respiration to cope with cellular stress and meet the ATP demands (Martinez Marignac et al. 2013). Although genetic lesions are absent in PI3K/AKT pathway in CLL, it is hyper activated by the microenvironment and therefore is a hot target for therapy. It is a key component of both chronic and tonic B-cell receptor-signaling pathways. Over the years, many PI3K inhibitors have been developed to treat lymphoid malignancies, starting with pan-PI3K inhibitors and gradually moved to isoform specific inhibitors. Some of the pan-PI3K inhibitors include copanlisib, buparlisib and GDC0941. PI3K δ responds to activation of many cell receptors like BCR, CD40, IL6, CXCR4 and 5 among others and therefore contributes to majority of the cancer hallmarks. Amongst the array of PI3K, AKT and mTOR inhibitors, it was the isoform specific PI3K inhibitors that were well tolerated as the others failed in clinical trials to high cytotoxity (Kelly et al. 2011).

Duvelisib is a small molecule inhibitor that binds to the ATP-binding site of the kinases, thereby preventing activation of the PI3Kδ/γ isoforms (Figure 60) (Winkler et al. 2013). It is currently in clinical trials as monotherapy # NCT02004522. It has shown better efficiency than idelalisib in inactivating AKT and reduced CLL cell survival in presence of stroma.

Duvelisib mitigates AKT and mTOR activity (Balakrishnan et al. 2015). In concert with these effects AKT on metabolic pathways, duvelisib treatment reduced glycolysis and

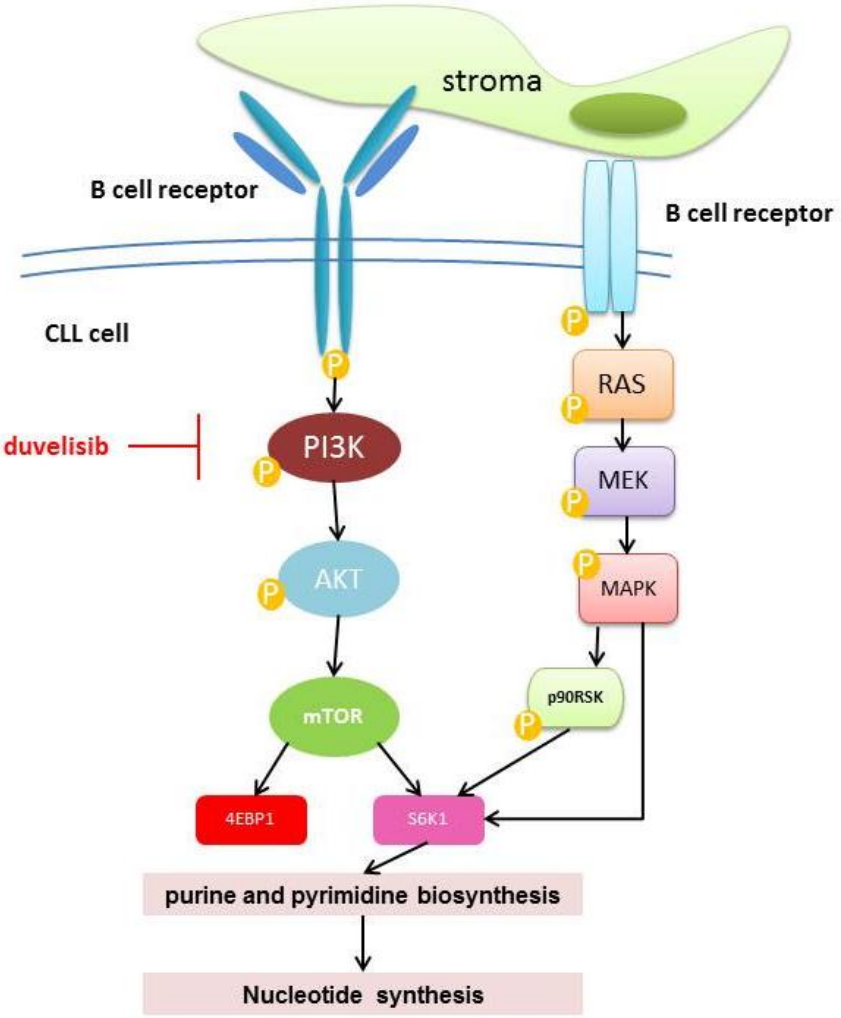

Figure 60. Targeting PI3K pathway inhibits cellular biosynthesis.

Contact with stroma enhances CLL survival and metabolism. Pharmacological inhibition using PI3K δ/γ inhibitor targets AKT pathway and impacts CLL cell metabolism and nucleotide biosynthesis. S6K1 ribosomal protein is activated by AKT and/or MAPK pathway, which in turn stimulates purine and pyrimidine synthesis, leading to an increase in the nucleotide pools.

mitochondrial respiration in CLL (Figure 41-42). Glycolysis was an anticipated target as it directly regulates glycolysis. Glucose uptake, nonetheless, was not affected (Figure 46).

It is speculated that glucose utilization by CLL cells is being affected because uptake of glucose did not decrease, and yet glycolysis and OxPhos were significantly down-regulated. Mitochondrial OCR may have decreased as AKT was postulated to regulate the function of mitochondrial ETC (Shaik et al. 2008) in addition to what was reported by Goo et al, i.e., AKT acting via 4E-BP-1 to control OxPhos. In context of CLL, there is no direct evidence of AKT affecting the mitochondrial complexes activity. Duvelisib did not impact mitochondrial biology or other functionalities tested in spite of mitigating the ATP levels in CLL cells (Figure 49). Moreover, the decline in CLL OxPhos and glycolysis with MK2206 demonstrated that the mitigation was AKT-dependent (Figure 44-45).

To evaluate if PI3K γ signaling is necessary for glycolysis and OxPhos, PI3K δ only inhibitor, idelalisib was used. Idelalisib also mitigated both the energy generating pathways, implying PI3K δ signaling alone is sufficient to curtail metabolism (Figure 44-45). Genetic ablation of PIK3CD, the gene coding for PI3K δ significantly lowered OCR and ECAR in mantle cell lymphoma cell line. This further demonstrates the importance of PI3K δ in regulating metabolism. This is the first study to highlight the significance of PI3K δ signaling in regulating CLL metabolism. Cell lines employed to create the knockout were those of mantle cell lymphoma, JeKo-1 and diffuse large B-cell lymphoma (DLBCL), Ly19. Ly19 cells failed to proliferate after separation from a mixed population of WT and KO cells.

PI3K δ knockout was also very toxic to cells, underlining its importance in proliferation and survival. These data explain why PI3K δ knockout is not tolerated in some cell lines. A recent study demonstrated the importance of PI3K pathway in survival of mature

B cells lacking B cell receptor (Srinivasan et al. 2009). In the same study, the significance of AKT signaling is highlighted when PTEN deletion rescued the cells.

BCR pathway is largely the central pathway in CLL. Since, PI3K and AKT fall under the umbrella of BCR signaling, I tested the significance and role of B cell receptor in CLL metabolism. PI3K/AKT act as second messengers for signals from a variety of receptors, therefore, the importance of BCR in context of metabolism is still under question.
BCR knockout cells from JeKo-1 cell line dramatically decreased OxPhos similar to PI3K knockout. BCR KO cells retained basal levels of p-AKT ser473 and p-MAPK thr44/42, similar to WT cells; however, they were unresponsive to IgM stimulation. Addition of IgM, abrogated their ability to further activate AKT and MAPK signaling. BCR signaling is of paramount important regarding every aspect of CLL survival and sustenance.

Future directions

'Firstly, amongst the prognostic factors considered for this study that correlated with glycolysis and OxPhos rates of CLL cells, ZAP 70 and IgVH status impacts the signaling of these cells; therefore, it would be necessary to test if patients' samples from ZAP 70 positive and IgVH unmutated CLL cohort respond better (cell death) to inhibition of OxPhos by PI3K inhibitors'

The exact mechanism underlying the augmentation of OxPhos in CLL cells, when it comes in contact with stroma in yet to be unfurled. The overall bioenergy (ATP) and biosynthesis (nucleotide pools) increased due to bone marrow stromal co-culture in CLL in a span of 24hrs. Tricarboxylic acid cycle (TCA) intermediates as well as OxPhos augmented,

suggesting energy in CLL cells is predominantly generated by oxidative metabolism in presence of microenvironment.

The pathways governing the metabolic activities are upregulated (PI3K/AKT/mTOR) in CLL. However, the downstream effectors of these pathways impacting mitochondrial metabolism are elusive.

Mitochondrial biogenesis may not the reason behind increase in OxPhos. Similarly, the activity of the electron transport chain does not particularly change upon stromal interaction with CLL. It maybe speculated that the increase of substrate availability to the ETC complexes could be a possibility as to why OxPhos was amplified. Carbon tracing experiments will give a better idea for delineating the substrate flow in the metabolic pathways.

STAT3 has been implicated in mitochondrial biogenesis. STAT3 could be impacting mitochondrial activity by localizing and thereby, interacting with complex I proteins. So far, only one study so far has been able to conclusively prove the relocation of STAT3 to mitochondria (Wegrzyn et al. 2009). Estov's group demonstrated that STAT3 is responsible for the dependence of CLL on fatty acid utilization. In the present study, phosphorylated STAT3 was one of the proteins whose levels were elevated upon stroma co-culture, upon RPPA analysis. Nonetheless, CLL cells were unable to fuel OxPhos upon providing fatty acid as a substrate, when tested using the extracellular flux analyzer. The utilization of intrinsic fatty acid to fuel OxPhos can be tested, by inhibiting fatty acid synthesis using a drug, etoximir that blocks the activity of fatty acid synthase. Carbon tracing as mentioned previously along with this experiment should identify the fuel source for OxPhos in CLL.

Cellular NADH/ NAD^+ ratio determines the redox state of a cell. This ratio in CLL needs to be measured after stroma co-culture to check for elevated substrate levels for complex I of mitochondria. Additionally, STAT3 inhibitors could be tested to check if OxPhos or glycolysis is affected.

Preliminary data from the metabolite analysis of CLL post stromal co-culture, indicated elevated DHODH enzyme activity, as orotate levels increased. This observation can be further extended using 10 patient samples for stroma co-cultures and for longer time points (48hrs), then assay OxPhos, DHODH activity (by spectrophotometry) and pyrimidine pools (by mass spectroscopy). This would give us an insight, if OxPhos induction and DHODH activity are correlated and increased DHODH activity corresponds to pyrimidine synthesis.

The major pathway in CLL resulting in increased purine and pyrimidine synthesis, upon stroma co-culture still remains elusive. While ribosomal protein S6 is phosphorylated upon co-culture in CLL, it could be activated via mTOR signaling or MAPK signaling. BCR KO in JeKo-1 cell lines abrogated MAPK signaling, whereas, AKT phosphorylation at Ser473 remained intact (not shown), indicating mTOR activity maybe unperturbed. If NTP pools in BCR KO JeKo-1 cells show a drop in purine and pyrimidine levels when compared to wild-type cells when measured, it is implied that MAPK pathway mainly regulates nucleotide synthesis in malignant B cells. To further ensure that increase in activity of S6 protein leads to augmentation of purine and pyrimidine synthesis, microRNA targeting S6 can be employed. If suppression of S6 protein leads to decrease in NTP pools, then S6 is upstream of nucleotide synthesis as postulated. If the nucleotide levels do not decrease, upon loss of S6 activity, then an alternative pathway for nucleotide metabolism like c-MYC needs

to be tested (Liu et al. 2008). Additional BCR KO cell lines should be used to test this hypothesis.

RNA sequencing may help identify non coding RNAs, that regulate metabolism (Tomasetti et al. 2014) in CLL and whose expression is altered upon co-culture. MicroRNAs (miRs) are reported to localize to mitochondria and influence ATP synthesis (Das et al. 2012). These miRs are also implicated in mediating tumor-stroma interactions (Bronisz et al. 2012, Ell and Kang 2013). It would be interesting to check if any of the miRs whose expression is affected, control mitochondrial metabolism in CLL.

This study underpins the necessity for using drugs that target cancer cell metabolism. CLL relapse rates can be decreased and disease free survival can be prolonged, if metabolic pathways are targeted. Existing drugs like the kinase and AKT inhibitors have a dual role, they repress the activity of the target pathway as well as affect metabolism. Meanwhile, drugs that specifically inhibit mitochondrial respiration and glycolysis are being tested (Toogood 2008, Mathupala et al. 2009, Liu et al. 2012). Drugs should be tailored to target oncogenes or pathways that are hyper activated in CLL along with cell metabolism, as solely targeting metabolism may not be beneficial to CLL as the disease is compartmentalized and as cells in circulation do not proliferate. The anti-metabolic drugs can be used against residual disease after traditional chemotherapy.

Using anti-metabolites for therapy is not a new concept. First antimetabolites that were used in cancer therapy were purine and pyrimidine analogous. 5-flurouracil was one of them. Gemcitabine is another popular drug that inhibits DNA and RNA synthesis, therefore it is used a frontline treatment for pancreatic and metastatic breast cancers (www.cancer.org).

Fludarabine, which is highly effective for treatment of CLL, is purine analogue that targets DNA synthesis. And clearly, interaction with stroma is providing a survival advantage for CLL cells not just by activating the pathways for cell survival and anti-apoptotic protein, but also by increasing the RNA synthesis as well as protein translation.

References

Aarhus, R., R. M. Graeff, D. M. Dickey, T. F. Walseth and H. C. Lee (1995). "ADP-ribosyl cyclase and CD38 catalyze the synthesis of a calcium-mobilizing metabolite from NADP." J Biol Chem **270**(51): 30327-30333.

Alcazar, I., M. Marques, A. Kumar, E. Hirsch, M. Wymann, A. C. Carrera and D. F. Barber (2007). "Phosphoinositide 3-kinase gamma participates in T cell receptor-induced T cell activation." J Exp Med **204**(12): 2977-2987.

Andrews, Z. B., S. Diano and T. L. Horvath (2005). "Mitochondrial uncoupling proteins in the CNS: in support of function and survival." Nat Rev Neurosci **6**(11): 829-840.

Arvisais, E. W., A. Romanelli, X. Hou and J. S. Davis (2006). "AKT-independent phosphorylation of TSC2 and activation of mTOR and ribosomal protein S6 kinase signaling by prostaglandin F2alpha." J Biol Chem **281**(37): 26904-26913.

Balakrishnan, K., J. A. Burger, M. Fu, T. Doifode, W. G. Wierda and V. Gandhi (2014). "Regulation of Mcl-1 expression in context to bone marrow stromal microenvironment in chronic lymphocytic leukemia." Neoplasia **16**(12): 1036-1046.

Balakrishnan, K., M. Peluso, M. Fu, N. Y. Rosin, J. A. Burger, W. G. Wierda, M. J. Keating, K. Faia, S. O'Brien, J. L. Kutok and V. Gandhi (2015). "The phosphoinositide-3-kinase (PI3K)-delta and gamma inhibitor, IPI-145 (Duvelisib), overcomes signals from the PI3K/AKT/S6 pathway and promotes apoptosis in CLL." Leukemia **29**(9): 1811-1822.

Banin, S., L. Moyal, S. Shieh, Y. Taya, C. W. Anderson, L. Chessa, N. I. Smorodinsky, C. Prives, Y. Reiss, Y. Shiloh and Y. Ziv (1998). "Enhanced phosphorylation of p53 by ATM in response to DNA damage." Science **281**(5383): 1674-1677.

Barretina, J., J. Junca, A. Llano, A. Gutierrez, A. Flores, J. Blanco, B. Clotet and J. A. Este (2003). "CXCR4 and SDF-1 expression in B-cell chronic lymphocytic leukemia and stage of the disease." Ann Hematol **82**(8): 500-505.

Ben-Sahra, I., J. J. Howell, J. M. Asara and B. D. Manning (2013). "Stimulation of de novo pyrimidine synthesis by growth signaling through mTOR and S6K1." Science **339**(6125): 1323-1328.

Benistant, C., H. Chapuis and S. Roche (2000). "A specific function for phosphatidylinositol 3-kinase alpha (p85alpha-p110alpha) in cell survival and for phosphatidylinositol 3-kinase beta (p85alpha-p110beta) in de novo DNA synthesis of human colon carcinoma cells." Oncogene **19**(44): 5083-5090.

Berger, N. A., J. W. Adams, G. W. Sikorski, S. J. Petzold and W. T. Shearer (1978). "Synthesis of DNA and poly(adenosine diphosphate ribose) in normal and chronic lymphocytic leukemia lymphocytes." J Clin Invest **62**(1): 111-118.

Bergmann, M. A., B. F. Eichhorst, R. Busch, D. Adorf, S. Stilgenbauer, M. J. Eckart, C. M. Wendtner, M. Hallek and Gcllsg (2007). "Prospective evaluation of prognostic parameters in early stage chronic lymphocytic leukemia (CLL): Results of the CLL1-protocol of the German CLL study group (GCLLSG)." Blood **110**(11): 193a-193a.

Bernier, G. M. (1980). "beta 2-Microglobulin: structure, function and significance." Vox Sang **38**(6): 323-327.

Bi, L., I. Okabe, D. J. Bernard and R. L. Nussbaum (2002). "Early embryonic lethality in mice deficient in the p110beta catalytic subunit of PI 3-kinase." Mamm Genome **13**(3): 169-172.

Bi, L., I. Okabe, D. J. Bernard, A. Wynshaw-Boris and R. L. Nussbaum (1999). "Proliferative defect and embryonic lethality in mice homozygous for a deletion in the p110alpha subunit of phosphoinositide 3-kinase." J Biol Chem **274**(16): 10963-10968.

Brody, J. I. and K. Merlie (1970). "Metabolic and biosynthetic features of lymphocytes from patients with diabetes mellitus: similarities to lymphocytes in chronic lymphocytic leukaemia." Br J Haematol **19**(2): 193-201.

Brody, J. I., F. A. Oski and D. E. Singer (1969). "Impaired pentose phosphate shunt and decreased glycolytic activity in lymphocytes of chronic lymphocytic leukemia. Metabolic pathway." Blood **34**(4): 421-429.

Bronisz, A., J. Godlewski, J. A. Wallace, A. S. Merchant, M. O. Nowicki, H. Mathsyaraja, R. Srinivasan, A. J. Trimboli, C. K. Martin, F. Li, L. Yu, S. A. Fernandez, T. Pecot, T. J. Rosol, S. Cory, M. Hallett, M. Park, M. G. Piper, C. B. Marsh, L. D. Yee, R. E. Jimenez, G. Nuovo, S. E. Lawler, E. A. Chiocca, G. Leone and M. C. Ostrowski

(2012). "Reprogramming of the tumour microenvironment by stromal PTEN-regulated miR-320." Nat Cell Biol **14**(2): 159-167.

Brown, J. R. (2011). "The treatment of relapsed refractory chronic lymphocytic leukemia." Hematology Am Soc Hematol Educ Program **2011**: 110-118.

Brown, J. R., M. Hanna, B. Tesar, L. Werner, N. Pochet, J. M. Asara, Y. E. Wang, P. Dal Cin, S. M. Fernandes, C. Thompson, L. Macconaill, C. J. Wu, Y. Van de Peer, M. Correll, A. Regev, D. Neuberg and A. S. Freedman (2012). "Integrative genomic analysis implicates gain of PIK3CA at 3q26 and MYC at 8q24 in chronic lymphocytic leukemia." Clin Cancer Res **18**(14): 3791-3802.

Brunet, A., A. Bonni, M. J. Zigmond, M. Z. Lin, P. Juo, L. S. Hu, M. J. Anderson, K. C. Arden, J. Blenis and M. E. Greenberg (1999). "Akt promotes cell survival by phosphorylating and inhibiting a Forkhead transcription factor." Cell **96**(6): 857-868.

Burger, J. A., M. Burger and T. J. Kipps (1999). "Chronic lymphocytic leukemia B cells express functional CXCR4 chemokine receptors that mediate spontaneous migration beneath bone marrow stromal cells." Blood **94**(11): 3658-3667.

Burger, J. A. and N. Chiorazzi (2013). "B cell receptor signaling in chronic lymphocytic leukemia." Trends Immunol **34**(12): 592-601.

Burger, J. A., M. P. Quiroga, E. Hartmann, A. Burkle, W. G. Wierda, M. J. Keating and A. Rosenwald (2009). "High-level expression of the T-cell chemokines CCL3 and CCL4 by chronic lymphocytic leukemia B cells in nurselike cell cocultures and after BCR stimulation." Blood **113**(13): 3050-3058.

Burger, J. A., N. Tsukada, M. Burger, N. J. Zvaifler, M. Dell'Aquila and T. J. Kipps (2000). "Blood-derived nurse-like cells protect chronic lymphocytic leukemia B cells from spontaneous apoptosis through stromal cell-derived factor-1." Blood **96**(8): 2655-2663.

Butcher, E. C. and L. J. Picker (1996). "Lymphocyte homing and homeostasis." Science **272**(5258): 60-66.

Caligaris-Cappio, F. and T. J. Hamblin (1999). "B-cell chronic lymphocytic leukemia: a bird of a different feather." J Clin Oncol **17**(1): 399-408.

Canman, C. E. and D. S. Lim (1998). "The role of ATM in DNA damage responses and cancer." Oncogene **17**(25): 3301-3308.

Cantley, L. C. (2002). "The phosphoinositide 3-kinase pathway." Science **296**(5573): 1655-1657.

Carew, J. S., Y. Zhou, M. Albitar, J. D. Carew, M. J. Keating and P. Huang (2003). "Mitochondrial DNA mutations in primary leukemia cells after chemotherapy: clinical significance and therapeutic implications." Leukemia **17**(8): 1437-1447.

Carlucci, F., F. Rosi, C. Di Pietro, E. Marinello, M. Pizzichini and A. Tabucchi (1997). "Purine nucleotide metabolism: specific aspects in chronic lymphocytic leukemia lymphocytes." Biochim Biophys Acta **1360**(3): 203-210.

Caron, F., C. Jacq and J. Rouviere-Yaniv (1979). "Characterization of a histone-like protein extracted from yeast mitochondria." Proc Natl Acad Sci U S A **76**(9): 4265-4269.

Cerezo, M., H. J. Bandelt, I. Martin-Guerrero, M. Ardanaz, A. Vega, A. Carracedo, A. Garcia-Orad and A. Salas (2009). "High mitochondrial DNA stability in B-cell chronic lymphocytic leukemia." PLoS One **4**(11): e7902.

Cerniglia, G. J., S. Dey, S. M. Gallagher-Colombo, N. A. Daurio, S. Tuttle, T. M. Busch, A. Lin, R. Sun, T. V. Esipova, S. A. Vinogradov, N. Denko, C. Koumenis and A. Maity (2015). "The PI3K/Akt Pathway Regulates Oxygen Metabolism via Pyruvate Dehydrogenase (PDH)-E1alpha Phosphorylation." Mol Cancer Ther **14**(8): 1928-1938.

Chan, J. C., K. M. Hannan, K. Riddell, P. Y. Ng, A. Peck, R. S. Lee, S. Hung, M. V. Astle, M. Bywater, M. Wall, G. Poortinga, K. Jastrzebski, K. E. Sheppard, B. A. Hemmings, M. N. Hall, R. W. Johnstone, G. A. McArthur, R. D. Hannan and R. B. Pearson (2011). "AKT promotes rRNA synthesis and cooperates with c-MYC to stimulate ribosome biogenesis in cancer." Sci Signal **4**(188): ra56.

Chen, L., J. Apgar, L. Huynh, F. Dicker, T. Giago-McGahan, L. Rassenti, A. Weiss and T. J. Kipps (2005). "ZAP-70 directly enhances IgM signaling in chronic lymphocytic leukemia." Blood **105**(5): 2036-2041.

Chen, L., G. Widhopf, L. Huynh, L. Rassenti, K. R. Rai, A. Weiss and T. J. Kipps (2002). "Expression of ZAP-70 is associated with increased B-cell receptor signaling in chronic lymphocytic leukemia." Blood **100**(13): 4609-4614.

Chiorazzi, N., K. R. Rai and M. Ferrarini (2005). "Chronic lymphocytic leukemia." N Engl J Med **352**(8): 804-815.

Clayton, E., G. Bardi, S. E. Bell, D. Chantry, C. P. Downes, A. Gray, L. A. Humphries, D. Rawlings, H. Reynolds, E. Vigorito and M. Turner (2002). "A crucial role for the p110delta subunit of phosphatidylinositol 3-kinase in B cell development and activation." J Exp Med **196**(6): 753-763.

Crespo, M., F. Bosch, N. Villamor, B. Bellosillo, D. Colomer, M. Rozman, S. Marce, A. Lopez-Guillermo, E. Campo and E. Montserrat (2003). "ZAP-70 expression as a surrogate for immunoglobulin-variable-region mutations in chronic lymphocytic leukemia." N Engl J Med **348**(18): 1764-1775.

Cui, B., L. Chen, S. Zhang, M. Mraz, J. F. Fecteau, J. Yu, E. M. Ghia, L. Zhang, L. Bao, L. Z. Rassenti, K. Messer, G. A. Calin, C. M. Croce and T. J. Kipps (2014). "MicroRNA-155 influences B-cell receptor signaling and associates with aggressive disease in chronic lymphocytic leukemia." Blood **124**(4): 546-554.

Cuni, S., P. Perez-Aciego, G. Perez-Chacon, J. A. Vargas, A. Sanchez, F. M. Martin-Saavedra, S. Ballester, J. Garcia-Marco, J. Jorda and A. Durantez (2004). "A sustained activation of PI3K/NF-kappaB pathway is critical for the survival of chronic lymphocytic leukemia B cells." Leukemia **18**(8): 1391-1400.

Cuttner, J. (1992). "Increased incidence of hematologic malignancies in first-degree relatives of patients with chronic lymphocytic leukemia." Cancer Invest **10**(2): 103-109.

Damle, R. N., F. M. Batliwalla, F. Ghiotto, A. Valetto, E. Albesiano, C. Sison, S. L. Allen, J. Kolitz, V. P. Vinciguerra, P. Kudalkar, T. Wasil, K. R. Rai, M. Ferrarini, P. K. Gregersen and N. Chiorazzi (2004). "Telomere length and telomerase activity delineate distinctive replicative features of the B-CLL subgroups defined by immunoglobulin V gene mutations." Blood **103**(2): 375-382.

Damle, R. N., S. Temburni, C. Calissano, S. Yancopoulos, T. Banapour, C. Sison, S. L. Allen, K. R. Rai and N. Chiorazzi (2007). "CD38 expression labels an activated subset within chronic lymphocytic leukemia clones enriched in proliferating B cells." Blood **110**(9): 3352-3359.

Damle, R. N., T. Wasil, F. Fais, F. Ghiotto, A. Valetto, S. L. Allen, A. Buchbinder, D. Budman, K. Dittmar, J. Kolitz, S. M. Lichtman, P. Schulman, V. P. Vinciguerra, K. R. Rai, M. Ferrarini and N. Chiorazzi (1999). "Ig V gene mutation status and CD38

expression as novel prognostic indicators in chronic lymphocytic leukemia." Blood **94**(6): 1840-1847.

Das, S., M. Ferlito, O. A. Kent, K. Fox-Talbot, R. Wang, D. Liu, N. Raghavachari, Y. Yang, S. J. Wheelan, E. Murphy and C. Steenbergen (2012). "Nuclear miRNA regulates the mitochondrial genome in the heart." Circ Res **110**(12): 1596-1603.

Datta, S. R., H. Dudek, X. Tao, S. Masters, H. Fu, Y. Gotoh and M. E. Greenberg (1997). "Akt phosphorylation of BAD couples survival signals to the cell-intrinsic death machinery." Cell **91**(2): 231-241.

Deaglio, S., T. Vaisitti, S. Serra, V. Audrito, C. Bologna, G. D'Arena, L. Laurenti, D. Gottardi and F. Malavasi (2011). "CD38 in chronic lymphocytic leukemia: from bench to bedside?" Mini Rev Med Chem **11**(6): 503-507.

DeBerardinis, R. J., J. J. Lum, G. Hatzivassiliou and C. B. Thompson (2008). "The biology of cancer: metabolic reprogramming fuels cell growth and proliferation." Cell Metab **7**(1): 11-20.

DeFrancesco, L. and G. Attardi (1981). "In situ photochemical crosslinking of HeLa cell mitochondrial DNA by a psoralen derivative reveals a protected region near the origin of replication." Nucleic Acids Res **9**(22): 6017-6030.

Demaria, M., C. Giorgi, M. Lebiedzinska, G. Esposito, L. D'Angeli, A. Bartoli, D. J. Gough, J. Turkson, D. E. Levy, C. J. Watson, M. R. Wieckowski, P. Provero, P. Pinton and V. Poli (2010). "A STAT3-mediated metabolic switch is involved in tumour transformation and STAT3 addiction." Aging (Albany NY) **2**(11): 823-842.

Deprez, J., D. Vertommen, D. R. Alessi, L. Hue and M. H. Rider (1997). "Phosphorylation and activation of heart 6-phosphofructo-2-kinase by protein kinase B and other protein kinases of the insulin signaling cascades." J Biol Chem **272**(28): 17269-17275.

Diehl, J. A., M. Cheng, M. F. Roussel and C. J. Sherr (1998). "Glycogen synthase kinase-3beta regulates cyclin D1 proteolysis and subcellular localization." Genes Dev **12**(22): 3499-3511.

Ding, W., T. D. Shanafelt, C. E. Lesnick, C. Erlichman, J. F. Leis, C. Secreto, T. R. Sassoon, T. G. Call, D. A. Bowen, M. Conte, S. Kumar and N. E. Kay (2014). "Akt inhibitor MK2206 selectively targets CLL B-cell receptor induced cytokines, mobilizes

lymphocytes and synergizes with bendamustine to induce CLL apoptosis." Br J Haematol **164**(1): 146-150.

Dohner, H., S. Stilgenbauer, A. Benner, E. Leupolt, A. Krober, L. Bullinger, K. Dohner, M. Bentz and P. Lichter (2000). "Genomic aberrations and survival in chronic lymphocytic leukemia." N Engl J Med **343**(26): 1910-1916.

Dong, S., D. Guinn, J. A. Dubovsky, Y. Zhong, A. Lehman, J. Kutok, J. A. Woyach, J. C. Byrd and A. J. Johnson (2014). "IPI-145 antagonizes intrinsic and extrinsic survival signals in chronic lymphocytic leukemia cells." Blood **124**(24): 3583-3586.

Dreger, P., J. Schetelig, N. Andersen, P. Corradini, M. van Gelder, J. Gribben, E. Kimby, M. Michallet, C. Moreno, S. Stilgenbauer, E. Montserrat, C. L. L. European Research Initiative on, B. the European Society for and T. Marrow (2014). "Managing high-risk CLL during transition to a new treatment era: stem cell transplantation or novel agents?" Blood **124**(26): 3841-3849.

Dumontet, C., J. Drai, J. Bienvenu, E. N. Berard, C. Thieblemont, F. Bouafia, F. Bayle, I. Moullet, G. Salles and B. Coiffier (1999). "Profiles and prognostic values of LDH isoenzymes in patients with non-Hodgkin's lymphoma." Leukemia **13**(5): 811-817.

Durig, J., M. Naschar, U. Schmucker, K. Renzing-Kohler, T. Holter, A. Huttmann and U. Duhrsen (2002). "CD38 expression is an important prognostic marker in chronic lymphocytic leukaemia." Leukemia **16**(1): 30-35.

Eagle, H. (1955). "Nutrition needs of mammalian cells in tissue culture." Science **122**(3168): 501-514.

Ell, B. and Y. Kang (2013). "MicroRNAs as regulators of tumor-associated stromal cells." Oncotarget **4**(12): 2166-2167.

Engelman, J. A., J. Luo and L. C. Cantley (2006). "The evolution of phosphatidylinositol 3-kinases as regulators of growth and metabolism." Nat Rev Genet **7**(8): 606-619.

Enns, G. M., C. L. Hoppel, S. J. DeArmond, S. Schelley, N. Bass, K. Weisiger, D. Horoupian and S. Packman (2005). "Relationship of primary mitochondrial respiratory chain dysfunction to fiber type abnormalities in skeletal muscle." Clin Genet **68**(4): 337-348.

Evans, D. R. and H. I. Guy (2004). "Mammalian pyrimidine biosynthesis: fresh insights into an ancient pathway." J Biol Chem **279**(32): 33035-33038.

Ferreira, P. G., P. Jares, D. Rico, G. Gomez-Lopez, A. Martinez-Trillos, N. Villamor, S. Ecker, A. Gonzalez-Perez, D. G. Knowles, J. Monlong, R. Johnson, V. Quesada, S. Djebali, P. Papasaikas, M. Lopez-Guerra, D. Colomer, C. Royo, M. Cazorla, M. Pinyol, G. Clot, M. Aymerich, M. Rozman, M. Kulis, D. Tamborero, A. Gouin, J. Blanc, M. Gut, I. Gut, X. S. Puente, D. G. Pisano, J. I. Martin-Subero, N. Lopez-Bigas, A. Lopez-Guillermo, A. Valencia, C. Lopez-Otin, E. Campo and R. Guigo (2014). "Transcriptome characterization by RNA sequencing identifies a major molecular and clinical subdivision in chronic lymphocytic leukemia." Genome Res **24**(2): 212-226.

Fink, S. R., S. A. Smoley, K. J. Stockero, S. F. Paternoster, E. C. Thorland, D. L. Van Dyke, T. D. Shanafelt, C. S. Zent, T. G. Call, N. E. Kay and G. W. Dewald (2006). "Loss of TP53 is due to rearrangements involving chromosome region 17p10 approximately p12 in chronic lymphocytic leukemia." Cancer Genet Cytogenet **167**(2): 177-181.

Foster, F. M., C. J. Traer, S. M. Abraham and M. J. Fry (2003). "The phosphoinositide (PI) 3-kinase family." J Cell Sci **116**(Pt 15): 3037-3040.

Fruman, D. A. and L. C. Cantley (2014). "Idelalisib--a PI3Kdelta inhibitor for B-cell cancers." N Engl J Med **370**(11): 1061-1062.

Ghia, P., N. Chiorazzi and K. Stamatopoulos (2008). "Microenvironmental influences in chronic lymphocytic leukaemia: the role of antigen stimulation." J Intern Med **264**(6): 549-562.

Gobessi, S., L. Laurenti, P. G. Longo, S. Sica, G. Leone and D. G. Efremov (2007). "ZAP-70 enhances B-cell-receptor signaling despite absent or inefficient tyrosine kinase activation in chronic lymphocytic leukemia and lymphoma B cells." Blood **109**(5): 2032-2039.

Goo, C. K., H. Y. Lim, Q. S. Ho, H. P. Too, M. V. Clement and K. P. Wong (2012). "PTEN/Akt signaling controls mitochondrial respiratory capacity through 4E-BP1." PLoS One **7**(9): e45806.

Gopal, A. K., B. S. Kahl, S. de Vos, N. D. Wagner-Johnston, S. J. Schuster, W. J. Jurczak, I. W. Flinn, C. R. Flowers, P. Martin, A. Viardot, K. A. Blum, A. H. Goy, A. J. Davies, P. L. Zinzani, M. Dreyling, D. Johnson, L. L. Miller, L. Holes, D. Li, R. D. Dansey,

W. R. Godfrey and G. A. Salles (2014). "PI3Kdelta inhibition by idelalisib in patients with relapsed indolent lymphoma." N Engl J Med **370**(11): 1008-1018.

Gottlob, K., N. Majewski, S. Kennedy, E. Kandel, R. B. Robey and N. Hay (2001). "Inhibition of early apoptotic events by Akt/PKB is dependent on the first committed step of glycolysis and mitochondrial hexokinase." Genes Dev **15**(11): 1406-1418.

Gough, D. J., A. Corlett, K. Schlessinger, J. Wegrzyn, A. C. Larner and D. E. Levy (2009). "Mitochondrial STAT3 supports Ras-dependent oncogenic transformation." Science **324**(5935): 1713-1716.

Hahn-Windgassen, A., V. Nogueira, C. C. Chen, J. E. Skeen, N. Sonenberg and N. Hay (2005). "Akt activates the mammalian target of rapamycin by regulating cellular ATP level and AMPK activity." J Biol Chem **280**(37): 32081-32089.

Hallek, M., L. Wanders, M. Ostwald, R. Busch, R. Senekowitsch, S. Stern, H. D. Schick, I. Kuhn-Hallek and B. Emmerich (1996). "Serum beta(2)-microglobulin and serum thymidine kinase are independent predictors of progression-free survival in chronic lymphocytic leukemia and immunocytoma." Leuk Lymphoma **22**(5-6): 439-447.

Hamada, K., T. Sasaki, P. A. Koni, M. Natsui, H. Kishimoto, J. Sasaki, N. Yajima, Y. Horie, G. Hasegawa, M. Naito, J. Miyazaki, T. Suda, H. Itoh, K. Nakao, T. W. Mak, T. Nakano and A. Suzuki (2005). "The PTEN/PI3K pathway governs normal vascular development and tumor angiogenesis." Genes Dev **19**(17): 2054-2065.

Hamblin, T. J., Z. Davis, A. Gardiner, D. G. Oscier and F. K. Stevenson (1999). "Unmutated Ig V(H) genes are associated with a more aggressive form of chronic lymphocytic leukemia." Blood **94**(6): 1848-1854.

Heintel, D., D. Kienle, M. Shehata, A. Krober, E. Kroemer, I. Schwarzinger, D. Mitteregger, T. Le, A. Gleiss, C. Mannhalter, A. Chott, J. Schwarzmeier, C. Fonatsch, A. Gaiger, H. Dohner, S. Stilgenbauer, U. Jager and C. L. L. S. Group (2005). "High expression of lipoprotein lipase in poor risk B-cell chronic lymphocytic leukemia." Leukemia **19**(7): 1216-1223.

Henderson, J. F., J. H. Fraser and E. E. McCoy (1974). "Methods for the study of purine metabolism in human cells in vitro." Clin Biochem **7**(4): 339-358.

Henderson, J. F. and A. R. P. Paterson (1973). Nucleotide metabolism; an introduction. New York,, Academic Press.

Herishanu, Y., P. Perez-Galan, D. Liu, A. Biancotto, S. Pittaluga, B. Vire, F. Gibellini, N. Njuguna, E. Lee, L. Stennett, N. Raghavachari, P. Liu, J. P. McCoy, M. Raffeld, M. Stetler-Stevenson, C. Yuan, R. Sherry, D. C. Arthur, I. Maric, T. White, G. E. Marti, P. Munson, W. H. Wilson and A. Wiestner (2011). "The lymph node microenvironment promotes B-cell receptor signaling, NF-kappaB activation, and tumor proliferation in chronic lymphocytic leukemia." Blood **117**(2): 563-574.

Herman, S. E., A. L. Gordon, E. Hertlein, A. Ramanunni, X. Zhang, S. Jaglowski, J. Flynn, J. Jones, K. A. Blum, J. J. Buggy, A. Hamdy, A. J. Johnson and J. C. Byrd (2011). "Bruton tyrosine kinase represents a promising therapeutic target for treatment of chronic lymphocytic leukemia and is effectively targeted by PCI-32765." Blood **117**(23): 6287-6296.

Herman, S. E., A. L. Gordon, A. J. Wagner, N. A. Heerema, W. Zhao, J. M. Flynn, J. Jones, L. Andritsos, K. D. Puri, B. J. Lannutti, N. A. Giese, X. Zhang, L. Wei, J. C. Byrd and A. J. Johnson (2010). "Phosphatidylinositol 3-kinase-delta inhibitor CAL-101 shows promising preclinical activity in chronic lymphocytic leukemia by antagonizing intrinsic and extrinsic cellular survival signals." Blood **116**(12): 2078-2088.

Hickey, F. B. and T. G. Cotter (2006). "BCR-ABL regulates phosphatidylinositol 3-kinase-p110gamma transcription and activation and is required for proliferation and drug resistance." J Biol Chem **281**(5): 2441-2450.

Hirai, H., H. Sootome, Y. Nakatsuru, K. Miyama, S. Taguchi, K. Tsujioka, Y. Ueno, H. Hatch, P. K. Majumder, B. S. Pan and H. Kotani (2010). "MK-2206, an allosteric Akt inhibitor, enhances antitumor efficacy by standard chemotherapeutic agents or molecular targeted drugs in vitro and in vivo." Mol Cancer Ther **9**(7): 1956-1967.

Hirsch, E., V. L. Katanaev, C. Garlanda, O. Azzolino, L. Pirola, L. Silengo, S. Sozzani, A. Mantovani, F. Altruda and M. P. Wymann (2000). "Central role for G protein-coupled phosphoinositide 3-kinase gamma in inflammation." Science **287**(5455): 1049-1053.

Hofbauer, S. W., P. W. Krenn, J. Pinomicronn Hofbauer, S. Pucher, D. Asslaber, A. Egle, T. N. Hartmann and R. Greil (2015). "The AKT1 isoform plays a dominant role in the

survival and chemoresistance of chronic lymphocytic leukaemia cells." Br J Haematol.

Hosnijeh, F. S., Q. Lan, N. Rothman, C. San Liu, W. L. Cheng, A. Nieters, P. Guldberg, A. Tjonneland, D. Campa, A. Martino, H. Boeing, A. Trichopoulou, P. Lagiou, D. Trichopoulos, V. Krogh, R. Tumino, S. Panico, G. Masala, E. Weiderpass, J. M. Huerta Castano, E. Ardanaz, N. Sala, M. Dorronsoro, J. R. Quiros, M. J. Sanchez, B. Melin, A. S. Johansson, J. Malm, S. Borgquist, P. H. Peeters, H. B. Bueno-de-Mesquita, N. Wareham, K. T. Khaw, R. C. Travis, P. Brennan, A. Siddiq, E. Riboli, P. Vineis and R. Vermeulen (2014). "Mitochondrial DNA copy number and future risk of B-cell lymphoma in a nested case-control study in the prospective EPIC cohort." Blood **124**(4): 530-535.

Hsu, P. P. and D. M. Sabatini (2008). "Cancer cell metabolism: Warburg and beyond." Cell **134**(5): 703-707.

Hu, H., A. Juvekar, C. A. Lyssiotis, E. C. Lien, J. G. Albeck, D. Oh, G. Varma, Y. P. Hung, S. Ullas, J. Lauring, P. Seth, M. R. Lundquist, D. R. Tolan, A. K. Grant, D. J. Needleman, J. M. Asara, L. C. Cantley and G. M. Wulf (2016). "Phosphoinositide 3-Kinase Regulates Glycolysis through Mobilization of Aldolase from the Actin Cytoskeleton." Cell **164**(3): 433-446.

Huang, M. and L. M. Graves (2003). "De novo synthesis of pyrimidine nucleotides; emerging interfaces with signal transduction pathways." Cell Mol Life Sci **60**(2): 321-336.

Itoyama, T., R. S. Chaganti, Y. Yamada, K. Tsukasaki, S. Atogami, H. Nakamura, M. Tomonaga, K. Ohshima, M. Kikuchi and N. Sadamori (2001). "Cytogenetic analysis and clinical significance in adult T-cell leukemia/lymphoma: a study of 50 cases from the human T-cell leukemia virus type-1 endemic area, Nagasaki." Blood **97**(11): 3612-3620.

Jiang, Z. Y., Q. L. Zhou, K. A. Coleman, M. Chouinard, Q. Boese and M. P. Czech (2003). "Insulin signaling through Akt/protein kinase B analyzed by small interfering RNA-mediated gene silencing." Proc Natl Acad Sci U S A **100**(13): 7569-7574.

Jitschin, R., M. Braun, M. Qorraj, D. Saul, K. Le Blanc, T. Zenz and D. Mougiakakos (2015). "Stromal cell-mediated glycolytic switch in CLL cells involves Notch-c-Myc signaling." Blood **125**(22): 3432-3436.

Jitschin, R., A. D. Hofmann, H. Bruns, A. Giessl, J. Bricks, J. Berger, D. Saul, M. J. Eckart, A. Mackensen and D. Mougiakakos (2014). "Mitochondrial metabolism contributes to oxidative stress and reveals therapeutic targets in chronic lymphocytic leukemia." Blood **123**(17): 2663-2672.

Jones, M. E. (1980). "Pyrimidine nucleotide biosynthesis in animals: genes, enzymes, and regulation of UMP biosynthesis." Annu Rev Biochem **49**: 253-279.

Jouaville, L. S., P. Pinton, C. Bastianutto, G. A. Rutter and R. Rizzuto (1999). "Regulation of mitochondrial ATP synthesis by calcium: evidence for a long-term metabolic priming." Proc Natl Acad Sci U S A **96**(24): 13807-13812.

Kelly, C. J., K. Hussien, E. Fokas, P. Kannan, R. J. Shipley, T. M. Ashton, M. Stratford, N. Pearson and R. J. Muschel (2014). "Regulation of O2 consumption by the PI3K and mTOR pathways contributes to tumor hypoxia." Radiother Oncol **111**(1): 72-80.

Kelly, K. R., J. H. Rowe, S. Padmanabhan, S. T. Nawrocki and J. S. Carew (2011). "Mammalian target of rapamycin as a target in hematological malignancies." Target Oncol **6**(1): 53-61.

Kienle, D., A. Benner, A. Krober, D. Winkler, D. Mertens, A. Buhler, T. Seiler, U. Jager, P. Lichter, H. Dohner and S. Stilgenbauer (2006). "Distinct gene expression patterns in chronic lymphocytic leukemia defined by usage of specific VH genes." Blood **107**(5): 2090-2093.

Kim, S., P. Mangin, C. Dangelmaier, R. Lillian, S. P. Jackson, J. L. Daniel and S. P. Kunapuli (2009). "Role of phosphoinositide 3-kinase beta in glycoprotein VI-mediated Akt activation in platelets." J Biol Chem **284**(49): 33763-33772.

Kini, A. R., N. E. Kay and L. C. Peterson (2000). "Increased bone marrow angiogenesis in B cell chronic lymphocytic leukemia." Leukemia **14**(8): 1414-1418.

Kipps, T. J., E. Tomhave, L. F. Pratt, S. Duffy, P. P. Chen and D. A. Carson (1989). "Developmentally restricted immunoglobulin heavy chain variable region gene expressed at high frequency in chronic lymphocytic leukemia." Proc Natl Acad Sci U S A **86**(15): 5913-5917.

Kitada, S., J. Andersen, S. Akar, J. M. Zapata, S. Takayama, S. Krajewski, H. G. Wang, X. Zhang, F. Bullrich, C. M. Croce, K. Rai, J. Hines and J. C. Reed (1998). "Expression of apoptosis-regulating proteins in chronic lymphocytic leukemia: correlations with In vitro and In vivo chemoresponses." Blood **91**(9): 3379-3389.

Klein, U., Y. Tu, G. A. Stolovitzky, M. Mattioli, G. Cattoretti, H. Husson, A. Freedman, G. Inghirami, L. Cro, L. Baldini, A. Neri, A. Califano and R. Dalla-Favera (2001). "Gene expression profiling of B cell chronic lymphocytic leukemia reveals a homogeneous phenotype related to memory B cells." J Exp Med **194**(11): 1625-1638.

Koczula, K. M., C. Ludwig, R. Hayden, L. Cronin, G. Pratt, H. Parry, D. Tennant, M. Drayson, C. M. Bunce, F. L. Khanim and U. L. Gunther (2015). "Metabolic plasticity in CLL: adaptation to the hypoxic niche." Leukemia: 1-9.

Kohn, A. D., S. A. Summers, M. J. Birnbaum and R. A. Roth (1996). "Expression of a constitutively active Akt Ser/Thr kinase in 3T3-L1 adipocytes stimulates glucose uptake and glucose transporter 4 translocation." J Biol Chem **271**(49): 31372-31378.

Koppenol, W. H., P. L. Bounds and C. V. Dang (2011). "Otto Warburg's contributions to current concepts of cancer metabolism." Nat Rev Cancer **11**(5): 325-337.

Krober, A., T. Seiler, A. Benner, L. Bullinger, E. Bruckle, P. Lichter, H. Dohner and S. Stilgenbauer (2002). "V(H) mutation status, CD38 expression level, genomic aberrations, and survival in chronic lymphocytic leukemia." Blood **100**(4): 1410-1416.

Kurtova, A. V., K. Balakrishnan, R. Chen, W. Ding, S. Schnabl, M. P. Quiroga, M. Sivina, W. G. Wierda, Z. Estrov, M. J. Keating, M. Shehata, U. Jager, V. Gandhi, N. E. Kay, W. Plunkett and J. A. Burger (2009). "Diverse marrow stromal cells protect CLL cells from spontaneous and drug-induced apoptosis: development of a reliable and reproducible system to assess stromal cell adhesion-mediated drug resistance." Blood **114**(20): 4441-4450.

Lafarge, S. T., J. B. Johnston, S. B. Gibson and A. J. Marshall (2014). "Adhesion of ZAP-70+ chronic lymphocytic leukemia cells to stromal cells is enhanced by cytokines and blocked by inhibitors of the PI3-kinase pathway." Leuk Res **38**(1): 109-115.

Lafarge, S. T., H. Li, S. D. Pauls, S. Hou, J. B. Johnston, S. B. Gibson and A. J. Marshall (2015). "ZAP70 expression directly promotes chronic lymphocytic leukaemia cell adhesion to bone marrow stromal cells." Br J Haematol **168**(1): 139-142.

Landau, D. A., S. L. Carter, P. Stojanov, A. McKenna, K. Stevenson, M. S. Lawrence, C. Sougnez, C. Stewart, A. Sivachenko, L. Wang, Y. Wan, W. Zhang, S. A. Shukla, A. Vartanov, S. M. Fernandes, G. Saksena, K. Cibulskis, B. Tesar, S. Gabriel, N. Hacohen, M. Meyerson, E. S. Lander, D. Neuberg, J. R. Brown, G. Getz and C. J. Wu (2013). "Evolution and impact of subclonal mutations in chronic lymphocytic leukemia." Cell **152**(4): 714-726.

Lanham, S., T. Hamblin, D. Oscier, R. Ibbotson, F. Stevenson and G. Packham (2003). "Differential signaling via surface IgM is associated with VH gene mutational status and CD38 expression in chronic lymphocytic leukemia." Blood **101**(3): 1087-1093.

Laplante, M. and D. M. Sabatini (2012). "mTOR signaling in growth control and disease." Cell **149**(2): 274-293.

Li, C., Y. Li, L. He, A. R. Agarwal, N. Zeng, E. Cadenas and B. L. Stiles (2013). "PI3K/AKT signaling regulates bioenergetics in immortalized hepatocytes." Free Radic Biol Med **60**: 29-40.

Li, Z., H. Jiang, W. Xie, Z. Zhang, A. V. Smrcka and D. Wu (2000). "Roles of PLC-beta2 and -beta3 and PI3Kgamma in chemoattractant-mediated signal transduction." Science **287**(5455): 1046-1049.

Lim, H. Y., Q. S. Ho, J. Low, M. Choolani and K. P. Wong (2011). "Respiratory competent mitochondria in human ovarian and peritoneal cancer." Mitochondrion **11**(3): 437-443.

Liu, Y., Y. Cao, W. Zhang, S. Bergmeier, Y. Qian, H. Akbar, R. Colvin, J. Ding, L. Tong, S. Wu, J. Hines and X. Chen (2012). "A small-molecule inhibitor of glucose transporter 1 downregulates glycolysis, induces cell-cycle arrest, and inhibits cancer cell growth in vitro and in vivo." Mol Cancer Ther **11**(8): 1672-1682.

Liu, Y. C., F. Li, J. Handler, C. R. Huang, Y. Xiang, N. Neretti, J. M. Sedivy, K. I. Zeller and C. V. Dang (2008). "Global regulation of nucleotide biosynthetic genes by c-Myc." PLoS One **3**(7): e2722.

Lu, C. L., L. Qin, H. C. Liu, D. Candas, M. Fan and J. J. Li (2015). "Tumor cells switch to mitochondrial oxidative phosphorylation under radiation via mTOR-mediated hexokinase II inhibition--a Warburg-reversing effect." PLoS One **10**(3): e0121046.

Malavasi, F., A. Funaro, S. Roggero, A. Horenstein, L. Calosso and K. Mehta (1994). "Human CD38: a glycoprotein in search of a function." Immunol Today **15**(3): 95-97.

Manshouri, T., Z. Estrov, A. Quintas-Cardama, J. Burger, Y. Zhang, A. Livun, L. Knez, D. Harris, C. J. Creighton, H. M. Kantarjian and S. Verstovsek (2011). "Bone marrow stroma-secreted cytokines protect JAK2(V617F)-mutated cells from the effects of a JAK2 inhibitor." Cancer Res **71**(11): 3831-3840.

Marti, G. E., V. Zenger, N. E. Caproaso, M. Brown, G. C. Washington, P. Carter, G. Schechter and P. Noguchi (1989). "Antigenic expression of B-cell chronic lymphocytic leukemic lymphocytes." Anal Quant Cytol Histol **11**(5): 315-323.

Martinez Marignac, V. L., S. Smith, N. Toban, M. Bazile and R. Aloyz (2013). "Resistance to Dasatinib in primary chronic lymphocytic leukemia lymphocytes involves AMPK-mediated energetic re-programming." Oncotarget **4**(12): 2550-2566.

Mathupala, S. P., Y. H. Ko and P. L. Pedersen (2009). "Hexokinase-2 bound to mitochondria: cancer's stygian link to the "Warburg Effect" and a pivotal target for effective therapy." Semin Cancer Biol **19**(1): 17-24.

Matutes, E., K. Owusu-Ankomah, R. Morilla, J. Garcia Marco, A. Houlihan, T. H. Que and D. Catovsky (1994). "The immunological profile of B-cell disorders and proposal of a scoring system for the diagnosis of CLL." Leukemia **8**(10): 1640-1645.

Menzel, T., Z. Rahman, E. Calleja, K. White, E. L. Wilson, R. Wieder and J. Gabrilove (1996). "Elevated intracellular level of basic fibroblast growth factor correlates with stage of chronic lymphocytic leukemia and is associated with resistance to fludarabine." Blood **87**(3): 1056-1063.

Mitchell, P. (1961). "Coupling of phosphorylation to electron and hydrogen transfer by a chemi-osmotic type of mechanism." Nature **191**: 144-148.

Mizoguchi, M., C. L. Nutt, G. Mohapatra and D. N. Louis (2004). "Genetic alterations of phosphoinositide 3-kinase subunit genes in human glioblastomas." Brain Pathol **14**(4): 372-377.

Moon, K. D., C. B. Post, D. L. Durden, Q. Zhou, P. De, M. L. Harrison and R. L. Geahlen (2005). "Molecular basis for a direct interaction between the Syk protein-tyrosine kinase and phosphoinositide 3-kinase." J Biol Chem **280**(2): 1543-1551.

Mustelin, T. and K. Tasken (2003). "Positive and negative regulation of T-cell activation through kinases and phosphatases." Biochem J **371**(Pt 1): 15-27.

Nishio, M., T. Endo, N. Tsukada, J. Ohata, S. Kitada, J. C. Reed, N. J. Zvaifler and T. J. Kipps (2005). "Nurselike cells express BAFF and APRIL, which can promote survival of chronic lymphocytic leukemia cells via a paracrine pathway distinct from that of SDF-1alpha." Blood **106**(3): 1012-1020.

Ono, M., S. Bolland, P. Tempst and J. V. Ravetch (1996). "Role of the inositol phosphatase SHIP in negative regulation of the immune system by the receptor Fc(gamma)RIIB." Nature **383**(6597): 263-266.

Orchard, J. A., R. E. Ibbotson, Z. Davis, A. Wiestner, A. Rosenwald, P. W. Thomas, T. J. Hamblin, L. M. Staudt and D. G. Oscier (2004). "ZAP-70 expression and prognosis in chronic lymphocytic leukaemia." Lancet **363**(9403): 105-111.

Oscier, D. G., A. C. Gardiner, S. J. Mould, S. Glide, Z. A. Davis, R. E. Ibbotson, M. M. Corcoran, R. M. Chapman, P. W. Thomas, J. A. Copplestone, J. A. Orchard and T. J. Hamblin (2002). "Multivariate analysis of prognostic factors in CLL: clinical stage, IGVH gene mutational status, and loss or mutation of the p53 gene are independent prognostic factors." Blood **100**(4): 1177-1184.

Pankov, R. and K. M. Yamada (2002). "Fibronectin at a glance." J Cell Sci **115**(Pt 20): 3861-3863.

Patel, V., L. S. Chen, W. G. Wierda, K. Balakrishnan and V. Gandhi (2014). "Impact of bone marrow stromal cells on Bcl-2 family members in chronic lymphocytic leukemia." Leuk Lymphoma **55**(4): 899-910.

Pflug, N., J. Bahlo, T. D. Shanafelt, B. F. Eichhorst, M. A. Bergmann, T. Elter, K. Bauer, G. Malchau, K. G. Rabe, S. Stilgenbauer, H. Dohner, U. Jager, M. J. Eckart, G. Hopfinger, R. Busch, A. M. Fink, C. M. Wendtner, K. Fischer, N. E. Kay and M. Hallek (2014). "Development of a comprehensive prognostic index for patients with chronic lymphocytic leukemia." Blood **124**(1): 49-62.

Rai, K. R., A. Sawitsky, E. P. Cronkite, A. D. Chanana, R. N. Levy and B. S. Pasternack (1975). "Clinical staging of chronic lymphocytic leukemia." Blood **46**(2): 219-234.

Rassenti, L. Z., L. Huynh, T. L. Toy, L. Chen, M. J. Keating, J. G. Gribben, D. S. Neuberg, I. W. Flinn, K. R. Rai, J. C. Byrd, N. E. Kay, A. Greaves, A. Weiss and T. J. Kipps (2004). "ZAP-70 compared with immunoglobulin heavy-chain gene mutation status as a predictor of disease progression in chronic lymphocytic leukemia." N Engl J Med **351**(9): 893-901.

Rathmell, J. C., C. J. Fox, D. R. Plas, P. S. Hammerman, R. M. Cinalli and C. B. Thompson (2003). "Akt-directed glucose metabolism can prevent Bax conformation change and promote growth factor-independent survival." Mol Cell Biol **23**(20): 7315-7328.

Ries L.A.G., E. M. P., Kosary C.L., Hankey B.F., Miller B.A., Clegg L., Mariotto A., Fay M.P., Feuer E.J. & Edwards B.K. 9 (eds) (2003) "SEER Cancer Statistics Review, 1975–2000."

Robitaille, A. M., S. Christen, M. Shimobayashi, M. Cornu, L. L. Fava, S. Moes, C. Prescianotto-Baschong, U. Sauer, P. Jenoe and M. N. Hall (2013). "Quantitative phosphoproteomics reveal mTORC1 activates de novo pyrimidine synthesis." Science **339**(6125): 1320-1323.

Rosenwald, A., A. A. Alizadeh, G. Widhopf, R. Simon, R. E. Davis, X. Yu, L. Yang, O. K. Pickeral, L. Z. Rassenti, J. Powell, D. Botstein, J. C. Byrd, M. R. Grever, B. D. Cheson, N. Chiorazzi, W. H. Wilson, T. J. Kipps, P. O. Brown and L. M. Staudt (2001). "Relation of gene expression phenotype to immunoglobulin mutation genotype in B cell chronic lymphocytic leukemia." J Exp Med **194**(11): 1639-1647.

Rozman, C. and E. Montserrat (1995). "Chronic lymphocytic leukemia." N Engl J Med **333**(16): 1052-1057.

Sano, H., S. Kane, E. Sano, C. P. Miinea, J. M. Asara, W. S. Lane, C. W. Garner and G. E. Lienhard (2003). "Insulin-stimulated phosphorylation of a Rab GTPase-activating protein regulates GLUT4 translocation." J Biol Chem **278**(17): 14599-14602.

Sasaki, T., J. Irie-Sasaki, R. G. Jones, A. J. Oliveira-dos-Santos, W. L. Stanford, B. Bolon, A. Wakeham, A. Itie, D. Bouchard, I. Kozieradzki, N. Joza, T. W. Mak, P. S. Ohashi, A. Suzuki and J. M. Penninger (2000). "Function of PI3Kgamma in thymocyte

development, T cell activation, and neutrophil migration." Science **287**(5455): 1040-1046.

Sawyer, C., J. Sturge, D. C. Bennett, M. J. O'Hare, W. E. Allen, J. Bain, G. E. Jones and B. Vanhaesebroeck (2003). "Regulation of breast cancer cell chemotaxis by the phosphoinositide 3-kinase p110delta." Cancer Res **63**(7): 1667-1675.

Schroder, A. E., A. Greiner, C. Seyfert and C. Berek (1996). "Differentiation of B cells in the nonlymphoid tissue of the synovial membrane of patients with rheumatoid arthritis." Proc Natl Acad Sci U S A **93**(1): 221-225.

Shaik, Z. P., E. K. Fifer and G. Nowak (2008). "Akt activation improves oxidative phosphorylation in renal proximal tubular cells following nephrotoxicant injury." Am J Physiol Renal Physiol **294**(2): F423-432.

Skorski, T., A. Bellacosa, M. Nieborowska-Skorska, M. Majewski, R. Martinez, J. K. Choi, R. Trotta, P. Wlodarski, D. Perrotti, T. O. Chan, M. A. Wasik, P. N. Tsichlis and B. Calabretta (1997). "Transformation of hematopoietic cells by BCR/ABL requires activation of a PI-3k/Akt-dependent pathway." EMBO J **16**(20): 6151-6161.

Spaargaren, M., E. A. Beuling, M. L. Rurup, H. P. Meijer, M. D. Klok, S. Middendorp, R. W. Hendriks and S. T. Pals (2003). "The B cell antigen receptor controls integrin activity through Btk and PLCgamma2." J Exp Med **198**(10): 1539-1550.

Srinivasan, L., Y. Sasaki, D. P. Calado, B. Zhang, J. H. Paik, R. A. DePinho, J. L. Kutok, J. F. Kearney, K. L. Otipoby and K. Rajewsky (2009). "PI3 kinase signals BCR-dependent mature B cell survival." Cell **139**(3): 573-586.

Stamatopoulos, K. (2009). "CLL: promiscuity leads to risks." Blood **114**(17): 3508-3509.

Stephens, L. R., A. Eguinoa, H. Erdjument-Bromage, M. Lui, F. Cooke, J. Coadwell, A. S. Smrcka, M. Thelen, K. Cadwallader, P. Tempst and P. T. Hawkins (1997). "The G beta gamma sensitivity of a PI3K is dependent upon a tightly associated adaptor, p101." Cell **89**(1): 105-114.

Subramaniam, P. S., D. W. Whye, E. Efimenko, J. Chen, V. Tosello, K. De Keersmaecker, A. Kashishian, M. A. Thompson, M. Castillo, C. Cordon-Cardo, U. P. Dave, A. Ferrando, B. J. Lannutti and T. G. Diacovo (2012). "Targeting nonclassical oncogenes for therapy in T-ALL." Cancer Cell **21**(4): 459-472.

Sujobert, P., V. Bardet, P. Cornillet-Lefebvre, J. S. Hayflick, N. Prie, F. Verdier, B. Vanhaesebroeck, O. Muller, F. Pesce, N. Ifrah, M. Hunault-Berger, C. Berthou, B. Villemagne, E. Jourdan, B. Audhuy, E. Solary, B. Witz, J. L. Harousseau, C. Himberlin, T. Lamy, B. Lioure, J. Y. Cahn, F. Dreyfus, P. Mayeux, C. Lacombe and D. Bouscary (2005). "Essential role for the p110delta isoform in phosphoinositide 3-kinase activation and cell proliferation in acute myeloid leukemia." Blood **106**(3): 1063-1066.

Tili, E., J. J. Michaille, Z. Luo, S. Volinia, L. Z. Rassenti, T. J. Kipps and C. M. Croce (2012). "The down-regulation of miR-125b in chronic lymphocytic leukemias leads to metabolic adaptation of cells to a transformed state." Blood **120**(13): 2631-2638.

Tomasetti, M., J. Neuzil and L. Dong (2014). "MicroRNAs as regulators of mitochondrial function: role in cancer suppression." Biochim Biophys Acta **1840**(4): 1441-1453.

Tonegawa, S. (1983). "Somatic generation of antibody diversity." Nature **302**(5909): 575-581.

Toogood, P. L. (2008). "Mitochondrial drugs." Curr Opin Chem Biol **12**(4): 457-463.

Vander Heiden, M. G., L. C. Cantley and C. B. Thompson (2009). "Understanding the Warburg effect: the metabolic requirements of cell proliferation." Science **324**(5930): 1029-1033.

Vanhaesebroeck, B., S. J. Leevers, K. Ahmadi, J. Timms, R. Katso, P. C. Driscoll, R. Woscholski, P. J. Parker and M. D. Waterfield (2001). "Synthesis and function of 3-phosphorylated inositol lipids." Annu Rev Biochem **70**: 535-602.

Vanhaesebroeck, B., M. J. Welham, K. Kotani, R. Stein, P. H. Warne, M. J. Zvelebil, K. Higashi, S. Volinia, J. Downward and M. D. Waterfield (1997). "P110delta, a novel phosphoinositide 3-kinase in leukocytes." Proc Natl Acad Sci U S A **94**(9): 4330-4335.

Vu, T. H., M. Sciacco, K. Tanji, C. Nichter, E. Bonilla, S. Chatkupt, P. Maertens, S. Shanske, J. Mendell, M. R. Koenigsberger, L. Sharer, E. A. Schon, S. DiMauro and D. C. DeVivo (1998). "Clinical manifestations of mitochondrial DNA depletion." Neurology **50**(6): 1783-1790.

Vuillier, F., G. Dumas, C. Magnac, M. C. Prevost, A. I. Lalanne, P. Oppezzo, E. Melanitou, G. Dighiero and B. Payelle-Brogard (2005). "Lower levels of surface B-cell-receptor

expression in chronic lymphocytic leukemia are associated with glycosylation and folding defects of the mu and CD79a chains." Blood **105**(7): 2933-2940.

Warburg, O. (1956). "On the origin of cancer cells." Science **123**(3191): 309-314.

Ward, P. S. and C. B. Thompson (2012). "Metabolic reprogramming: a cancer hallmark even warburg did not anticipate." Cancer Cell **21**(3): 297-308.

Wegrzyn, J., R. Potla, Y. J. Chwae, N. B. Sepuri, Q. Zhang, T. Koeck, M. Derecka, K. Szczepanek, M. Szelag, A. Gornicka, A. Moh, S. Moghaddas, Q. Chen, S. Bobbili, J. Cichy, J. Dulak, D. P. Baker, A. Wolfman, D. Stuehr, M. O. Hassan, X. Y. Fu, N. Avadhani, J. I. Drake, P. Fawcett, E. J. Lesnefsky and A. C. Larner (2009). "Function of mitochondrial Stat3 in cellular respiration." Science **323**(5915): 793-797.

Whiteman, E. L., H. Cho and M. J. Birnbaum (2002). "Role of Akt/protein kinase B in metabolism." Trends Endocrinol Metab **13**(10): 444-451.

Wierda, W. G., S. O'Brien, X. Wang, S. Faderl, A. Ferrajoli, K. A. Do, J. Cortes, D. Thomas, G. Garcia-Manero, C. Koller, M. Beran, F. Giles, F. Ravandi, S. Lerner, H. Kantarjian and M. Keating (2007). "Prognostic nomogram and index for overall survival in previously untreated patients with chronic lymphocytic leukemia." Blood **109**(11): 4679-4685.

Wiestner, A., A. Rosenwald, T. S. Barry, G. Wright, R. E. Davis, S. E. Henrickson, H. Zhao, R. E. Ibbotson, J. A. Orchard, Z. Davis, M. Stetler-Stevenson, M. Raffeld, D. C. Arthur, G. E. Marti, W. H. Wilson, T. J. Hamblin, D. G. Oscier and L. M. Staudt (2003). "ZAP-70 expression identifies a chronic lymphocytic leukemia subtype with unmutated immunoglobulin genes, inferior clinical outcome, and distinct gene expression profile." Blood **101**(12): 4944-4951.

Winkler, D. G., K. L. Faia, J. P. DiNitto, J. A. Ali, K. F. White, E. E. Brophy, M. M. Pink, J. L. Proctor, J. Lussier, C. M. Martin, J. G. Hoyt, B. Tillotson, E. L. Murphy, A. R. Lim, B. D. Thomas, J. R. Macdougall, P. Ren, Y. Liu, L. S. Li, K. A. Jessen, C. C. Fritz, J. L. Dunbar, J. R. Porter, C. Rommel, V. J. Palombella, P. S. Changelian and J. L. Kutok (2013). "PI3K-delta and PI3K-gamma inhibition by IPI-145 abrogates immune responses and suppresses activity in autoimmune and inflammatory disease models." Chem Biol **20**(11): 1364-1374.

Wise, D. R. and C. B. Thompson (2010). "Glutamine addiction: a new therapeutic target in cancer." Trends Biochem Sci **35**(8): 427-433.

Woyach, J. A., A. J. Johnson and J. C. Byrd (2012). "The B-cell receptor signaling pathway as a therapeutic target in CLL." Blood **120**(6): 1175-1184.

Yancopoulos, G. D. and F. W. Alt (1986). "Regulation of the assembly and expression of variable-region genes." Annu Rev Immunol **4**: 339-368.

Yang, Z. Z., O. Tschopp, M. Hemmings-Mieszczak, J. Feng, D. Brodbeck, E. Perentes and B. A. Hemmings (2003). "Protein kinase B alpha/Akt1 regulates placental development and fetal growth." J Biol Chem **278**(34): 32124-32131.

Yuan, T. L., H. S. Choi, A. Matsui, C. Benes, E. Lifshits, J. Luo, J. V. Frangioni and L. C. Cantley (2008). "Class 1A PI3K regulates vessel integrity during development and tumorigenesis." Proc Natl Acad Sci U S A **105**(28): 9739-9744.

Zhang, W., D. Trachootham, J. Liu, G. Chen, H. Pelicano, C. Garcia-Prieto, W. Lu, J. A. Burger, C. M. Croce, W. Plunkett, M. J. Keating and P. Huang (2012). "Stromal control of cystine metabolism promotes cancer cell survival in chronic lymphocytic leukaemia." Nat Cell Biol **14**(3): 276-286.

Zhao, J. J., H. Cheng, S. Jia, L. Wang, O. V. Gjoerup, A. Mikami and T. M. Roberts (2006). "The p110alpha isoform of PI3K is essential for proper growth factor signaling and oncogenic transformation." Proc Natl Acad Sci U S A **103**(44): 16296-16300.

Zhou, Y., E. O. Hileman, W. Plunkett, M. J. Keating and P. Huang (2003). "Free radical stress in chronic lymphocytic leukemia cells and its role in cellular sensitivity to ROS-generating anticancer agents." Blood **101**(10): 4098-4104.

Vita

Hima V. Vangapandu was born in Visakhapatnam, Andhra Pradesh, India on March 27th to the parents of V. Rama Krishna and P. Jyothi as a single child. She grew up in Hyderabad and Visakhapatnam, Andhra Pradesh. She attended school at St. Joseph's Girls' High School, Visakhapatnam from 1998-2002. She completed her 11th and 12th grades from Sri Chaitanya Junior college from 2002-2004. Hima graduated with a degree in Bachelors of Technology from a college affiliated to Jawaharlal Nehru Technological University, Hyderabad in 2008. She came to United States of America in 2008, to pursue higher education. She received a Masters' degree in Biomedical Sciences from University of South Carolina, School of Medicine at Columbia, South Carolina. In August, 2012, she enrolled in The University of Texas Graduate School of Biomedical Sciences at Houston and later joined the laboratory of Dr. Varsha Gandhi in the Department of Experimental Therapeutics, MD Anderson Cancer Center and affiliated with the Experimental Therapeutics Academic Program (ETAP). Hima conducted her Ph.D work under Gandhi's advisory. And she will complete all the requirements of Doctor of Philosophy degree in March 2016.

During Hima's graduate training, she received multiple travel awards from both UT-GSBS and ETAP to attend the annual meetings of American Association of Cancer Research (AACR), where she presented her work. She also received a research award from ETAP in 2014. Hima received UT MD Anderson Alumni and Faculty Association Award in Translational Research in 2014. In addition, she also received Student Apple Award in 2015 from ETAP for her volunteer activities towards the program. She received Floyd Haar, M.D., Endowed Memorial Research Award in Memory of Freda Haar of 2015-2016 through UT GSBS for her research in leukemia.

Publications

Vangapandu, H. and Gandhi, V. Chronic lymphocytic leukemia at genomic level. In. Multitargeted Approach to Treatment of Cancer, Ed. Varsha Gandhi, Kapil Mehta, Rajesh Grover, Sen Pathak and Bharat B. Aggarwal, Springer Production; Heidelberg, Germany, 2014.

Stellrecht CM, **Vangapandu HV**, Le XF, Mao W, Shentu S. ATP directed agent, 8-chloro-adenosine, induces AMP activated protein kinase activity, leading to autophagic cell death in breast cancer cells. *Journal of Hematology and Oncology*, 7(23) 1756-8722, 2014.

Jorgez CJ, Wilken N, Addai J, Newberg J, Pastsuzak A, Bournat J, Mukherjee S, **Vangapandu HV**, Sahin A, Rosenfeld JA, Lipshultz LI, Lamb DJ. Genomic and genetic variation in E2F transcription factor-1 in men with nonobstructive azoospermia *Fertility and Sterility*, 103(1):44-52.e12015.

Jorgez CJ, Rosenfeld JA, Wilken NR; **Vangapandu HV**, Sahin A; Pham D, Carvalho CM, e Bandholz A, Miller A, Weaver DD, Burton B, Babu D, Bamforth JS, Wilks T, Flynn DP, Roeder E, Patel A, Cheung SW, Lupski JR, Lamb DJ. Genitourinary Defects Associated with Genomic Deletions in 2p15 Encompassing OTX1. *PLoS One*,2014. 9(9): p. e107028.

Shull AY, Clendenning ML, Ghoshal-Gupta S, Farrell CL, **Vangapandu HV**, Dudas L, Wilkerson B, Buckhaults PJ 2013 Somatic Mutations, Allele Loss, and DNA Methylation of the Cub and Sushi Multiple Domains 1 (CSMD1) Gene Reveals Association with Early Age of Diagnosis in Colorectal Cancer Patients. *PLoS ONE* 8(3).

Tannour-Louet M, Lewis SK, Louet JF, Stewart J, Addai JB, Sahin A, **Vangapandu HV**, Lewis AL, Dittmar K, Pautler RG, Zhang L, Smith RG, Lamb DJ (2013) Increased expression of CYP24A1 correlates with advanced stages of prostate cancer and can cause resistance to vitamin D3-based therapies. *FASEB J* fj.13-236109.

Vangapandu H and Ai W. Kruppel like factor (KLF4) a Transcription factor with diverse context dependent functions. *Gene Ther Mol Biol* Vol 13, 194-203, 2009.

Permanent Address:

50-121-29/21

Balayya Sastri Layout, Seethammadhara,

Visakhapatnam, Andhra Pradesh

India, 530013